N62-17561

# TECHNICAL INFORMATION SERIES

R62SD31

# EVALUATIONS OF SPACE VEHICLE SHIELDING

N.F. DOW, S.P. SHEN AND J.F. HEYDA

SPACE SCIENCES LABORATORY

GENERAL ⓖ ELECTRIC

MISSILE AND SPACE VEHICLE DEPARTMENT

# SPACE SCIENCES LABORATORY

## SPACE MECHANICS OPERATION

EVALUATIONS OF SPACE VEHICLE SHIELDING

by

Norris F. Dow, S. P. Shen, and J. F. Heyda

R62SD31 - Class I
April 1962

## MISSILE AND SPACE VEHICLE DEPARTMENT

## GENERAL ELECTRIC

## SUMMARY                    /75 6 /

A general method of evaluating the efficiency of space vehicle shielding

is developed and used to compare various active and passive systems for

protection against ionizing radiation. Available permanent magnets are found

useless for active shielding, and combined active-passive systems in general

are determined to be inefficient. On the other hand, evaluations show that

active electrostatic shielding may have possibilities for weight savings if

electrical conditions (presently unknown) are favorable therefor in space.

Further, a positive potential improvement is calculated for an active

shielding system which utilizes superconducting $Nb_3Sn$ to provide a

confined magnetic flux to deflect incident charged particles; this potential

points toward substantial reductions in shield weight for the protection of

large vehicles from highly energetic particles. Recommendations are

made for further research, particularly for flight experiments to measure

directionality of solar flare protons.

# TABLE OF CONTENTS

Table of Contents - Continued

Table of Contents - Continued

# INTRODUCTION

## The Problem and Its Significance

Despite many uncertainties (ref. 1) which complicate the evaluation of

the ionizing radiation hazard to manned space flight, the conclusion is

inescapable that shielding is a most serious problem. No attempt will be

made in this report to reproduce the many studies that have been made to

evaluate the hazard (such as refs. 2-6); rather their results will be accepted as

representative of the present state of knowledge (or ignorance) of the three

types of ionizing radiation for which shielding of man must be considered -

qualitatively essentially as follows:

1. <u>The geomagnetically trapped (Van Allen) radiation</u> - which evidently

consists of both protons and electrons of numbers and intensities which vary

greatly with time and position. From the standpoint of shield design, the

important characteristics of this radiation are: (1) that at some altitudes

substantial numbers of protons of energies up to some 700 Mev have been

measured, (2) that the energies of the electrons are much less than this -

they are generally measured in Kev rather than Mev, and (3) that the

particles are not isotropic but have some directional properties, as they

spiral about the (often distorted) geomagnetic lines for force.

2. <u>The radiation resulting from solar flares</u> - which is generally accepted

to consist primarily of protons. The numbers and energies of the protons

apparently vary enormously from flare to flare, with the only correlating

factor that biggest flares occur least frequently. For shielding, design

1

thus becomes a matter of probabilities, i. e. , the more energetic the particle that can be shielded, the longer the spacecraft may fly before the probability of encounter of dangerous dosage becomes excessive.

3.  Galactic cosmic rays - the composition and numbers of which seem to be non-controversial, consisting mostly of protons of extremely high energies.  The cosmic radiation is perhaps still of problematical seriousness as regards the design of shielding, however.  Biological dosages produced by (1) the few heavy primaries mixed in among the protons and by (2) the secondaries produced from the primaries by nuclear collisions within the shield itself are of uncertain magnitude; they generally are agreed to be negligible for short exposures, but certainly they accumulate dosage (whatever the rate) as time goes on in space.

The foregoing qualitative summarization of the ionizing radiation hazards may perhaps give the general impression that a shielding problem exists but a quantitative assessment of the significance of the problem is more difficult.  Several authors have contributed sample evaluations - Keller for the Van Allen belts (ref. 2), Abel for solar flares (ref. 6), and Wallner and Kaufman (ref. 4) for cosmic radiation - and perhaps the best available measurement of the problem is to combine these as suggested in reference 7 to weigh the amount of shielding required on a probability basis for varying length missions in space.  Such an appraisal is presented in figure 1.

Discounting heavily the absolute values of weight depicted in figure 1 (as the authors whose results have been transcribed thereon would assuredly urge), one can still infer from the figure that while for short space flights the shielding

2

problem may be solvable without unreasonable weight penalties, for long

space missions - particularly if one adds together the requirements for

solar flares and cosmic rays - shield weights may become prohibitive.

## Directions for Research

On the basis of the foregoing evaluation of the significance of the

ionizing radiation in space, the attack on the shielding problem is logically

made in two directions. One explores possibilities of substantial reductions

in shield weight; the other examines further the seriousness of the contri-

bution of secondary radiation to the accumulation of dosage.

Possibilities of substantial reductions in the weight of simple, passive

shielding are not evident. The deceleration of protons by excitation and

ionization of the atoms of the shield material is sufficiently well understood

to eliminate any liklihood of the discovery of an order-of-magnitude more

effective shield material and, by the same token, only minor improvements

are accessible through the use of optimum combinations of materials as will

be shown later in this report.

While research directed toward improved passive shielding thus does

not seem to warrant much emphasis, unresolved questions about the hazard

of galactic cosmic radiation interacting with shielding still need attention.

The secondary radiations produced by collisions between incident, highly

energetic protons and nuclei within the shield are not well understood.

Indeed, dosages accumulated from cosmic ray/shield interactions during

long space flights may be substantial if the secondaries produced are much

greater than past calculations (ref. 4) show, and the problem deserves the

3

active research it is receiving (for example, ref. 8). Experiments in this area to investigate the phenomena involved should also penetrate the Bev range appropriate to cosmic radiation. The end result of this research inevitably must be a negative one, however, for at best it will pinpoint the shield thicknesses and flight durations at which the weight of passive shielding becomes prohibitive, or possibly the point at which, because of the secondaries produced, passive shielding becomes worse than no shielding at all.

The only possible direction for substantial increases in shield efficiency that is apparent at present is through the development of active shielding systems, utilizing electromagnetic or electrostatic fields to divert the incident particles from the region to be shielded. Perhaps the first to propose this concept was Singer (ref. 9). The enormities of the magnetic moments (or voltages) required were emphasized by Dow (ref. 10), and first achieved in concept by Levy (ref. 11), utilizing the newly discovered superconducting characteristics of $Nb_3Sn$ (ref. 12). Despite the long path between concept and application, Levy's work is significant because it is the first demonstration of a potential for a breakthrough in radiation shield design. The indication thus has been clearly given that studies of active shielding are desirable directions for research.

## Scope of this Report

This report describes the first steps in the directions suggested to be
appropriate in the preceding section, together with the results of preliminary
work necessary before even these first steps could be taken with confidence.

The preliminary studies included:

(1)  The development of simplified trajectory equations for
     charged particles moving through a retarding medium in
     electrostatic and electromagnetic fields.  (The approximating
     assumptions used and the derivations of these equations are
     presented in Appendix A. )

(2)  The Development of a Valid Method of Evaluation of the
     efficiency of various shielding systems.  (This development
     is presented in the following section of this report. )

The first of these studies permits the investigation either of active systems
incorporating magnetic materials or of combination active/passive systems
in which incident particles are both attenuated and diverted.  The second
makes it possible to avoid the problem that evaluation by sample design
for specific conditions may be misleading.

The main body of the report is concerned with First Approximation
Evaluations of Active Shielding Systems.  Various electrostatic, electro-
magnetic, and combination active/passive systems are considered and eval-
uated via the general method of comparison developed.  As might be expected,
the interesting potential of the active approach found by Levy (ref. 11) for a

5

magnetic dipole field is shown to be only a good first step. Not surprisingly, greater potentials are achievable; in particular a superconducting, electromagnetic, confined-flux system is described which conceptually compares most favorably (1) with any other active approach so far considered for shielding high-energy particles from volumes big enough for man, and (2) also compares favorably at all energies with corresponding first approximations to optimum passive systems.

Advanced Studies leading toward improved (second approximation) evaluations of both active and passive shielding are still in progress. These studies comprise (1) the analysis of results of a 3 Bev nuclear cascade experiment performed in the Brookhaven cosmotron, and (2) mathematical analyses of forbidden zones for as yet unexplored shielding field configuration. A status report of these investigations is given before the sections Results and Discussion, inasmuch as the advanced studies contribute thereto.

Conclusions and Recommendations are combined to suggest directions for future research emphasis in the quest for solutions to the radiation shielding problems.

# DEVELOPMENT OF A VALID METHOD OF EVALUATION

## Introduction

The fact that the geometries of shield and space to be shielded, as well as particle energy, affect the weight of shielding needed is well known to shield designers. The problem is not just one of minimization of shielded-volume surface, and the use of material found most effective on a weight basis (liquid hydrogen) from range-energy curves such as figure 2. Such curves represent just lower limits approached only as the radius of curvature of the shielded surface approaches infinity. As the radius decreases and the particle energy increases, the weight goes up, and the lighest material to use changes simply from liquid hydrogen to the denser, higher-atomic-number materials, seriatim (as pointed out in ref. 13).

In this section methods are developed for the systematic assessment of the interplay of geometry, energy, and shield weight required. The approach used is analogous to that employed in comparisons of weights of compression structures (for example, ref. 14) via the identification of a <u>Loading Index,</u> incorporating the important design conditions, against which the weight may be properly measured, to the end that a valid evaluation may be made of the weight efficiency of any type of shielding system for any combination of geometries and energies encountered. A particular objective is the establishment of a sound basis upon which to assess the efficiency of complex, active shielding systems for which evaluations from examples designed for specific, arbitrary conditions may be misleading.

7

## The Loading Index

The Loading Index Proposed incorporates the design conditions of kinetic energy of protons encountered and geometry of space to be shielded. As will be shown, measures of these conditions are appropriately combined as

$$L_i = \frac{CE^{1.75}}{r} \tag{1}$$

where

$L_i$ loading index, $\left[\dfrac{gms}{cm^3}\right]$

$E$ kinetic energy of protons, [Mev]

$r$ a length characteristic of the radius of the surface to be shielded, [cm.]

$C$ a dimensional constant used in the range/energy expression given as equation (2) below, $\left[\dfrac{gm}{cm^2 - Mev^{1.75}}\right]$

The parameter $\dfrac{CE^{1.75}}{r}$ derives from the simplified equation for the relationship between range and energy for protons

$$w_\infty = CE^{1.75} \tag{2}$$

where

$w_\infty$ weight of shielding required to stop normally incident protons by excitation and ionization of the atoms in the shield material, $\left[\dfrac{gm}{cm^2}\right]$

C & E as before

As a basis for comparison, hereafter in this report a value of 0.00110 $\dfrac{gm}{cm^2 - Mev^{1.75}}$ will be used for the value of C in the Loading Index. This

value, applicable to the element having the greatest shielding effectiveness (liquid hydrogen), is assumed as a logical standard against which to measure other shield materials and systems. With this value equation (2) is accurate, within ±5% of the more detailed expressions represented by the curves of figure 2, for energies from 50 to 500 Mev.

## Loading Index Evaluation of Passive Shielding

The use of the Loading Index for the evaluation of the weight efficiency of shielding will be illustrated in this section by application to passive shielding. The purpose here is primarily to show how the evaluation method works. To this end, implications regarding the use of composite materials and ideal shapes - not generally made clear in papers on space vehicle shielding (for example, ref. 15 and 16) - will be explored sufficiently to indicate the way in which the analysis appraises their significance.

Isotropic particles, simple materials, and a spherical shape. - Let us consider first a spherical volume to be shielded, by a single material of uniform thickness, from isotropic particles. The problem is to find the weight of material required for the given volume and for protons of given energy.

If the total weight of shield is W grams, and the volume to be shielded is $V_{Ref}$ cubic centimeters, where

$$V_{Ref} = \frac{4}{3} \pi r^3 \qquad (3)$$

then, as shown in Appendix B, except for small deviations at energies above 400 or 500 Mev, the variation of

9

$$\frac{W}{V_{Ref}} \text{ with } L_i = \frac{CE^{1.75}}{r} \tag{4}$$

can be depicted by a single curve for each shield material. Hence such a curve measures directly the weight-volume-energy relationship required. Further, a series of such curves for a series of materials indicates directly the relative weights of each, which is the lightest, and the actual weight required. A plot of this character for liquid hydrogen, polyethylene, aluminum, and lead is given in figure 3.

Low and to the left on figure 3 the curves are parallel, at a $45^{\circ}$ slope, and at the same height relative to one another that they are on range energy diagrams like figure 2. In this region the radius r effectively is approaching infinity and the low density materials are most efficient. For values of the Loading Index greater than approximately $0.01 \text{ gm/cm}^3$, however, (above energies of 40 Mev for a 4 ft. diameter sphere) geometry becomes important, and above $L_i \gtrsim 1 \frac{gm}{cm^3}$ (above $E \approx 500$ Mev for a 4 ft. sphere) the use of lead instead of liquid hydrogen, for example, can reduce shield weight by more than an order of magnitude.

That geometrical effects may indeed be of practical, not just academic interest may be inferred from the following examples taken from the literature. Using the 90 cm. inside radius chosen as representative in reference 15 and the particle energies considered appropriate therein for the May 1959 and February 1956 solar flares (275 and 1440 Mev, respectively), we find corresponding values of the Loading Index of 0.227 and 4.115 $\text{gm/cm}^3$. At the lower of these Index values, figure 3 shows the optimum material for

the May flare to be slightly higher on the atomic number scale than poly-
ethylene (Robey's choice of carbon is probably about the best that can be
done). For the February flare, however, (although the chart is quantitatively
not accurate at the high energies involved) figure 3 gives lead as the lightest
shielding material, and indeed calculations neglecting secondary effects
confirm that the use of lead would save 166,000 kgms. (44%) compared to
the carbon shield cited.

Evidently, even for the simple case of a one-material shield and a
spherical shape, geometrical effects need to be considered, and the Loading
Index is helpful in their evaluation.

Isotropic particles, a combination of materials, and a spherical shape. - Between
values of the Loading Index of 0.02 and 0.1 $gm/cm^3$, approximately, the over-
lapping character of the curves for liquid hydrogen and polyethylene suggests
the probability that a shield made by combining the two materials would weigh
less than one made of either material alone. Indeed, because of the extraordinary
stopping power of hydrogen, the possibility would seem to exist that the efficient
region of application of the combination liquid-hydrogen, polyethylene shield
may extend below and to the right of the "low" point defined by the $(CH_2)_n$
curve of figure 3.

An enlarged plot of the region of figure 3 under consideration is given in
figure 4. The curve for liquid hydrogen is identified by long dashes; that for
polyethylene by short dashes. Also plotted on figure 4 is a curve calculated
for a composite liquid-hydrogen, polyethylene shield optimized by the procedure

given in Appendix B (short and long dashes), and a section of the curve for

aluminum (the solid curve). As was anticipated, between the "low" points

of the curves for liquid hydrogen and polyethylene the composite is indeed

lighter than either material alone. The fact not so readily anticipated but

clearly brought out by the plot is that there is <u>no</u> region in which polyethylene

alone is lightest, for the composite curve is the lower until a heavier element

(in the illustration, aluminum) becomes more efficient than either $(CH_2)_n$ or

the composite.

Similar comparisons may be made for other combinations of materials,

and the most effective and their ranges of application defined, by means of

the Loading Index.

<u>Two-dimensionally isotropic particles</u>. - Two-dimensional isotropy, as

suggested by Singer (ref. 9), is of interest as an approximation of some

conditions in the geomagnetically trapped radiation belts. Similar directional

characteristics may possibly be of interest for some phases of solar flare

radiation. Applicable to two-dimensionally isotropic protons (see Appendix B)

is the same Loading Index $L_i = \dfrac{CE^{1.75}}{r}$ developed for complete, three-dimensional

isotropy. Shielding weight is generally less in the two-dimensional case,

however, as might be expected, and the magnitude of the weight difference

for various design conditions may now be measured from plots of $\dfrac{W}{V_{Ref}}$ vs. $L_i$

provided that proper interpretation is made of effects due to the difference in

shield shapes appropriate for the different directionalities.

An example of such a plot is figure 5, presenting curves of $\frac{W}{V_{Ref}}$ vs. $L_i$ for liquid hydrogen shielding for two- and three-dimensionally-isotropic protons. In order to compare relative weights for the two cases of directionality, the proper value of the "characteristic radius" r must be found for the shield for two-dimensional isotropy to correlate with the corresponding characteristic (spherical) radius for full isotropy. In the simplest case, in which a cylindrical shield is used for the two-dimensional case and the diameter is the same as that of the spherical shield for the three-dimensional case, the characteristic radii are equal and weights of each may be measured directly at the same value of the abscissa from the values of the ordinates of the two curves.

For equal volumes to be shielded, an infinite variety of cylindrical shield shapes, ranging from long, small-diameter shields to short, large diameter rings may be compared with a spherical shape.
For equal volumes

$$\frac{4}{3} \pi r^3_{Sph} = \pi r^2_{Cyl} \ell_{Cyl} \tag{5}$$

where

  r    radius, [cm.]

  $\ell$    length, [cm.]

Sph, Cyl refer to the sphere and the cylinder, respectively. The characteristic radius for the cylindrical shield is evidently $\sqrt[3]{\frac{4}{3}\left(\frac{r}{\ell}\right)_{Cyl}}$ times the radius of the comparable spherical shield, and the value of the Loading

Index for the sphere (for isotropic radiation) must be divided by $\sqrt[3]{\dfrac{4}{3}\left(\dfrac{r}{\ell}\right)}_{Cyl}$ to give the abscissa for the comparable cylindrical shield (for 2-dimensional isotropy) on a plot such as figure 5.

For example, suppose that a volume equivalent to that of a 100 cm. radius sphere is to be shielded by liquid hydrogen from 100 Mev protons. For the isotropic case

$$(L_i)_{Sph} = \frac{CE^{1.75}}{r_{Sph}} = \frac{0.0011(100)^{1.75}}{100} = 0.0348 \frac{gm}{cm^3} \tag{6}$$

and from figure 5 at this value of $L_i$

$$\left(\frac{W}{V_{Ref}}\right)_{Sph} = \frac{W}{\frac{4}{3}\pi(100)^3} = 0.16 \frac{gm}{cm^3} \tag{7}$$

and

$$W_{Sph} = 670,000 \text{ gm} \tag{8}$$

Let us compare this weight with the weights required to shield two-dimensionally isotropic particles with three cylindrical shapes - first a cylinder of equal radius to the sphere, and then ones one-tenth and ten times that value. For the same radius

$$(L_i)_{Cyl} = (L_i)_{Sph} = 0.0348 \frac{gm}{cm^3} \tag{9}$$

and from figure 5

$$\left(\frac{W}{V_{Ref}}\right)_{Cyl} = 0.08 \frac{gm}{cm^3} \tag{10}$$

or

$$W_{Cyl} = 335,000 \text{ gm}$$

which is one-half of the weight of the spherical shield for isotropic particles. In general, if the cylindrical shield is required to have the same radius as

14

the spherical shield, comparison of the curves of figure 5 shows that shielding for two-dimensional isotropy varies from 2/3 of the weight required for three-dimensional isotropy at low values of $L_i$ to a very small fraction of the weight at the high values of $L_i$ for which geometrical considerations are of prime importance.

Returning to the example, we find that for the cases in which the cylindrical radii are one-tenth and ten times the spherical radius

$$(L_i)_{Cyl_{r/10}} = \frac{0.0348}{\sqrt[3]{\frac{4}{3}\left(\frac{10}{133.3}\right)}} = 0.075 \ \frac{gm}{cm^3} \tag{11}$$

and

$$(L_i)_{Cyl_{10\ r}} = 0.01615 \ \frac{gm}{cm^3} \tag{12}$$

respectively, for which figure 5 gives

$$\left(\frac{W}{V_{Ref}}\right)_{Cyl_{r/10}} = 0.22 \ \frac{gm}{cm^3} \ , \quad W = 920,000 \ gm \tag{13}$$

and

$$\left(\frac{W}{V_{Ref}}\right)_{Cyl_{10\ r}} = 0.0365 \ \frac{gm}{cm^3} \ , \quad W = 153,000 \ gm \tag{14}$$

Evidently the lightest shield for two-dimensional isotropy is a large, thin ring, not a small tube. It is also evident that shielding weight for two-dimensionally isotropic particles can vary from somewhat more than to substantially less than the weight of similar spherical shielding for isotropic particles. The magnitude of the weight difference in any case can be determined from curves such as those of figure 5 if proper cognizance is taken of the significance of the "characteristic radius" employed therein.

Uni-directional particles. - The same Loading Index $L_i$ is also applicable (see Appendix B) in the case of uni-directional particles, again if proper interpretation is placed upon the meaning of "characteristic radius". Obviously in the uni-directional case even more than for the two-dimensional one, the weight of shielding for a given shielded volume can be changed at will by changing the shape - as from a pancake broadside to the radiation to a pencil pointed toward it.

For a simple spherical volume to be shielded, weights for various particle directionalities can be compared directly (as before) at given abscissa values on a plot such as figure 6. For example, the factor 4 difference to be expected between the isotropic case and that for uni-directional particles (the ratio of exposed surface areas of a disk and a sphere of equal radii) is found directly at low Index values where the curves are parallel. As emphasized in the derivation in Appendix B, however, the location of the curve for the uni-directional case depends entirely on the shape to be shielded, and this factor 4 applies only to a spherical volume.

Application of Loading Index to Evaluation of Active Shielding

Curves similar to those presented for passive shielding in figures 3 - 6 are also useful to assess active shielding systems. Precautions must be taken in using them for this purpose, however - perhaps more thoughtful precautions than those indicated in the preceding section to allow for shape effects with passive shielding - as the following discussion suggests.

16

(1) Precisely the same form of Loading Index derived for passive systems $\left(\dfrac{CE^{1.75}}{r}\right)$ is not generally directly applicable to active systems, to the extent that differing combinations of E and r for the active system which produce the same value of $L_i$ will usually not lead to a corresponding unique value of $\dfrac{W}{V_{Ref}}$ . Hence, while the weight of an active design may be evaluated relative to passive shielding as a plotted point on a graph such as figures 3 - 6, such an evaluation shows nothing about the location of the point for different values of E and r (even those which give rise to the same value of $\dfrac{CE^{1.75}}{r}$ ).

(2) Accordingly, to be general an evaluation of an active system should consider the effect of changes in both E and r to yield a plot for a family of active shields, representing, for example, weight variations with energy for constant radius, or the corresponding variation with radius for constant energy. These families of curves may then be compared with corresponding families for a passive shielding system, represented by a unique curve on a plot of $\dfrac{W}{V_{Ref}}$ vs. $L_i$. This type of comparison will be used to evaluate active shielding in this report.

(3) If the energy range under consideration extends appreciably above 400 Mev, the same precautions should be taken in evaluating passive shielding as suggested for active systems in (2) above. For protons above 400 or 500 Mev the $^{1.75}$ power law used to derive $L_i$ is not a

17

good approximation for range-energy relationships even on the

simple basis of attenuation by non-nuclear interactions. The higher

the energy, the poorer the approximation, and curves for evaluation

of shielding efficiency need to be identified by energy and radius.

Thus the advantage of the Loading Index is lost, and the possibility

of the derivation of a new Loading Index applicable to the high energy

range should be considered if extensive studies are undertaken in

that range.

Extension of Loading-Index Approach to Other than Mono-energetic Particles

The Loading Index has been derived herein with the implicit assumption

that one energy level E is representative of the design condition for incident

protons, although the fact is of course that the ionizing radiation in space is

not mono-energetic but consists of a spectrum of energies. Because of the

merit of the relative simplicity of the expression $\dfrac{CE^{1.75}}{r}$ , it is not proposed

to generalize further the Loading Index identified here as $L_i$. Instead in

this section it will be shown that the simple Loading Index concept can be

readily extended to account for other than mono-energetic particles.

For example, consider the case of solar flare protons. Various

expressions have been proposed to approximate the spectrum of energies

representative of these particles, typical of these being (from ref. 3)

$$N = \frac{X}{E^n} \tag{15}$$

where

N    number of particles (per $cm^2$ per sec. per ster-radian) of energy $> E$

18

$\chi$   a constant (suggested in ref. 3 as $3 \times 10^{13}$)

n   a constant (suggested in ref. 3 as 6)

Solving for E

$$E = \left(\frac{\chi}{N}\right)^{1/n} \tag{16}$$

Suppose this value of E substituted in the expression for $L_i$, so

$$(L_i)_{Spectrum} = \frac{C\left(\frac{\chi}{N}\right)^{1.75/n}}{r} \tag{17}$$

We now have a Loading Index applicable to a spectrum of energies and useful for measuring the weight of shielding required to reduce the particle flux to N. Notably, however, a similar result could have been achieved by the use of an effective value of E in the expression $\frac{CE^{1.75}}{r}$. This use of an effective value of E in the numerator of the expression is comparable to the use of a "characteristic radius" in the denominator, and is the approach recommended for generalizations to cases for other than mono-energetic particles.

# FIRST APPROXIMATION EVALUATIONS OF ACTIVE SHIELDING SYSTEMS

## Introduction

At the outset of this investigation, it was recognized that the path to a solution of the shielding problem would be a long one. Accordingly the step-by-step documentation of both pitfalls and encouraging prospects seemed desirable. To a degree this section reproduces that documentation, beginning with discussions of the simplest possible shielding systems in the most elementary terms. In the reproduction of the first studies (ref. 17-18) for inclusion here some effort has been expended to up-grade them in the light of present knowledge, as by the use of the more general appraisals permitted by the Loading-Index approach (ref. 19). Similar up-grading has been done in other areas in consonance with results generated as the study proceeded.

The studies are presented in the order in which they were carried out, progressing from the first look at shielding for uni-directional particles through the two-dimensionally isotropic case to shielding for isotropic particles (ref. 20).

## Uni-directional Particles

The simplest possible problem to consider assumes that the energetic charged particles to be shielded are approaching the space vehicle in straight, parallel lines, and that the vehicle is precisely oriented so that the shield is interposed like an umbrella between the particles and the space to be shielded.

Because of its simplicity, this case makes a useful starting point regardless of what the relationship may be between it and the realities of the ionizing radiation in space. Four approaches will be evaluated for this case:

(1) Umbrella-like disks of various materials (passive shielding) to provide reference weights for comparison with active shielding systems.

(2) A solid ring of permanent magnet material to retard and divert the particles.

(3) An electrostatic shield in the form of a hollow thin-walled cylinder with a center electrode to perform in the same manner as the magnetic shield.

(4) A combination of magnetic, electrostatic, and passive systems.

The shape of the volume to be shielded was assumed to be spherical for simplicity.

Passive shielding. - In the ideal situation in which the shielding disk is perfectly alined between particles and space to be shielded, shield weights are in direct proportion to those given by the usual range-energy relations (ref. 21). On a plot of $\frac{W}{V_{Ref}}$ vs. $\frac{CE^{1.75}}{r}$, the weights of these disks are represented by parallel straight lines of 45° slope, with hydrogen the lightest (see figure 7). The greater the allowance for misalinement, the more umbrella shaped the shield becomes, and, particularly at high values of the Loading Index the greater the weight penalty. The effect of misalinement is shown on figure 8 for the four materials considered in figure 7 and for an assumed angle of misalinement of 1/2 degree. The curves on this figure are

21

now reminiscent of those for more complex directionalities (such as fig. 3), crossing one another as they progress to the higher values of, $\dfrac{CE^{1.75}}{r}$ .

In the plot of figure 8 advantage is taken of the properties of the Loading Index to shrink families of energies and sizes into single curves. Thus a general representation of shield weights is provided for all values of r and E (up to $E \approx 400$ or 500 Mev) for the assumed 1/2 degree misalinement.

This plot and that of figure 7 for perfect alinement will be used as bases for comparison for the active systems investigated.

Permanent magnet shielding disk. - The concept of magnetic material to divert incident protons has been proposed by Dank (ref. 10) and Hughes (ref. 22). Following Dank's suggestion, the model evaluated here uses a ring magnet of Alnico V material as sketched in figure 9 to divert the incident particles away from the (spherical) space to be shielded. Calculations were made of the minimum weights required for active shielding of this type on the basis of the following assumptions:

(1) The residual magnetic flux in the Alnico V material was 12,400 gauss, and uniform throughout the material.

(2) The incident uni-directional protons were both retarded and diverted by the magnetic ring, and the resultant path within the Alnico V material was approximated by the equations given in Appendix A, leading to the angles of diversion $\alpha_{exit}$ plotted in figure 10. After passage through the magnet, the protons were assumed to continue in straight lines.

(3)  An approximate expression was used for the weight of mast

required to support the ring magnet, namely

$$W_{Mast} = 0.00002\,rH^2 \tag{18}$$

where

$W_{Mast}$  mast weight, [gm.]

r  radius of shielded volume, [cm.]

H  mast height, [cm.]

In order to minimize weight, the thickness of Alnico V was tapered as

required in the radial direction to provide just enough attenuation and

deflection of the particles so that at the given energy and mast height

they would just miss the space to be shielded.

The results of these weight calculations are plotted in figure 11 for the

ideal case in which there is no angular misalinement between the incident,

uni-directional particles and the axis of the shielding system.  Figure 11

shows that for high energy particles and for small radii to be shielded

there is indeed some potential weight saving for this active shielding concept,

provided that the required perfection of alinement can be maintained.

The potential weight saving depends critically, however, upon the

perfection of alinement of particles and shield.  Calculations made for a

one-half degree angular misalinement showed such small differences from

the weight required for passive (iron) shielding that no attempt was made to

pictorialize them upon a plot such as that of figure 8.  The only weight savings

achieved through the magnetization in this case were those made possible by

slight reductions in thickness at the edges of the "umbrella" where those

particles which would almost miss the shielded volume anyway could be diverted by the magnetic flux the little more required.

Electrostatic shielding. - An electrostatic shielding system analogous to the permanent magnet system just considered may be made in the form of a hollow, thin-walled cylindrical shell (the negative electrode) of approximately the diameter of the sphere to be shielded, concentric about a small diameter cylinder (the positive electrode). This system is sketched in figure 12.

To divert protons incident parallel to the axis of the cylinder, the length required for such an electrostatic shield is plotted in figure 13 against the voltage applied between inner and outer electrodes. As before, two cases are considered: (1) perfectly axial protons, and (2) a misalinement of one-half degree. The equations used for the calculation of the curves of figure 13 are given in Appendix A.

In order to evaluate the efficiency of such a shielding system, assumptions must be made regarding the weight of material required to provide the electrode surfaces in space. Calculations of the (collapsing) hydrostatic pressures created by the potential difference between the center electrode and the outer shell electrode reveal that they are generally small, of the order of

$$p = (5.65 \times 10^{-11}) \frac{V^2}{r} \tag{19}$$

where

$p$    inward-acting pressure on shell electrode, $[\frac{gm}{cm^2}]$

$V$    applied potential, $[\frac{volts}{cm}]$

$r$    radius of shield, $[cm.]$

24

Even these small pressures could collapse a flimsy shell, however, so the assumption is made that the shell thickness must be proportional to the pressure, with a value equivalent to that giving a stress in aluminum of 10,000 psi. Assuming the same weight for the center electrode as for the mast for the Alnico V shield, we develop the following expression for total weight of electrode -

$$W_{Elect.} = (2rH \times 10^{-5})(H + 2\pi V^2 \times 10^{-11}) \tag{20}$$

Weights of electrodes were calculated from this expression for both perfectly alined and 1/2 degree misalined uni-directional particles, with the results plotted in figures 14 and 15. It is clear from these figures that for uni-directional particles the weight of electrodes for electrostatic shielding is negligible compared to passive shielding. Furthermore, unlike the permanent magnet shielding considered, the electrostatic system can accommodate some misalinement without undue weight disadvantage.

Weights required for the generation and maintenance of the deflecting voltages are not included in the calculations leading to the curves of figures 14 and 15. Indeed these curves represent a kind of lower limit to the system weight which would be actually required - as a first step in evaluation. If, for example, these curves had fallen above the curves for passive shielding, electrostatic shielding could be dismissed as not worth more detailed study. Since they do fall so far below, further study is warranted, and some of the effects of additional weights required by practical considerations will be investigated in subsequent sections herein.

Combination active-passive shielding systems. - In order to investigate the possibility that combination active-passive shielding systems may be more effective than either system alone, two examples will be considered: (1) an Alnico V magnet deflector behind a polyethylene retarder, and (2) an electrostatic field combined with a series of polyethylene screens to provide a combined retarding - deflecting medium.

The reasoning which suggests that a combination system may be effective goes as follows. Because of the high velocity of the incident protons, they pass through the deflecting field in such a short time that there is little opportunity for them to be accelerated away from their initial paths. Hence, if properly retarded, they may perhaps be more effectively deflected. That such increased effectiveness does not obtain is not apparent in advance, but is illustrated by the chosen examples.

First for the combination Alnico V - $(CH_2)_n$ system the high energy range (500 Mev) is selected as representative of the regime showing the greatest potential for the permanent-magnet system (see fig. 11). Then thicknesses of polyethylene sufficient to decelerate the protons to 200 and 100 Mev are interposed between the incident, uni-directional particles and the magnetic disk of figure 9, and the proportions of the mast and magnet are optimized as before with the results plotted on figure 16.

The top curve on figure 16 represents the weight of polyethylene (passive) shielding alone; the bottom curve that of the Alnico V system alone for 500 Mev, uni-directional protons. The two intermediate curves are for the combination system. Both of these latter curves show only slight weight

savings over the simple polyethylene passive system, even for the higher values of the Loading Index $\frac{CE^{1.75}}{r}$ . At the lower values of the Index the curve for the combination system with the thicker polyethylene cover actually crosses above that for the $(CH_2)_n$ alone. There is no evidence of advantage for the combination compared to the active system by itself.

For the second example, utilizing polyethylene screens disposed along an electrostatic field to simulate a low density or foamlike retarding-deflecting material, calculations were made of voltage-proportion relations for various "foam" densities (fig. 17). The employment of these results in calculations of minimum weight shields quickly demonstrated that the appreciable voltage reductions shown by the dashed curves compared to the solid curve on figure 17 are never practically accessible, requiring so much retarding material that the weight is excessive, and the optimum is always back near the solid (no retarding material curve). Only for very thin, well-separated screens (as for example those giving an effective density 0.001 times that for solid polyethylene) is the concept which the example was supposed to evaluate approximated, and even such a low density material does little other than to decrease the effectiveness of the system (see fig. 18). Because the results shown on figure 18 for $\eta = 0.001$ were so unpromising, no further combinations were evaluated.

## Two-Dimensionally Isotropic Particles

Introduction. - Thus far we have considered the most elementary shielding concepts with the simplest possible geometry of incident particles. These first studies have shown: (1) little promise for combined active-passive

27

systems, (2) only a minor potential for an active, permanent magnet system even if the most ideal directional conditions exist. At the same time, the potential on the elementary basis for electrostatic diversion of protons has appeared substantial, and worthy of investigation on a basis bearing more resemblance to reality. Accordingly, in this section electrostatic shielding will be evaluated further for the somewhat more realistic situation of two-dimensionally isotropic protons.

Whether the energetic particles in space are at all directional or really essentially isotropic is still to some extent an open question. The protons trapped by the earth's magnetic field are indeed directional to the extent that they spiral about the magnetic lines of force. Protons produced by solar flares, however, are not known to follow any such well-ordered trajectories. At the outset, at least, they apparently have some directional characteristics, for: (1) flares occurring on the side of the sun away from the earth generally do not produce the phenomena associated with solar-flare protons near the earth (ref. 23); (2) many flares observed on the earthward side of the sun also produce no proton events near the earth (ref. 23). Thus, the possibility exists that the protons may stream out together in some general direction (rather than all directions) from the sun - a possibility compatible with observations (1) and (2). By the same token, (1) implies that the particles are not reflected back past the sun as by some kind of magnetic mirror. Hence the protons may be confined to a spherical (or cylindrical) angle of something less than $2\pi$ ster-radians (or $\pi$ radians) opening out from the sun. Isotropy of particle motion within this angle appears somewhat

incompatible with confinement of particles therein.

That the local directionality of the geomagnetically trapped protons is not badly represented by two-dimensional isotropy has been suggested by Singer (ref. 9). In this case, the particles are assumed to move in planes perpendicular to the magnetic lines of force; i.e., the lead angle of the spiral traced by their path is assumed small. Two-dimensional isotropy is also not incompatible with the noted observations of solar-flare effects; it contains as a special case uni-directional particles, and perhaps may be considered as a rough approximation for particles having partially random directionality over a spherical angle approaching $2\pi$ ster-radians and having a generally preferred direction away from the apex of that angle. Accordingly, two-dimensional isotropy is of practical interest for the Van Allen radiation belt environment, and may be of some (and even conceivably of major) interest for the solar-flare environment. Two-dimensionally isotropic protons are therefore assumed as the next design condition for the evaluation of electrostatic shielding, according to the model proposed in the following section.

Electrostatic shielding system considered. - The electrostatic shielding system investigated consists of three large flat circular-plate electrodes. The center plate (the positive electrode) is concentric with the sphere to be shielded. The other two plates (the negative electrodes) are parallel to the center plate and separated from it a distance approximately equal to the radius of the sphere. Thus, with the center electrode alined parallel to

29

the plane of motion of the energetic particles, they will be deflected away from the sphere no matter what their direction of approach. The electrodes must be proportioned to divert the incident protons at the given impressed electrostatic potential, and the electrode structure must withstand the force of attraction between the center and outer electrodes.

Assumptions and methods of computation. - For the purpose of this evaluation, rather conservative assumptions were made to design the electrodes. In the first place, as has been shown previously, a spherical volume to be shielded is not the most efficient shape to use for two-dimensional isotropy even for passive shielding - because it unnecessarily separates the deflecting electrodes, it is especially unsuited for the electrostatic diversion system under consideration. The assumption of a sphere to be shielded (rather than an edgewise disk) is approximately the same as an assumption of misalinement of an optimum shape with the plane in which the particles move. On the other hand, optimization of shape to be shielded for the electrostatic system appears more objectionable (and certainly less conservatively evaluates the active system) than to accept this fictitious misalinement. As will be shown, the conservatism used here in no way damages the general results achieved.

The second conservative assumption is that made regarding the structural weight required to support the electrodes. For simplicity each outer electrode is assumed made as a sandwich plate of tapering thickness, the weight of which is given by the formula

$$W_{Elect.} = 2.4\pi t_o (H^2 - 3rH - 12r^2) \tag{21}$$

30

where

$W_{Elect.}$ weight of one electrode, [gm.]

$t_o$ face thickness of sandwich at center of disk (aluminum

alloy), [cm.]

$r$ radius of spherical volume to be shielded, [cm.]

$H+r$ radius of disk, [cm.]

The weight of the center electrode is arbitrarily assumed to be one-half

that of the outer electrodes, because the forces acting upon it oppose and

cancel each other. The forces on the outer electrodes determine the value

of $t_o$ and the face thicknesses used here were calculated from the formula

$$t_o = \left(2.24 \times 10^{-9}\right) \left(\frac{HV}{\sqrt{r}}\right) \tag{22}$$

with

$V$ voltage gradient between center and outer electrodes, $\left[\frac{volts}{cm}\right]$

Other symbols as before

This formula, derived essentially to maintain the face stress at the

disk center below 50 ksi is again an arbitrary approximation. The reason

that it is considered to be conservative is that numberless ways are open

to the designer to alleviate bending stresses on the electrodes, as by external

braces. Hence the total electrode weight calculated here should be amenable

to reduction in practice. Once again the fact that this conservatism does not

hurt the end results will be evidenced by the results themselves.

Optimization of proportions of electrodes employing the assumed relation-

ships among voltage, size, and weights leads to unrealistically high values of

applied voltage. A more suitable evaluation procedure in this case accordingly

31

appeared to be to select arbitrary voltages and to determine the associated
sizes and weights. The results of this procedure are plotted on figure 20
for shielding 100 Mev protons, and the results of an inverse procedure in
which the voltage is restricted to 1,000,000 volts and the particle energy
is varied are plotted on figure 21.

Results. - Despite the several assumptions made in the development of the
evaluation procedure which led to the curves of figures 20, and 21, the
following conclusions can be drawn without equivocation from the results:

(1)  The potential weight saving of the active electrostatic system
     compared to passive shielding is substantially less for two-
     dimensional isotropy than it appeared to be for uni-directional
     particles.

(2)  Within the range considered, the potential weight saving for the
     active, electrostatic system increased as the applied voltage
     increased, as the radius of the volume to be shielded increased,
     and as the energy of the particles to be shielded increased.

(3)  Effective electrostatic shielding will require the maintenance of
     voltages on the electrodes of approximately 1,000,000 volts
     or higher.

## Isotropic Particles

Introduction. - The development of techniques for producing niobium-tin wire
of sufficiently high quality to make possible the attainment of superconductivity

in high-intensity magnetic fields (ref. 12) opens up interesting possibilities for active, electromagnetic shielding for isotropic protons. As vehicle geometries and particle energies vary, the appropriateness of such shielding varies, and how great this variation is, and indeed just how effective the superconducting, electromagnetic approach may be should be evaluated.

An excellent first cut at such an evaluation has been made by Levy (ref. 11), utilizing an unconfined magnetic field produced by a toroidal shell which serves as both superconductor and shielded volume. Levy's evaluation yielded several substantial contributions, as follows:

(1) The unconfined-magnetic-flux, superconducting toroid becomes most attractive when the particle energy to be shielded is high and the volume to be shielded is large.

(2) The weight of insulation needed to maintain the temperature of the superconducting material as required near absolute zero is negligible compared to the weights of the other parts of the system.

(3) The major portion of the weight in this active shielding system is that of structure required to support the stresses induced by the enormous electrical currents in the toroidal shell.

Because induced stresses vary as the square of the current, a shield configuration requiring less current to protect the shielded volume than needed to produce the simple, dipole-like shielding field considered by Levy should be of less total weight. One such configuration is shown schematically in figure 22. With this configuration the magnetic flux is confined within the superconducting coil windings, external to the volume to be shielded. The

entire diversion of the incident, energetic particles accordingly also takes place within the coils essentially in the manner suggested by Hughes (ref. 22). As will be shown, this concentration of magnetic flux leads to order-of-magnitude reductions in shielding currents required and, consequently, to the practical elimination of current-induced stresses.

With the configuration of superconducting $Nb_3Sn$ shown in figure 22, and with virtually the same assumptions as in reference 11, calculations have been made of minimum shielding weights required for isotropic particles of various energies, and for a range of volumes to be shielded. The results are compared herein with those for Levy's unconfined-flux, toroidal-shell shield as well as with passive shielding. In these calculations a few restrictive assumptions and approximations were made for reasons of necessity and expediency. In the following section these assumptions and approximations are described so that their influence upon the results can be assessed. In general, for the purpose of evaluation of system potential, the calculations should yield answers of the same (or greater) validity as those in previous studies. Areas in which further resolutions of unknowns are desirable will be discussed in the section "Results and Discussion".

Shielding concept. - Superconducting $Nb_3Sn$ is supposed wound in spirals about the hollow volumes shown in figure 22, to produce confined, uniform magnetic fields surrounding a five-sided (essentially spherical) enclosed shielded volume. Thus a proton penetrating through the outside layer of insulation and $Nb_3Sn$ is caused to take a circular path whose radius depends upon the particle energy and magnetic flux intensity. Because particles are

34

assumed to approach from all directions, coil sizes and fluxes must be chosen to prevent penetration of the shielded volume for the worst angle of incidence; these choices will be detailed in the paragraph headed "Optimization".

As shown in figure 22, the shield is divided into five sections: an "equatorial" band which is essentially toroidal, two polar caps which are hollow conical frustums with central posts at the poles, and two intermediate sections. The division into five sections is an arbitrary one which results in a number of essentially radially-disposed webs or posts of $Nb_3Sn$ which serve only to complete the circuit between inner and outer surfaces. Although perhaps somewhat more efficient winding configurations might be found, the weight of material in these radial elements (determined to provide sufficient conducting material) is generally not a substantial enough fraction of the whole to be of prime concern. Nonuniformity of winding at different radii is neglected.

Particularly at the lower particle energies and larger winding thicknesses, a not insignificant part of the shielding is contributed by deceleration of the particles during their passage through thermal insulation and superconducting material. Account has been taken of this deceleration in the manner described under "Optimization". To evaluate the effectiveness of a combined active-passive shield like this for isotropic particles, calculations also were made for the case in which various thicknesses of polyethylene were added on the outer surface to provide additional deceleration, as will be described.

Current densities. - Allowable superconducting current densities were selected to correspond with the best results described in the pioneering work reported in reference 12. Allowable current was assumed to vary with magnetic flux according to the relationship

$$\bar{i} = \frac{10^{10}}{B} \qquad (23)$$

where

$\bar{i}$    current density, $[\frac{amps}{cm^2}]$

$B$    magnetic flux density, $[gauss]$

Variations in allowable current densities with size of niobium-tin wire were neglected.

Magnetic flux densities. - Magnetic fluxes were calculated, on the assumption of unit permeability, from the elementary coil equation

$$B = \frac{4\pi}{10} (\bar{i} \ b) \qquad (24)$$

where

$b$    wire thickness (square cross-section wire), $[cm.]$

Optimization. - The optimization procedure has as its objective the determination of the combinations of $Nb_3Sn$ wire thickness, and spacing between inner and outer coil walls which provide minimum-weight protection at given particle energies and shield sizes. To find these minima, the following steps were taken:

(1) The "worst" angle of incidence for the particles was found for each energy and $Nb_3Sn$ wire thickness. At the worst angle, the maximum spacing between inner and outer shield walls (hence the greatest

36

system weight) is required to bring the proton just to rest at (and usually nearly tangent to) the inner shield surface. To find the spacing, the trajectory equation of Appendix A for K = 0 (no retarding medium between inner and outer walls) was employed as follows:

$$x = v_o M (\sin \alpha_{Exit} - \sin \alpha_o) \qquad (25)$$

where

$x$      spacing

$v_o$      particle velocity after passing through the external insulation and outer wall, $[\frac{cm}{sec}]$

$M$      proton mass/charge ratio divided by the magnetic flux intensity, $[sec]$. (See Appendix A)

$\alpha$      angle of proton path to normal $[deg.]$. The value of $\alpha_{Exit}$ was chosen to make this thickness of inner wall plus insulation at that angle just sufficient to stop protons of velocity $v_o$. (Except for the thickest coils $\alpha_{Exit}$ is not very different from $90°$.)

(2) For each particle energy and selected shielded volume, the total weight of shielding (plus insulation, of weight as calculated in ref. 11) corresponding to the spacing found above was plotted against the thickness of $Nb_3Sn$ used, and the minima were picked from these plots.

Stresses. - Stresses induced in the coils by the currents circulating therein are of two primary types: (1) compressive stresses induced by the currents flowing parallel to each other in successive coil turns, (2) tensile stresses induced within

37

each individual turn by the oppositely flowing currents (or components thereof) across the coil.

Compressive stresses were calculated from the formula available from many sources (for example, ref. 24)

$$\sigma = -2\left(\frac{I}{b}\right)^2 \times 10^{-5} \tag{26}$$

where

$\sigma$     stress, $[gm/cm^2]$ (minus sign indicates compression)

I     current per wire, $[amps]$

Integration around a loop gives a similar expression for the hoop tension induced in a circular coil. The only difference turns out to be a factor - 1/2, and the equation is

$$\sigma = \left(\frac{I}{b}\right)^2 \times 10^{-5} \tag{27}$$

For the current densities assumed herein, formulas (26) and (27) yield maximum stress values at the thickest windings, amounting to compressive stresses (tending to squeeze adjacent coils together) of approximately - 280 $kgm/cm^2$ and tensile stresses tending to pull each turn of the coil apart of approximately +140 $kgm/cm^2$. The niobium-tin can perhaps withstand the compression by itself. The hoop tension could be easily carried if desired, for example, by less than 0.012 cm. thickness of aluminum-alloy sheet wrapped around the windings. This is a weight increase of less than 2% in the worst case, and so the weight of structure required to carry current-induced stresses has been neglected in the present study.

In addition to primary stresses, local secondary stresses or stress concentrations occur, as for example those required to hold the windings on

the radially disposed webs. Because the secondary stresses are of a local nature, they are assumed to require only local reinforcement, and the weight of material needed therefore is neglected here.

Results. - The results of the calculations are presented and compared in figures 24-25, but first in figure 23 Levy's results (ref. 11) are re-presented on a Loading Index basis to establish a frame of reference within which to measure the confined-flux system. Figure 23 re-emphasizes Levy's conclusion that (neglecting secondaries) a superconducting toroid is more effective than passive shielding only at very high particle energies (>500 Mev), and at large shielded volumes. (Quantitatively the curves for passive shielding, it should be remembered, are slightly in error at these very high energies, but not substantially enough to change the picture.)

The active, "contained-flux" system considered here is shown in figure 24 to become competitive with passive shielding at lower energies than the unconfined-flux system. As before, the active system becomes more attractive as particle energy and shielded volume increase, surpassing an order-of-magnitude decrease in weight in large sizes at 500 Mev.

# ADVANCED STUDIES

Studies pertinent to refinement of the evaluations of active and passive

systems for shielding space vehicles from ionizing radiation, and to the

determination of directions toward improved deflecting field configurations

for active shielding have been initiated, and progress thereon is reported

in this section. These studies are in two areas: the first considers the

secondary radiation associated with the nuclear cascade produced by

highly energetic protons incident on shield material; the second investigates

the creation by electrostatic fields of forbidden zones for isotropic charged

particles. Here the appropriateness of each study to the problem at hand

is briefly reviewed, and then progress on the investigations is described.

## Secondary Radiation from Highly Energetic Incident Protons

Introduction. - Throughout this report evaluations of various approaches

to the shielding problem have used as a basis the weights of passive

shielding calculated from available range-energy curves (as in fig. 2) for

stopping incident protons by electromagnetic interactions within the

shielding material. This basis was used, even though its limitations were

recognized, for want of curves which adequately describe the attenuation

of incident radiation via nuclear as well as electromagnetic interactions, the

production of secondary radiation and its attenuation, and the evaluation of

the effectiveness of the resultants.

Even in the absence of such better attenuation curves, some qualitative

assessment of the influence of nuclear interactions on the evaluations of

shielding systems can be made. In the first place for low incident energies (less than about 100 Mev) the nuclear interactions are relatively unimportant, and available range-energy relations are probably adequate to provide a basis for evaluation. In this range, however, as shown elsewhere in this report, there is the least need for active shielding because simple passive shielding is relatively effective. For higher incident energies - energies appropriate to solar-flare protons and for which active systems may be desired - the evaluation process is certainly complicated by the secondary effects.

Complications arise particularly because at high incident energies a critical range of material thickness exists for which the biological effects of radiation emerging from the shield may be worse than from the incident radiation itself, i.e., as shield thickness is increased from zero the radio-biological effects behind the shield increase to a maximum before the thickness becomes great enough so that the over-all effects are attenuated.

Active shielding systems, if effective enough so that they are of less weight than passive shielding, may fall directly into this regime of material thicknesses for which dosage from secondary radiation is maximized. Thus, even though active systems may divert the primary particles from the shielded region and so completely eliminate the dosage from them, during the diversion process the particles may encounter just that thickness of material which generates the greatest secondary dose. Two important questions obviously arise: (1) Quantitatively what are the secondary dosages, and how do they vary with material, thickness, and incident energy? (2) Is the radiation scattered in all directions, or does it follow the directions of

41

the incident particles? (The latter question is most pertinent to the relative evaluations of active and passive systems, inasmuch as active systems may not simply interpose their mass between incident particles and shielded volume.) The cosmotron experiment described in Appendix C provides some answers to both of these questions.

Preliminary results and discussion. - The primary result so far evident from the data obtained from the 3 Bev experiment described in Appendix C is that the incident proton beam and the secondaries therefrom are still well collimated after passage through substantial thickness of material. Further, a first tentative evaluation of the secondary effects by interpretation from the measured production of $Na^{24}$ in the aluminum foils suggests that for this energy at the worst thickness secondary radiation may multiply dosage behind the shield by a factor three. At substantially larger thicknesses, on the other hand, (thicknesses approaching the range calculated from simple range-energy relations) the total attenuation of both primary and secondary radiation is indicated to be appreciably greater than would be expected if nuclear interactions are neglected.

The lack of scattering evidenced in the experiment may be an effect which is somewhat favorable for active shielding systems, if their masses can be lumped into regions such that primary directions of particle incidence miss the shielded volume. A simple, if not necessarily realistic, illustration of the point would be the electrostatic system of figure 19 in which the only particles penetrating the disk electrodes do so in directions which are aimed away from the shielded volume. By contrast, even for the directional

particles assumed, a passive shield can only channel any unattenuated radiation into the volume which it is trying to protect.

The multiplication of dosage at critical thicknesses has worrisome implications for both active and passive systems. Substantial multiplication factors equal to or greater than the tentative value of three of this experiment, are to be expected only for the most energetic particles, - either galactic cosmic rays or those few solar flare protons in the Bev or greater range encountered in the most rarely occurring giant events. Discounting the latter because of their infrequent occurrance, we are still confronted by the cosmic ray problem, and the danger that with multiplication factors of this magnitude or greater the accumulated dosage therefrom may be serious. Differences between active and passive systems in this situation are not clear. The active systems may operate below the most critical thicknesses; the passive systems may be above them. At this stage the only positive indication is that more conclusive evaluations of cosmic ray dosages behind shields of various thicknesses are needed.

Finally the substanial attenuation produced by nuclear interactions at high energies in thick shields is favorable to passive shielding designed for particles in the Bev range. If such shielding (for the most rare giant flare) is required, more accurate evaluations of the relative weights of active and passive systems therefor are desirable than those made here. Appreciable differences in the comparisons because of such attenuations by nuclear interactions are not expected up to about 500 Mev.

Introduction. - While the configuration of a system of electrodes to provide electrostatic shielding for directional energetic particles is conceptually straightforward (as in the cases illustrated in figs. 12 and 19 for example), a correspondingly effective configuration for isotropic particles is not straightforward at all. Electrostatic shielding is known to be capable of providing "forbidden zones" for isotropic particles, but at least in the simplest case the voltages required match the particle energies to be shielded (ref. 10). The difference between the voltages required with the models considered herein for uni-directional and two-dimensionally isotropic particles and that of reference 10 for isotropy is that in the first case the particles were just diverted enough for their initial paths to miss the shielded volume, whereas in the latter case the particles were repelled, i. e., even, if need be, caused to reverse direction. Evidently a configuration using other than this "brute force" repulsion is desirable.

In order to provide a basis for the development of diversionary rather than repulsive electrostatic shielding fields, a mathematical study was made (see Appendix D) of a series of field configurations of gradually increasing complexity. The scope, results and implications of this study are presented in the following sections.

Scope. - The scope of this study of "forbidden zones" in electrostatic fields was limited to elementary arrays of point and line charges, in part because of complexities of analysis but also because, as will be shown, greater complexity in this direction is not justified. The problems considered

began with the case of two point charges, and grew from there to cover three and four point charges, a ring, and three line charges. The fact that in the actual case a spectrum of energies is encountered was also considered, and the flux reduction produced by electrostatic shielding for non-monoenergetic particles was evaluated.

Results and implications. - While the results of this field configuration study are essentially contained in the equations derived in Appendix D, the implications of these results perhaps become more clear if evaluated in terms of the simple spherical electrostatic shield previously considered (ref. 10). For the sphere, the surface voltage required to reject protons was shown numerically equal to the incident particle energy in electron volts. This corresponds to the limit of the case of two point charges (Case 1 (a) of Appendix D) as their separation $2c \rightarrow 0$. For $c = 0$ in equation (D-7), the equi-potential curve is given by

$$x^2 + y^2 = \frac{4}{a^2} \tag{28}$$

which is a circle of radius

$$r = \frac{2}{a} = \frac{2qq_1}{\frac{1}{2} Jv_\infty^2} = \frac{4qq_1}{2\left(\frac{1}{2} mv_\infty^2\right)} \tag{29}$$

where

$$\frac{1}{2} mv_\infty^2 = \text{incident particle energy, [ergs]} \tag{30}$$

$$J = 4\pi \epsilon_o m = m \text{ [in absolute electrostatic units ]}$$

Substituting $1.6 \times 10^{-6}$ ergs/Mev, and $4.8 \times 10^{-10}$ stat-coulombs (the

proton charge) for q we get

$$E = (300 \times 10^{-6}) \left( \frac{2q_1}{2/a} \right) \qquad (31)$$

where

E = particle energy rejected at radius 2/a, [Mev]

This agrees with the expression for the sphere in reference 10, with a

factor 2 difference to account for the fact that here there are two charges $q_1$.

Evidently, then, the "forbidden zone" here corresponds exactly to that

created in the "brute force" way in reference 10.

If now the two charges are allowed to separate, the "forbidden zone"

elongates into a "dog-bone" shape, and the pertinent question to be answered

is: "Does the shielded volume show any marked increases, indicative of a

favorable shape effect?" A qualitative answer to this question is afforded

by figure 26 in which the equi-potential curves are sketched for a series

of increasing separations of the charges. There is no suggestion in this

representation that any appreciable advantage is achieved by the changing

shape of the potential lines.

Perhaps even more discouraging is the case of three charges, positive

at the center and negative on the two outer "electrodes". The equi-potential

curve for this configuration superimposed on the circular one for no outer

electrodes (fig. 27) shows that the negative charges, rather than attracting

protons away from the center tend to reduce the over-all effectiveness.

Significant in this regard is the result of the investigation of flux

reduction for non-monoenergetic particles   Liouville's theorem, applied

(Appendix D) to the case of a large number of electrically charged particles

isotropically distributed with energy E moving in an electrostatic field, shows that the particle flux across a surface at a point P, where the potential is $\varphi^*(P)$, is $1 + \dfrac{\varphi^*(P)}{E}$ times the flux at the same point in the absence of the field. This result, depending solely upon the potential at P and not upon the shape of the equipotential surface or gradients created, indicates that "forbidden zones" of the nature investigated operate via the brute force repulsion mechanism rather than by diverting particles.

# RESULTS AND DISCUSSION

## Results

The results of this study are as follows:

1. The development of the Loading Index. - A new, general method of comparison of shielding systems of space vehicles for energetic particles has been developed. This method utilizes a "Loading Index" which incorporates the design conditions of particle energy and vehicle geometry. With the aid of this method, several approaches to the shielding problem have been evaluated, as follows.

2. The evaluation of active, permanent-magnet shielding. - Active, permanent magnet umbrella-like shielding has been found ineffectual even for the most favorable assumption (uni-directionality) of particle incidence. This ineffectivness, associated with the small path deflection angles induced during the brief passage of the energetic particles through the relatively weak permanent magnetic flux, was demonstrated by a lack of weight saving compared to passive shielding for even practically unrealistically small angular deviations from ideal uni-directionality of incident particles.

3. The evaluation of electrostatic shielding. - The weight of electrodes required for active, electrostatic shielding was found to be a function of particle energy and directionality, and of the size of vehicle to be shielded. For uni-directional particles the electrode weight was determined to be small, indeed almost negligible, for all energies and volumes to be shielded. For

two-dimensionally isotropic particles the electrode weights were found much less than corresponding weights of passive shielding for high particle energies and large volumes to be shielded, but not very different from passive shielding weights for low energy particles and small shielded volumes. Electrode configurations suitable for isotropic particles were not found in this investigation.

4. The evaluation of combined active-passive shielding. - For the several types of combined active-passive shielding systems evaluated no synergistics effects of combination were found. The combined systems were calculated to be always heavier than the related active systems, generally not much lighter than the corresponding passive systems, and sometimes the combination was the heaviest of all.

5. The evaluation of an active, enclosed-flux, superconducting, electromagnetic shielding system. - An enclosed-flux, electromagnetic shielding system utilizing superconducting niobium-tin was found conceptually to offer promise of substantial improvement over Levy's (ref. 11) unconfined magnetic flux system. Weight savings for these systems (as for active systems in general) compared to passive shielding were found potentially greatest for shielding large volumes from particles of high energies.

6. The investigation of the penetration of a collimated beam of 3 Bev protons into passive shielding. - Irradiation of a one by one by three foot iron block with a collimated stream of 3 Bev protons in the Brookhaven cosmotron showed that both proton stream and secondary radiation therefrom

is still well collimated after passage through substantial thickness of material. A very tentative evaluation of the data obtained suggest that at critical thicknesses dosages from secondaries produced by highly energetic particles (cosmic rays) may be of concern for long space flights, although at substantial thicknesses the total attenuation is appreciably greater than would be expected from range-energy relations based simply on electromagnetic interactions.

7. The analysis of electrostatic shielding field configurations. - In the analysis of a series of simple, unconfined electrostatic field configurations, it was shown that for isotropic particles of energy E the flux across a surface where the potential is $\varphi^*$ (P) is $1 + \dfrac{\varphi^* \ (P)}{E}$ times the flux for $\varphi^*$ (P) = 0. Thus appreciable flux reductions are achieved only as $\varphi^*$ (P) approaches the order of -E. Evidently for all configurations considered the unconfined electrostatic shielding was of the "brute force", repulsion (rather than diversion) type, since the required values of $\varphi^*$ (P) were associated with electrode voltages comparable to the particle energies in electron volts.

<div align="center">Discussion</div>

The results given in the preceding section are for the most part self-explanatory, and accordingly discussion will be limited here to those few areas in which important corollaries to the results may be derived. This discussion is given below in the same numbered sequence as the results with which the discussion is associated. As will be seen, much of the

following material pertains to the influence of secondary radiation, induced

by collisions between incident energetic particles and nuclei in shield

material.

1. Effects of secondary radiation on the Loading Index evaluation of

shielding efficiency. - The Loading Index approach is still a useful one

for the evaluation of shielding when secondary radiation is considered as

well as the primary, incident particles themselves. To be sure, the Index

$\frac{CE^{1.75}}{r}$ has the same sort of reduced utility as in the evaluation of active

shielding, and curves of $\frac{W}{V_{Ref}}$ vs. $\frac{CE^{1.75}}{r}$ need to be drawn both for

constant, identified values of incident energy E and of resultant dose

attenuation (or equivalent) within the shielded volume. With the curves

properly identified, however, the evaluation procedure is valid for

determining relative merits of various types of shielding, and particularly

for comparison with the basic weights needed to stop the primary particles.

Indeed plots of this type would be most useful to clarify the important of

secondaries, in the various regimes of energies and geometries, for passive

shielding with appropriate materials.

2. Active, umbrella-like (shadow) shielding. - Without question the

unencouraging potentials calculated for the permanent magnet system

derive in large measure from the unsuitability of Alnico V as an active

shielding material. Alnico V is more effective for attenuating than for

diverting particles (because its residual magnetism is inadequate), so

that it is inherently a combined active-passive system, and, as has been

shown, combination systems do not look attractive. Undoubtedly the use of a superconducting $Nb_3Sn$ magnetic lens in place of an Alnico V disk would have yielded a more promising result; such a system was not considered because the assumption of uni-directional particles appeared unrealistic enough to be useful only for eliminating such unlikely candidates as available permanent magnets.

Uni-directionality may not be totally unrealistic, however, although the only likely occurrence thereof would seem to be during the earliest stages of a solar flare. Here the first, most energetic protons may approach a vehicle in space for a brief time as a stream of semi-parallel particles. While as time goes on the particle paths may be more and more randomized, the high energies of these hypothetical early protons streams may justify some special shielding. Two questions then need to be answered:

(1) Is there some degree of uni-directionality during some portion of encounter of solar-flare protons?

(2) Is there enough of a dose during such an encounter to merit umbrella-like consideration?

If positive answers are found to these questions, further examination of more sophisticated active, umbrella-like shielding may be in order.

3. Electrostatic shielding. - The importance of particle directionality is emphasized by the results of the studies of electrostatic shielding. To be sure directionality has a profound effect upon shield weight required even for simple passive shielding (see fig. 6), but the weight differences associated with different degrees of directionality for electrostatic shielding are even

more substantial. As yet a satisfactory configuration of electrodes for the electrostatic shielding of isotropic particles has not (to the authors' knowledge) been found. Accordingly if electrostatic shielding is to be considered further for protection from solar flares, either data must be obtained to show that solar flare protons are truly non-isotropic or an effective electrode configuration for isotropic particles must be invented. Measurements of particle directionalities are considered further under the section "Conclusions and Recommendations"; here let us examine further what the findings so far imply about the possible invention of the isotropic electrostatic shield.

First, they imply that it must be a configuration that confines and so concentrates the deflecting potential gradient. The unconfined field studies of Heyda (Appendix D) showed pretty clearly that unconfined fields require impractically high voltages to reject particles of the energy range of interest, nor do they give the slightest hint that cleverness in electrode layout can effect any reduction in the voltage required. Second, they indicated that the problem is an electrical not a mechanical one, for the forces between electrodes in all cases required a minimum of structure to be accommodated. Third, and perhaps in the long run most important, there is the finding that even with confined fields high voltages (though of the one to ten million volt range, not the hundreds of millions of volts range as for unconfined fields) will be required.

This last implication is suggested to be most important because little is known about the rate of charge leakage or of electrical breakdown at high voltages in space. Because the elemental particles in space are mostly

ions, even though scare they may trigger electrode discharge at prohibitively low potentials. Data to evaluate the electrical insulation properties of space for this problem will not be easily obtained on the ground, and if an attractive configurational concept is found, flight experiments may be needed to measure high voltage leakage rates in space.

No discussion of electrostatic shielding is complete without some mention of the voltage generating equipment which has so far been ignored in this study. Estimates of weights and powers required are unfortunately not feasible, for lack of just the kind of data described in the preceding paragraph. The generation of voltages in the one million to ten million volt range can be accomplsihed readily on the ground with available, compact (but not optimized from a weight standpoint) Van Der Graff generators. Electrostatic power generators have been suggested capable of construction for flight applications at about the weight of one pound per kilowatt (ref. 25). The power required for the shielding application, however, depends upon the rate of charge leakage, and as has been stated, this is essentially unknown.

A sequence of events is needed to clarify the future of the electrostatic shielding approach. First either an attractive configuration needs to be found for shielding isotropic particles or else a systematic directionality needs to be demonstrated for solar flare protons so that they can be shown amenable to shielding with a reasonable electrode design. Once either of these has been indicated to be a possibility, data on charge leakage rate in space need to be obtained, and the over-all electrostatic system weight evaluated.

4. <u>Combined active-passive shielding.</u> - To a degree any so-called "active"
shielding system is in actuality a combination "active-passive" system,
inasmuch as the active system components comprise material mass which
intercepts incident energetic particles, attenuates them, and generates
secondary radiation. The use of supplemental passive material has been
found not desirable to increase the attenuation of the primary particles.
The following argument suggests that supplementary material is also not
likely to make the combination system more attractive from the standpoint
of secondary radiation. Clearly if the active system alone has reduced the
material thickness below the critical range for maximum secondary dosage
production, the addition of passive material can only degrade the system. If
the active system has a thickness greater than the critical, supplemental
material is not apt to be more effective for the attenuation of the secondaries
than with a pure passive system. Again nothing is apparent which suggests
merit for the combination of the active and passive approaches.

One unexplored possibility still remains - that a combination system
configuration exists which uses passive material to help control the
directionality of incidence of particles and so achieves a synergistic
advantage. This possibility may deserve some further consideration; it will
be discussed again in paragraph 6 below.

5. <u>The use of superconducting material.</u> - The complexities of a superconducting,
electromagnetic shielding system are inherently abhorrent. Considering the
fact that niobium-tin wire is still a curiosity, we boggle at the extrapolation

to the use of it in quantities of tons for a space vehicle shielding system. The fact remains, however, that the only potential demonstrated so far for substantial reduction in the weight of shielding of large space vehicles from high energy isotropic protons is through the use of this concept. Studies of this approach should proceed into the area of preliminary design, to provide a better picture of the complexities encountered, and an evaluation of the penalties (such as electrical power supplies to start the current flowing) associated with the engineering conversion of the concept to application.

Both confined-flux and unconfined-flux systems deserve more detailed investigation. Areas to be studied include: (1) possibilities of "leaks", particularly around the pole pieces in the confined flux system, (2) evaluation of the importance of secondaries with both systems, and (3) exploration of better configurations which utilize the most favorable aspects of all approaches - directed toward the development of an attractive engineering design. Desirably the magnetic flux should be confined, at least away from regions where it may interact unfavorably with instrumentation, communication, or other functions; circulating currents and hence induced stresses should be minimized; still, the penetration of particles into shield system material is best avoided and thus the production of secondary radiation is minimized; leakage of particles into shielded volume should be negligible, but access thereto must not be prohibitively difficult. The achievement of the best compromise among these characteristics may well require a combination, semi-confined, semi-unconfined flux system.

6.  Active shielding and secondary radiation. - A great merit of the unconfined

magnetic flux approach proposed by Levy (ref. 11) is that incident particles

penetrate no material within the forbidden zones and thus generate no secondary

radiation.  Active systems in which particles penetrate material, on the other

hand, must seriously consider the secondary problem, and all systems must

take into account penetrating cosmic rays and the secondaries therefrom.

Somewhat greater flexibility of approach exists in the active than in the

passive case, however.  In the passive case the shielding must be interposed

between incident particles and space to be shielded, and as Shen's experiment

(Appendix C) has shown, this interposition does not divert the secondaries

away from the shielded volume.  By contrast, an active system may be

especially designed to reduce secondaries by directing primary particles

into paths which cause the secondaries produced to miss the shielded

volume.  The electrostatic shield for two-dimensionally isotropic particles

is an ideal example.


## CONCLUSIONS AND RECOMMENDATIONS

### Conclusions

The following conclusions are abstracted from the results and discussions

of the investigations reported herein.


1.  Permanent-magnet shielding useless. - Active, permanent-magnet (Alnico V)

shielding is ineffectual and offers no promise of improved efficiency compared to

passive shielding.

57

2.  Electrostatic diversion of particles possibly effective for favorable

conditions. - Active electrostatic shielding may have a potential for weight

saving compared to passive shielding if the rate of charge leakage in space

is not excessive.  The greatest potential saving is for shielding large vehicles

from high energy directional particles, and the potential reduces substantially

as the particles become less directional.  As yet a satisfactory configuration

for isotropic particles has not been found; unconfined electrostatic fields

for shielding isotropic particles require electrode voltages comparable to

particle energies in electron volts.

3.  Combination active-passive shielding undesirable. - Combined active-passive

shielding systems show no synergistic improvement over simple active or

passive systems alone.

4.  Superconducting system efficient in concept. - An active, confined magnetic

flux, superconducting $Nb_3Sn$ electromagnetic shielding system conceptually

has a potential for substantial weight savings for shielding large vehicles

from high energy, isotropic charged particles.

### Recommendations

The following recommendations are based upon the foregoing results and

conclusions:

1.  Flight measurements: directionality; charge leakage, and electric

breakdown. - Flight measurements should be made to determine in a

thoroughgoing fashion directionality characteristics of solar flare protons;

58

to evaluate the rate of leakage of high voltages from exposed surfaces of large area in space, and to evaluate electrical breakdown characteristics in the space environment.

2.  <u>Configuration of electrodes for isotropic particles.</u> - Further studies should be made directed toward the development of a suitable configuration for an electrostatic shield for isotropic particles.  These studies should concentrate upon designs in which the deflecting field is confined between electrode surfaces.

3.  <u>Designs of superconducting systems.</u> - Investigations of the use of superconducting materials like niobium - tin for active shielding should be carried forward into the preliminary design stage to provide evaluations of engineering problems and of practical complexities.

4.  <u>Evaluations of secondaries.</u> - Evaluations of effects of secondary radiation, and the implications thereof regarding active shielding systems should be further refined.  Particular consideration should be given to improved determinations of total dosage accumulated over long times from interactions of cosmic rays and vehicle shielding materials.

# APPENDIX A

## Preliminary Studies

In order to pave the way for the evaluation of various approaches to the shielding problem, several preliminary studies were carried out. First, approximations to trajectory equations for energetic charged particles subject to retarding and electromagnetic* or electrostatic forces were derived using essentially linearizing assumptions. Second, a general method of evaluation of shielding systems was developed, analogous to efficiency evaluations of vehicle structures, to provide a valid basis for comparisons among different approaches. Because the remainder of this investigation repeatedly draws upon the results of these preliminary studies, they are presented in some detail in this report - the development of the trajectory expressions in this Appendix, that of the evaluation method in Appendix B and within the main text.

Approximate trajectory equations for motion in a retarding medium and a uniform magnetic field. - In a magnetic field, the path of a charged particle is curved, and the radius of curvature is

$$r = \frac{mv}{Be} \tag{A-1}$$

where

    r    radius of curvature, [cm. ]

    m   mass of particle, [gms. ]

    v   velocity of particle, [cm/sec] (assumed below relativistic velocities)

---

*Trajectory equations for charged particles in a retarding medium and magnetic or electrostatic fields were derived in part in a study which preceded the present investigation (ref. 17).

e    electrostatic charge in particle, [stat-coulombs]

and B magnetic flux intensity at that point, [gauss]

Choosing a coordinate system with origin at the point of incidence of the charged particle on the surface of the retarding medium, and with x- and y-axes perpendicular and parallel to the surface at that point and perpendicular to the magnetic flux, we may write

$$\frac{(1 + y'^2)^{3/2}}{y''} = \frac{m}{Be} (\dot{x}^2 + \dot{y}^2)^{1/2} \tag{A-2}$$

where the dots represent derivatives with respect to time, and the primes derivatives with respect to x.

Noting that

$$(\dot{x}^2 + \dot{y}^2)^{1/2} = \dot{x} (1 + y'^2)^{1/2} \tag{A-3}$$

and letting

$$M = \frac{m}{Be} \tag{A-4}$$

We have

$$\frac{1 + y'^2}{y''} = M\dot{x} \tag{A-5}$$

Substituting $y' = u$ and integrating

$$u = \tan\left(\frac{\tau}{M} + C*\right) \tag{A-6}$$

where

$\tau$    time, [sec. ]

C*  constant of integration

Assuming that the deceleration of the particle is a constant with time - a crude approximation except for limited decelerations, but adequate for first evaluations such as this -

$$v = (\dot{x}^2 + \dot{y}^2)^{1/2} = K\tau + v_o \tag{A-7}$$

61

where

v, $v_o$  velocity, and initial velocity [cm/sec]

K    constant of proportionality, [cm/sec$^2$]

Combining (A-6) and (A-7), once again using the relationship given in (A-3), integrating, and employing the initial condition that the angle of incidence relative to the x-axis is $\alpha_o$ (radians) gives

$$x = KM^2\left[\cos\left(\frac{\tau}{M}+\alpha_o\right) + \frac{\tau}{M}\sin\left(\frac{\tau}{M}+\alpha_o\right) - \cos\alpha_o\right] + v_o M\left[\sin\left(\frac{\tau}{M}+\alpha_o\right) - \sin\alpha_o\right] \quad (A-8)$$

Similarly the expression for the sidewise deflection may be derived as

$$y = KM^2\left[\sin\left(\frac{\tau}{M}+\alpha_o\right) - \frac{\tau}{M}\cos\left(\frac{\tau}{M}+\alpha_o\right) - \sin\alpha_o\right] - v_o M\left[\cos\left(\frac{\tau}{M}+\alpha_o\right) - \cos\alpha_o\right] \quad (A-9)$$

Useful special cases are the equations of penetration at normal incidence

$$x_{\alpha_o=0} = KM^2\left[\cos\left(\frac{\tau}{M}\right) + \frac{\tau}{M}\sin\left(\frac{\tau}{M}\right) - 1\right] + v_o M \sin\left(\frac{\tau}{M}\right) \quad (A-10)$$

and for sidewise displacement at maximum penetration

$$y_{x=x_{max}} = KM^2(1-\sin\alpha_o) + v_o M\cos\alpha_o \quad (A-11)$$

For no retarding medium, K = 0, and equations (A-8) and (A-9) reduce to

$$x_{K=0} = v_o M\left[\sin\left(\frac{\tau}{M}+\alpha_o\right) - \sin\alpha_o\right] \quad (A-12)$$

$$y_{K=0} = -v_o M\left[\cos\left(\frac{\tau}{M}+\alpha_o\right) - \cos\alpha_o\right] \quad (A-13)$$

Or for normal incidence

$$x_{\substack{K=0\\\alpha_o=0}} = v_o M\left[\sin\left(\frac{\tau}{M}\right)\right] \quad (A-14)$$

And in this case maximum penetration corresponds to the radius

$$x_{\substack{max_{K=0}\\\alpha_o=0}} = v_o M \quad (A-15)$$

as would be expected.

62

Approximate trajectory equations for motion in a retarding medium and a uniform electrostatic field. - The rather special assumption is first made that the retarding medium is so distributed that it influences only motion in the x-direction and not in the y-direction. This assumption is applicable for the long paths with small sidewise deflections appropriate to the particle energies, deflecting voltages, and distributed retarding media to be considered. The x-axis is assumed perpendicular to the field and the y-axis is assumed parallel to it, and the approximation to the position of the particle at time $\tau$ is

$$x = v_o \tau \cos \alpha_o + 1/2 \, \eta \, K \, \tau^2 \tag{A-16}$$

$$y = K' V \tau^2 + v_o \tau \sin \alpha_o \tag{A-17}$$

Also

V    applied (constant) potential, [volts/cm]

K'    $4.8 \times 10''$ (for protons), [cm$^2$/volt-sec$^2$]

$\eta$    ratio of effective density of retarding medium to the

density of the material as a solid

For no retarding medium and incidence normal to the field

$$\eta K_{eff} = 0$$

$$\alpha_o = 0 \tag{A-18}$$

and the equations reduce to that of the expected parabola

$$x_{\substack{\eta K_{eff}=0 \\ \alpha_o=0}} = v_o \sqrt{\frac{y}{K'V}} \tag{A-19}$$

A convenient form for use in determining voltages required with no retarding material may be derived from equations (A-16) and (A-17) by

algebra, as

$$Vy = \frac{(v_o \cos \alpha_o)^2}{K'} \left[ \frac{1 - \frac{x}{y} \tan \alpha_o}{\left(\frac{x}{y}\right)^2} \right] \qquad (A-20)$$

This form was used for the calculation of the curves of figure 13. Similarly a useful form may be derived for $\alpha_o = 0$ but $\eta K_{eff} \neq 0$, as

$$Vy = \frac{-\eta K_{eff} \, y \left(\frac{x}{y}\right) + \left[ v_o + \sqrt{v_o^2 + 2\eta K_{eff} \, y \left(\frac{x}{y}\right)} \right] \left[ \sqrt{v_o^2 + 2\eta K_{eff} \, y \left(\frac{x}{y}\right)} \right]}{2K' \left(\frac{x}{y}\right)^2} \qquad (A-21)$$

This form was used to calculate the curves of figure 17.

# APPENDIX B

Derivation of Equations Pertinent to the Identification of a Loading Index

The range-energy relationship for (non-relativistic) protons as plotted in figure 2 can be approximated by an equation of the form

$$w_\infty = CE^{1.75} \qquad \text{(B-1)}$$

where

$w_\infty$     weight of flat material penetrated by protons having normal

incidence, $[gm/cm^2]$

$C$     dimensional constant, $\left[ \dfrac{gm}{cm^2 - Mev^{1.75}} \right]$

$E$     kinetic energy of protons, $[Mev]$

For liquid hydrogen

$$C_{H_2} \approx 0.0011 \; \frac{gm}{cm^2 - Mev^{1.75}} \qquad \text{(B-2)}$$

and equation (B-1) reproduces the curve of figure 2 with an error of less than 5% up to $E \approx 400$ Mev.

Equation (B-1) will now be employed to determine shield weights for various configurations and particle directionalities. From these examples a common parameter, identified here as the Loading Index, will be evident.

For a spherical shield and isotropic particles. -

$$W = \frac{4}{3} \pi \; (r_2^3 - r_{Sph}^3) \, \rho \qquad \text{(B-3)}$$

where

$W$     shield weight, $[gms.]$

$r_2$     outside radius, $[cm.]$

$r_{Sph}$     inside radius, [cm.]

$\rho$     material density, [gm/cm$^3$]

The weight per unit volume shielded is

$$\frac{W}{\frac{4}{3}\pi r_{Sph}^3} = \frac{W}{V_{Ref}} = \left[\left(\frac{r_2}{r_{Sph}}\right)^3 - 1\right]o \tag{B-4}$$

Now

$$r_2 = r_{Sph} + \frac{w_\infty}{\rho} \tag{B-5}$$

Or, employing (B-1)

$$r_2 = r_{Sph} + \frac{CE^{1.75}}{\rho} \tag{B-6}$$

And

$$\frac{W}{V_{Ref}} = \rho\left[\left(\frac{CE^{1.75}}{r_{Sph}}o + 1\right)^3 - 1\right] \tag{B-7}$$

Evidently $W/V_{Ref}$ is a function of the density of the shield material and

of the parameter $CE^{1.75}/r_{Sph}$ which contains the design conditions of particle

energy and radius to be shielded.


For a cylindrical shield and two-dimensionally isotropic particles. -

$$\frac{W}{V_{Ref}} = \frac{\pi \ell_{Cyl} (r_2^2 - r_{Cyl}^2)\rho}{\pi r_{Cyl}^2 \ell_{Cyl}} \tag{B-8}$$

with $r_{Cyl}$ the inside radius of the cylinder and $\ell_{Cyl}$ its length, and with

$$V_{Ref} = \pi r_{Cyl}^2 \ell_{Cyl} = \frac{4}{3}\pi r_{Sph}^3 \tag{B-9}$$

As before

$$r_2 = r_{Cyl} + \frac{CE^{1.75}}{\rho} \tag{B-10}$$

66

and

$$\frac{W}{V_{Ref}} = \rho \left[ \left( \frac{CE^{1.75}}{r_{Cyl}\rho} + 1 \right)^2 - 1 \right]$$ (B-11)

where the characteristic radius $r_{Cyl}$ is related to $r_{Sph}$ via equation (B-9). Here again the weight is a function of $\rho$ and $\frac{CE^{1.75}}{r}$. Because the quantity $\left( \frac{CE^{1.75}}{r_{Cyl}\rho} + 1 \right)$ appears only to the second power in (B-11) rather than to the third power as in (B-7), as would be expected, shield weight required for two-dimensional isotropy is generally less than for fully isotropic particles.

For a circular shield and uni-direction particles. - For uni-directional particles, the criterion which determines the size of shield is more nearly one of frontal area than volume. For a circular cross-section perpendicular to the incident particles, the frontal area $A_{Front}$ is

$$A_{Front} = \pi r^2_{Cir}$$ (B-12)

and the weight of shield is

$$W = \pi r^2_{Cir} \rho \left( \frac{w_\infty}{\rho} \right)$$ (B-13)

The volume to be shielded $V_{Ref}$ can be related to the frontal area through the use of a characteristic length $\ell_{Ave}$, thus;

$$V_{Ref} = \pi r^2_{Cir} \ell_{Ave}$$ (B-14)

and the relationship between the actual shape and a spherical volume is described by the equation

$$V_{Ref} = \frac{4}{3} \pi r^3_{Sph} = \pi r^2_{Cir} \ell_{Ave}$$ (B-15)

As before, we write an expression for the shield weight per unit volume shielded, as follows:

$$\frac{W}{V_{Ref}} = \frac{\pi\, r_{Cir}^2\, w_\infty}{\pi\, r_{Cir}^3\, \ell_{Ave}} \qquad\qquad (B-16)$$

Or, employing (B-1)

$$\frac{W}{V_{Ref}} = \frac{w_\infty}{\ell_{Ave}} = \frac{CE^{1.75}}{r_{Cir}} \left(\frac{r_{Cir}}{\ell_{Ave}}\right) \qquad\qquad (B-17)$$

In equation (B-17) the same sort of loading index $\dfrac{CE^{1.75}}{r_{Cir}}$ is identified as in the previously considered cases. Here, however, it is modified by a factor $\dfrac{r_{Cir}}{\ell_{Ave}}$ which accounts for the shape of the body. Furthermore, the relationship between the characteristic radius $r_{Cir}$ and the radius of the reference spherical volume is not direct but depends in part upon the characteristic length $\ell_{Ave}$ as noted in equation (B-15). The real difference, of course, between this case and the others is that whereas before the shape was uniquely specified, here it is not. In consequence a plot of $\dfrac{W}{V_{Ref}}$ vs. $L_i$ is no longer a unique curve but rather a family of curves, one for each value of $\dfrac{r_{Cir}}{\ell_{Ave}}$. For any specified shape of shield, however, $\dfrac{r_{Cir}}{\ell_{Ave}}$ is fixed; the plot does yield a single curve; and its location is a measure of the weight efficiency.

Optimization of Composite Liquid-Hydrogen, Polyethylene Shielding

The basis for optimization of the composite spherical shielding considered is the assumption that the relative effectiveness of liquid hydrogen and polyethylene for stopping protons is the same at any given energy level, i. e.,

68

one centimeter of polyethylene is generally as effective as 6.7 centimeters of liquid hydrogen approximately. On this basis, an equation for the thickness of liquid hydrogen required together with polyethylene to stop protons of a given energy can be written as follows:

$$t_{H_2 \text{Req'd}} = t_{H_2_0} - 6.7\, t_{(CH_2)_n} \tag{B-18}$$

where

$t_{H_2}$    thickness of liquid hydrogen required in combination, [cm.]

$t_{H_2_0}$    thickness of liquid hydrogen alone which will just stop the particles being considered, [cm.]

$t_{(CH_2)_n}$    thickness of polyethylene, [cm.]

The corresponding weight equation is

$$W = \frac{4}{3}\pi\left[0.07\,(r_3^3 - r_2^3) + 0.92\,(r_2^3 - r_{Sph}^3)\right] \tag{B-19}$$

where

W    total weight of composite, spherical shield, [gm.]

0.07 & 0.92    densities of liquid hydrogen and polyethylene, respectively, [gm/cm$^3$]

$r_{Sph}$    radius of spherical volume to be shielded, [cm.]

$r_2 - r_{Sph} = t_{(CH_2)_n}$ , [cm.]

$r_3 - r_2 = t_{H_2}$ , [cm.]

Equations (B-18) and (B-19) may readily be combined and the result minimized to provide the desired optimum. This procedure was used to calculate the composite curve of figure 4.

# APPENDIX C

## Nuclear Cascade Experiment

by

S. P. Shen

In what follows, we describe an experiment designed to study the nuclear cascade in dense matter as well as the depth variation of cosmic-ray activation products in meteorites. These two problems are nearly identical; in fact, first knowledge of attenuation curves at high energies came mainly from studies of the meteorite problem (ref. 26). To our knowledge, this experiment is the first systematic study of the nuclear cascade in dense matter in three dimensions.

An iron target 1 ft. x 1 ft. x 3 ft. was bombarded for 88 minutes in the external beam of the Brookhaven Cosmotron. About $2 \times 10^{13}$ 3-BeV protons entered perpendicularly the geometrical center of the 1 ft. x 1 ft. face. Considerable effort was spent in collimating the beam. Polaroid photographs of the final beam showed negligible angular divergence and a roughly elliptical beam cross-sectional area of about 2 cm. and 1 cm. semimajor and semiminor axis, respectively.

The development of the nuclear cascade in the target block was "mapped" by means of the following foils, which were sandwiched in the block throughout the bombardment:

(a) Al foils of various configurations and thicknesses. The Na-24 activity (15 hr. half-life) and F-18 activity (1.9 hr. half-life) produced in Al are measured.

(b) Indium foils. These are counted in gas-flow counters for their beta activity. If there is a substantial flux of slow neutrons, the beta activity of 54-minute In-116 should be prominent.

(c) Au foils of various configurations and thicknesses   The Tb-149 (4-hr. half-life) alpha activity induced by spallation reactions in Au is measured.

(d) Fe foils. These are studied by means of an 8" x 4" NaI scintillation crystal for their gamma-ray spectra. These measurements are still in progress.

The analysis of the data for the lateral spread of the nuclear cascade is partially complete. The analysis of the data for the longitudinal development of the cascade is in progress and is expected to be completed in the near future.

The preliminary lateral-spread data based on Na-24 activity in Al are summarized in figure 28. The abscissa represents the lateral distance measured from the axis of the cascade. Each abscissa division is roughly 1.4 inch. The ordinate represents the Na-24 activity in Al. The scala for the ordinate is linear but entirely arbitrary, i.e., the height of the six curves cannot as yet be intercompared. Each of the six curves represents the lateral spread of nuclear-active particles responsible for the production of Na-24 in Al at a particular depth in the target. The six depths are, as labelled, 82 gm/cm$^2$, 229 gm/cm$^2$, 332 gm/cm$^2$, 353 gm/cm$^2$, 455 gm/cm$^2$, and 663 gm/cm$^2$ (the depths here are expressed in "area density", i.e., the linear depth times the density of the material).

It must be emphasized that the data shown in figure 28 are very preliminary. In particular, these data have not yet been corrected for the effect of the finite cross-section of the incident beam. It can be seen nevertheless that the core of the cascade is extremely well-defined up to a depth of at least 350 gm/cm$^2$, after which it becomes less prominent.

In addition to the above data, measurement of the Tb-149 in the Au foils showed that beyond about 6 cm. from the cascade axis, nuclear-active particles of energy exceeding about 600 MeV are virtually absent at all depths.

# APPENDIX D

## Determination of Equi-Potential Surfaces for Some Electrostatic Field Configurations

### by

### J. F. Heyda

In this Appendix equations are derived and equi-potential curves, $-\phi^*(P) = E$, are sketched for several simple electrostatic field configurations to help guide the development of more complex configurations for application to active shielding. Through the application of Liouville's theorem to the case of a large number of electrically charged particles moving in an electrostatic field, it is shown that the particle flux across a surface having the potential $\phi^*(P)$ is equal to $1 + \dfrac{\phi^*(P)}{E}$ times the flux at the same point in the absence of the field.

Equi-potential curves for special electric fields. -

Case 1:  The field of two charged particles, $q_1$ and $q_2$.

Let the charges $q_1$ and $q_2$ be placed on the line Ox as shown in the sketch below
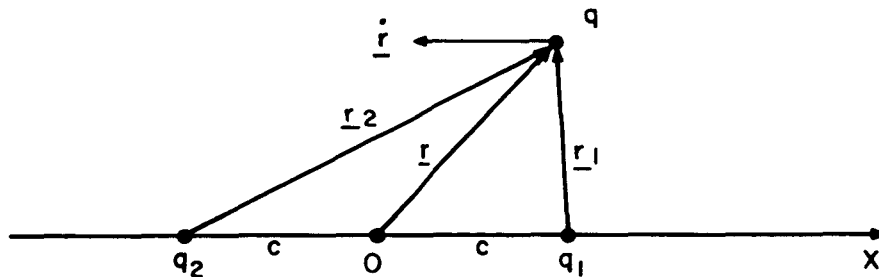


and let q be a charged particle of mass m.  Then the force acting on q is

$$\underline{F} = \frac{q}{4\pi \epsilon_o} \left[ \frac{q_1}{r_1^{\,3}} \, \underline{r}_1 + \frac{q_2}{r_2^{\,3}} \, \underline{r}_2 \right] + q \, \underline{\dot{r}} \times \underline{B} \qquad (D-1)$$

where $\underline{B}$ is the magnetic flux density due to the moving charges $q_1$, $q_2$; and $\epsilon_o$ is the electrical permittivity of space.

73

The equation of motion is then

$$m \ddot{\underline{r}} = \frac{q}{4 \pi \epsilon_o} \left[ \frac{q_1}{r_1^3} \underline{r}_1 + \frac{q_2}{r_2^3} \underline{r}_2 \right] + q \dot{\underline{r}} \times \underline{B} \qquad (D-2)$$

If we dot both sides of (D-2) with $\dot{\underline{r}}$ and integrate, we find

$$J \dot{\underline{r}}^2 = -2q \left( \frac{q_1}{r_1} + \frac{q_2}{r_2} \right) + \text{constant} \qquad (D-3)$$

where $J = 4 \pi \epsilon_o m$, and the constant is equal to

$$J v_o^2 + 2q \left( \frac{q_1}{r_{1_o}} + \frac{q_2}{r_{2_o}} \right) = C^{**} \qquad (D-4)$$

where $v_o$ is the relative speed of $q$ when $\underline{r}_1 = \underline{r}_{1_o}$ ; $\underline{r}_2 = \underline{r}_{2_o}$ .

If $(x, y)$ are Cartesian coordinates of $q$ relative to 0, then (D-3) may be written

$$J (\dot{x}^2 + \dot{y}^2) = C^{**} - 2q \left[ \frac{q_1}{\sqrt{(x-c)^2 + y^2}} + \frac{q_2}{\sqrt{(x+c)^2 + y^2}} \right] \qquad (D-5)$$

The constant $C^{**}$ is inherently positive since it may be interpreted as $J v_\infty^2$,

where $v_\infty$ is the particle speed beyond the effect of the field.

The locus of points where $\dot{x} = \dot{y} = 0$, namely

$$J v_\infty^2 = 2q \left[ \frac{q_1}{\sqrt{(x-c)^2 + y^2}} + \frac{q_2}{\sqrt{(x+c)^2 + y^2}} \right] \qquad (D-6)$$

if real defines the equi-potential curves which delineate regions of the plane

in which trajectories of $q$ do not enter.

If $q_1$ and $q_2$ are of the same sign and $q$ is of the opposite sign, then, as might

be expected, the relative speed of $q$ can never vanish, and no such equi-potential

curves exist.

74

<u>Case 1(a)</u>: $q_1$ $q_1$, and $q_2$ either all positive or all negative and $\left|q_1\right| = \left|q_2\right|$ .

Equation (D-6) now may be written as

$$\frac{1}{\sqrt{(x - c)^2 + y^2}} + \frac{1}{\sqrt{(x + c)^2 + y^2}} = a \tag{D-7}$$

where

$$a = \frac{Jv_\infty^2}{2q\,q_1} > 0$$

The curve defined by this equation is symmetric with respect to both axes

and the origin. It crosses the x-axis vertically when

$$x = \pm \left( \frac{1 + \sqrt{1 + a^2 c^2}}{a} \right) \tag{D-8}$$

and the y-axis horizontally when

$$y = \pm \sqrt{\frac{4}{a^2} - c^2} \tag{D-9}$$

The y - intercepts are real provided that $a$ c $< 2$, that is providing

$$q_1 \quad \frac{Jv_\infty^2 c}{4q} \tag{D-10}$$

When (D-10) is satisfied, the curve (D-7) has the following appearance
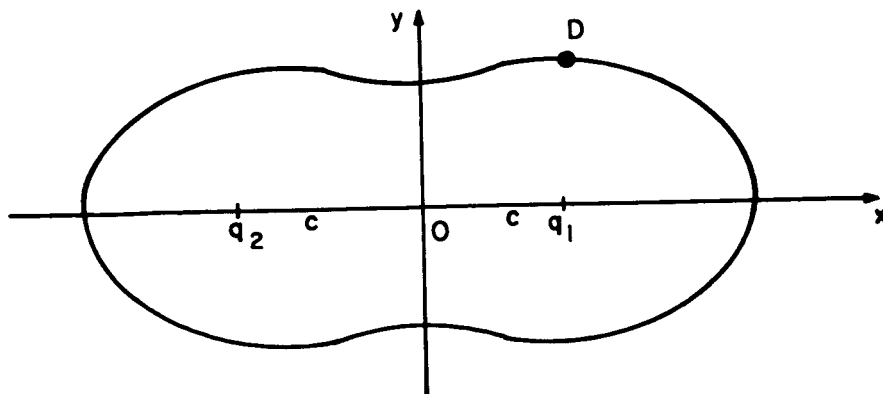
When (D-10) is not satisifed, the curve degenerates into two ovals about the charge locations $\pm$ c, 0. The shielded region can, therefore, be varied by adjusting c and $q_1$ in accordance with (D-10).

The maximum point D is obtained by solving simultaneously the pair of equations

$$x = c \left( \frac{r_2^3 - r_1^3}{r_2^3 + r_1^3} \right) \tag{D-11}$$

$$\frac{1}{r_1} + \frac{1}{r_2} = \alpha$$

<u>Case 1(b)</u>:  Either $\quad q > 0, \quad q_1 > 0, \quad q_2 < 0$

$\qquad\qquad\qquad$ or $\quad q < 0, \quad q_1 < 0, \quad q_2 > 0$ $\quad$ and $q_1 = -q_2$

Equation (D-6) now takes the form

$$\frac{1}{\sqrt{(x-c)^2 + y^2}} - \frac{1}{\sqrt{(x+c)^2 + y^2}} = \alpha \tag{D-12}$$

with

$$\alpha = \frac{J v_\infty^2}{2 q q_1} > 0$$

It is evident from equation (D-12) that points of zero relative velocity for q do not occur in the 2nd and 3rd quadrants. The equi-potential curve (D-12) intersects 0x vertically at $(x_1, 0)$ and $(x_2, 0)$, where $x_1 > x_2$, and

$$x_1 = \sqrt{c^2 + \frac{4 c q q_1}{J v_\infty^2}} \quad , \qquad x_2 = \frac{2 q q_1}{J v_\infty^2} \left[ -1 + \sqrt{1 + \left( \frac{J v_\infty^2 c}{2 q q_1} \right)^2} \right] \tag{D-13}$$

The curve is symmetric with respect to the x-axis, and has the appearance shown in the following sketch
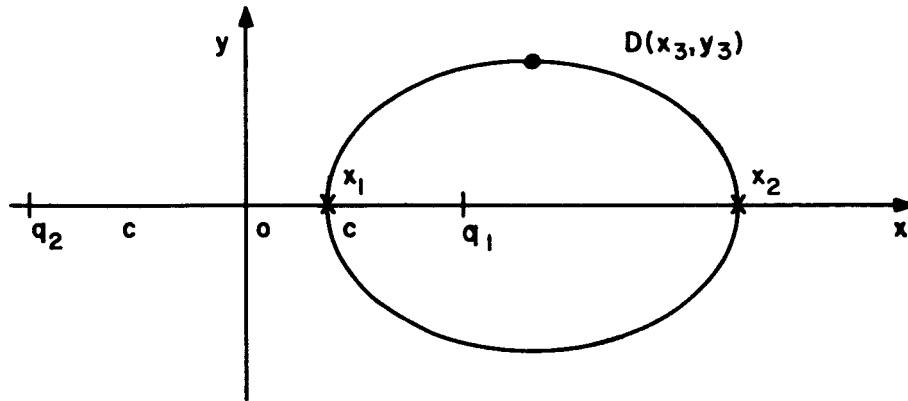


Point D $(x_3, y_3)$ where $y' = 0$ is obtained by solving simultaneously the equations

$$\frac{x + c}{r_2^3} = \frac{x - c}{r_1^3}$$

(D-14)

$$\frac{1}{r_1} - \frac{1}{r_2} = a$$

Case 1 (c):   Either   $q > 0$, $q_1 < 0$, $q_2 > 0$ $\Big\}$ and $q_1 = -q_2$

or   $q < 0$, $q_1 > 0$, $q_2 < 0$

This case is the mirror image of Case 1 (b), the shielded region now being bounded by a single oval about the charge $q_2$ instead of $q_1$.

Case 2 (a):   Three charges on 0x: $q > 0$, $q_1 > 0$, $q_2 > 0$, $q_3 > 0$; and $q_1 = q_2 = -q_3$. ($q_1$ @ c, 0; $q_2$ @ -c, 0; and $q_3$ @ 0)

The equi-potential curve here has the equation

$$\frac{1}{\sqrt{(x - c)^2 + y^2}} - \frac{1}{\sqrt{x^2 + y^2}} + \frac{1}{\sqrt{(x + c)^2 + y^2}} =$$

(D-15)

77

with

$$\alpha = \frac{Jv_\infty^2}{2qq_1} > 0$$

The curve is symmetric with respect to both axes and the origin. We need, therefore, to investigate it only in the first quadrant.

There will be an x-intercept to the right of c if the equation

$$\frac{1}{x - c} - \frac{1}{x} + \frac{1}{x + c} = \alpha \tag{D-16}$$

possesses a positive root. Since such a root must satisfy

$$\alpha x^3 - x^2 - \alpha c^2 x - c^2 = 0 \tag{D-17}$$

we see by Descartes' rule that there is exactly one such root.

There will be a positive x-intercept in the interval $0 < x < c$ if

$$\frac{1}{x + c} - \frac{1}{x} - \frac{1}{x - c} = \alpha \tag{D-18}$$

i.e. if

$$\alpha x^3 + x^2 + c (2 - \alpha c) x - c^2 = 0 \tag{D-19}$$

Since this polynomial has exactly one positive zero and is of opposite signs at 0 and c, there is definitely an x-intercept of (D-15) between 0 and c.

To find positive y-intercepts, we must solve the equation

$$\frac{2}{\sqrt{y^2 + c^2}} - \frac{1}{y} = \alpha \tag{D-20}$$

If we put $y = c \tan \theta$, equation (D-20) becomes

$$2 \sin \theta - 1 = \alpha c \tan \theta \tag{D-21}$$

Plotting separately the left and right members of (D-21) yields curves as follows:
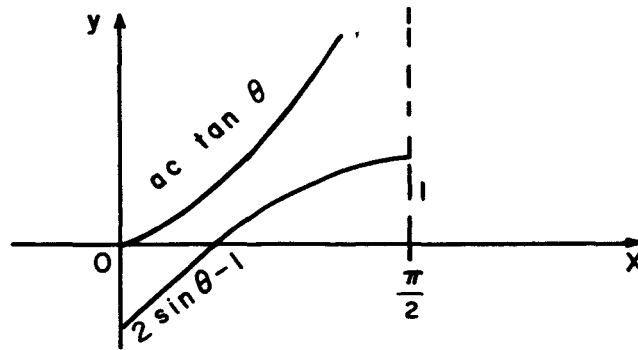


These curves will be tangent providing (D-21) and (D-22) as follows:

$$a\,c\,\sec^2\theta\ -\ 2\cos\theta\ =\ 0 \tag{D-22}$$

have a common root.   This yields the conditions

$$a\,c\ =\ 2\left[1-\frac{3\sqrt{2}}{2}\right]^{3/2}=\ 0.45,\ \theta\ =\ 52^\circ\ 30' \tag{D-23}$$

thus,  in summary,  we can say that

(1)   For $a\,c > 0.45$,  equation (D-15) has no  y-intercepts

(2)   For $a\,c\ =\ 0.45$,  there is one y-intercept at   $y\ =\ \dfrac{0.586}{a}$

(3)   For $a\,c < 0.45$,  two y-intercepts $y_1$, $y_2$ exist such that

$$\frac{c}{\sqrt{3}}\ <\ y,\ <\ y_2$$

The curve (D-15) has the general appearance shown in the following sketch, drawn for the case  $c = 1$,  $a = 0.25$
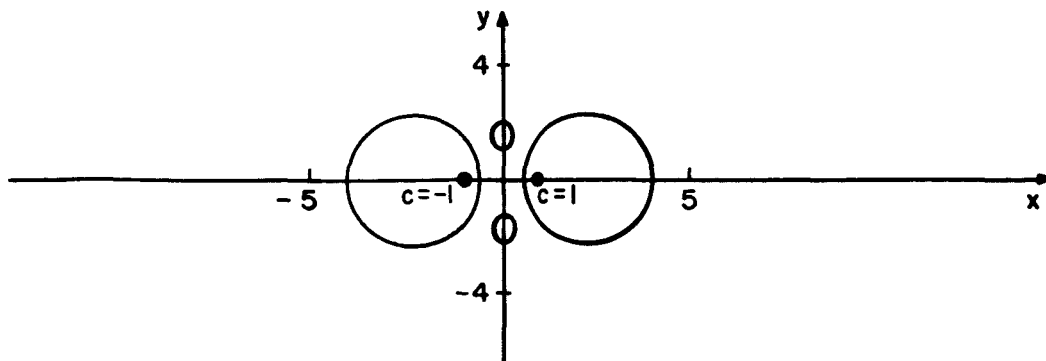
Case 2 (b): Same as case 2 (a) but with $q > 0$; $q_1 = q_2 < 0$; $q_3 > 0$

$$q_3 = -q_1 = -q_2$$

The equation of the equi-potential curve is now

$$\frac{1}{\sqrt{(x-c)^2 + y^2}} - \frac{1}{\sqrt{x^2 + y^2}} + \frac{1}{\sqrt{(x+c)^2 + y^2}} = -\alpha \qquad (D-24)$$

and it has the form sketched below for $c = 3.2$, $\alpha = 3.2$
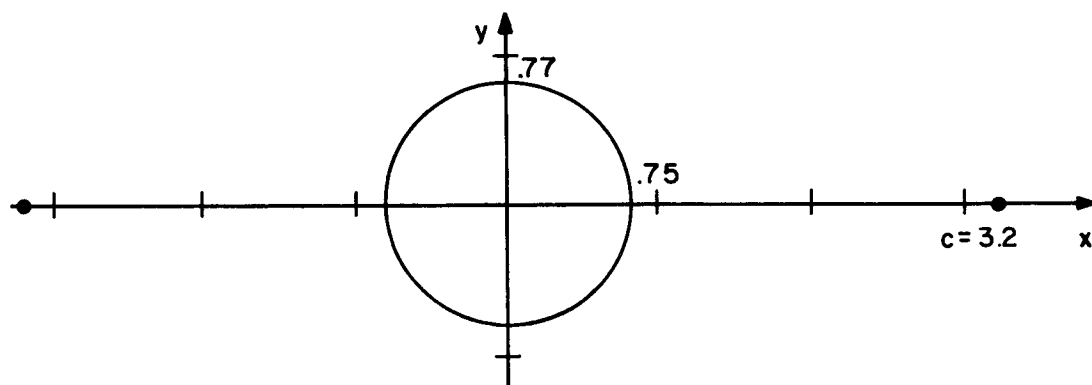


Case 3: Four charges

Consider four equal charges, all of the same sign as the moving charge $q$

and situated as shown in the following sketch
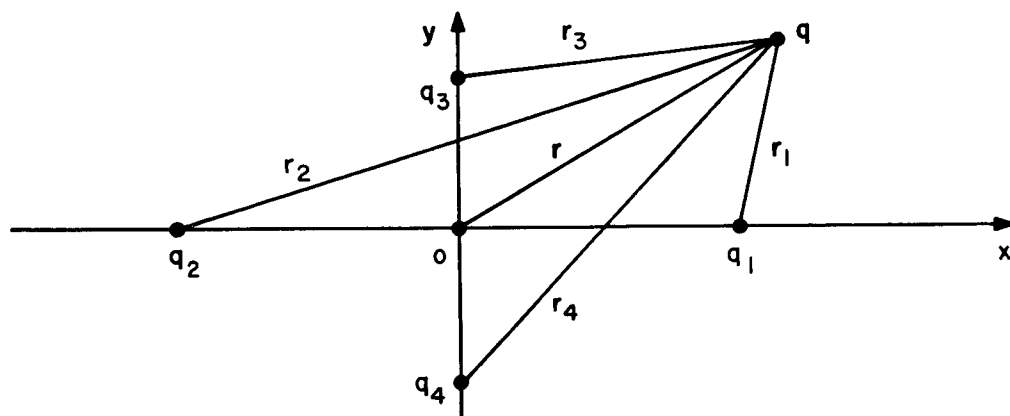


Corresponding to equation (D-3) we have

$$J \underline{\dot{r}}^2 = -2qq_1 \left[ \frac{1}{r_1} + \frac{1}{r_2} + \frac{1}{r_3} + \frac{1}{r_4} \right] + \text{constant} \qquad (D-25)$$

80

where the equi-potential curve is

$$\frac{1}{r_1} + \frac{1}{r_2} + \frac{1}{r_3} + \frac{1}{r_4} = a \qquad (D-26)$$

with

$$a = \frac{Jv_\infty^2}{2qq_1} > 0$$

This curve is symmetric with respect to both axes and the origin. The x- and y-intercepts are solutions of the equation

$$\frac{1}{|x-c|} + \frac{1}{|x+c|} + \frac{2}{\sqrt{x^2 + c^2}} = a \qquad (D-27)$$

whence intercepts > c satisfy

$$\frac{2x}{x^2 - c^2} + \frac{2}{\sqrt{x^2 + c^2}} = a \qquad (D-28)$$

and intercepts between 0 and c satisfy

$$\frac{2c}{c^2 - x^2} + \frac{2}{\sqrt{x^2 + c^2}} = a \qquad (D-29)$$

Consider equation (D-29) first, and put $x = c \tan \theta$. We find that for $0 < x < c$, i.e. for $0 < \theta < \frac{\pi}{2}$, we must have

$$2\cos^3\theta + (1-ac)\cos^2\theta - \cos\theta + \frac{ac}{2} = 0 \qquad (D-30)$$

This equation has no root in the interval $\frac{1}{\sqrt{2}} < \cos\theta < 1$, if $ac < 4$.

Now equation (D-28) under the same substitution $x = c \tan \theta$ becomes

$$\tan 2\theta = 2\cos\theta - ac \qquad (D-31)$$

which is seen to possess exactly one root in the range $x > c$, $\left( \frac{\pi}{4} < \theta < \frac{\pi}{2} \right)$

81

For $ac < 4$, the equi-potential curve has the form sketched below
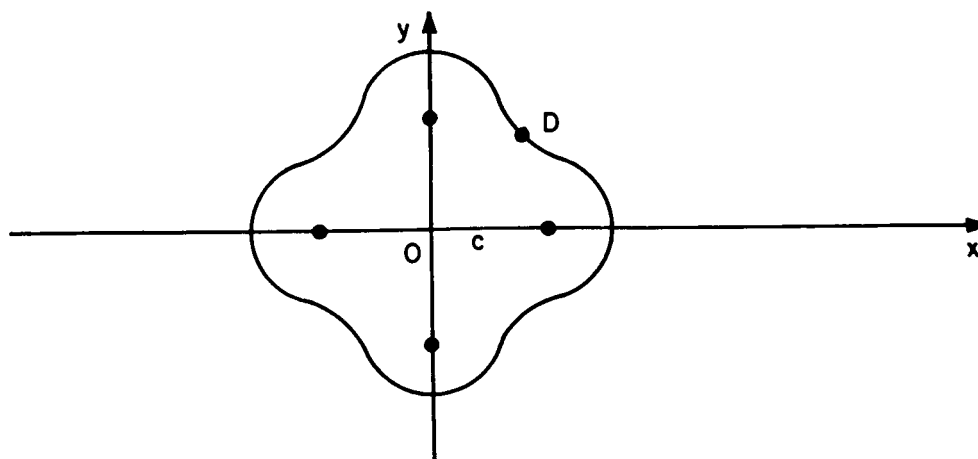


The closest that $x_1$ comes to $c$ is $x_1 = c \tan(54° 40') = 1.41c$.

When this happens, the curve deforms into four separate ovals about the four

charge foci.

The "dimple point" D is symmetrically located on the line $x = y$. It is

easy to show that $\overline{OD} \geq c$ providing $ac \leq 3.695$. Hence the shielded

region includes at least the full circle of radius $c$ providing the four equal

charges $q_i$ are chosen so that

$$q_i \geq \frac{J v_\infty^2 c}{7.39 q}$$

(D-32)

Case 5: Continuous charge distribution

As an extension of the last case, consider a continuous charge distribution

of density $\rho(x, y)$ at $(x, y)$ on a circle of radius $c$. Consider $\rho$ constant and

of the same sign as the moving charge $q$. (See following sketch.)
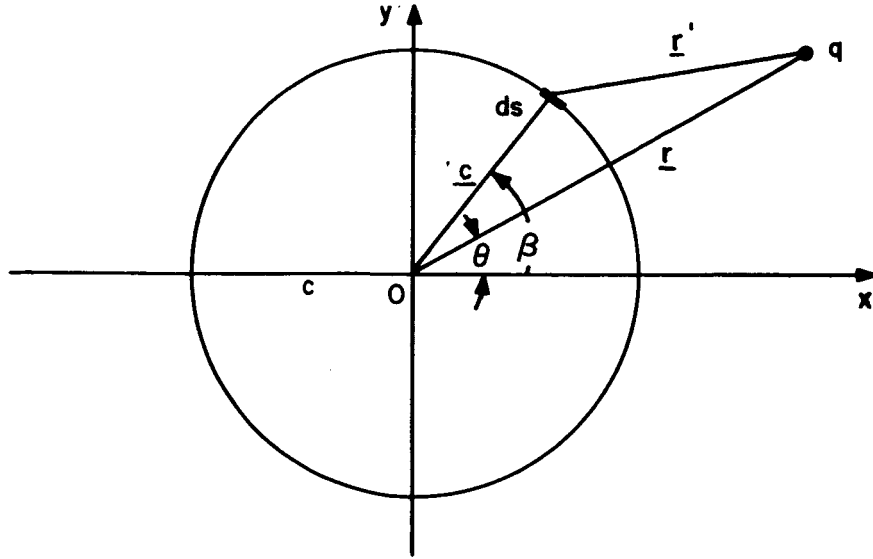
Then $\rho\,ds$ is the charge on element $ds$ of the circle of radius c. The equation of motion of the charge q (omitting the term involving $\underline{B}$ ) is

$$J\,\underline{\ddot{r}} \;=\; \rho\,q\,c \int_{o}^{2\pi} \frac{\underline{r}'\;d\beta}{r'^{3}} \tag{D-33}$$

A first integral of (D-33) is

$$J\,\underline{\dot{r}}^{2} \;=\; -\;2\,\rho\,q\,c \int_{o}^{2\pi} \frac{d\beta}{\sqrt{r^{2}+c^{2}-2\,r\,c\,\cos(\beta-\theta)}} \;+\; \text{constant} \tag{D-34}$$

The equi-potential curve is then

$$\int_{o}^{2\pi} \frac{d\beta}{\sqrt{r^{2}+c^{2}-2\,r\,c\,\cos(\beta-\theta)}} \;=\; \alpha \tag{D-35}$$

where now

$$\alpha \;=\; \frac{J\,v_{\infty}^{2}}{2\,\rho q\,c} \;>\; 0$$

In (D-35) let $\gamma = \beta - \theta$ to get

$$\int_{-\phi}^{2\pi-\theta} \frac{d\gamma}{\sqrt{r^2 + c^2 - 2rc\cos\gamma}} = a \qquad (D-36)$$

or, since the integrand is periodic of period $2\pi$

$$\int_{0}^{2\pi} \frac{d\gamma}{\sqrt{r^2 + c^2 - 2rc\cos\gamma}} = a \qquad (D-37)$$

Thus, the equi-potential curve is a circle whose radius $r$ is the positive root

of the equation

$$\frac{4}{r+c} K\left(\frac{2\sqrt{rc}}{r+c}\right) = a \qquad (D-38)$$

wherein $K(k)$ represents the complete elliptic integral of the first kind.

For a given value of $ac$ one determines $r$ from the relations.

$$r = \eta^2 c \qquad k = \frac{2\eta}{1+\eta^2} \qquad k K(k) = \frac{1}{2}\eta(ac) \qquad (D-39)$$

In general, the larger the charge density $\rho$, the greater the region shielded.

Case 6:   Three line charges

Consider three line charges, each of length $2\ell$, and having constant linear

charge density $\rho$, as shown in the following sketch:



84
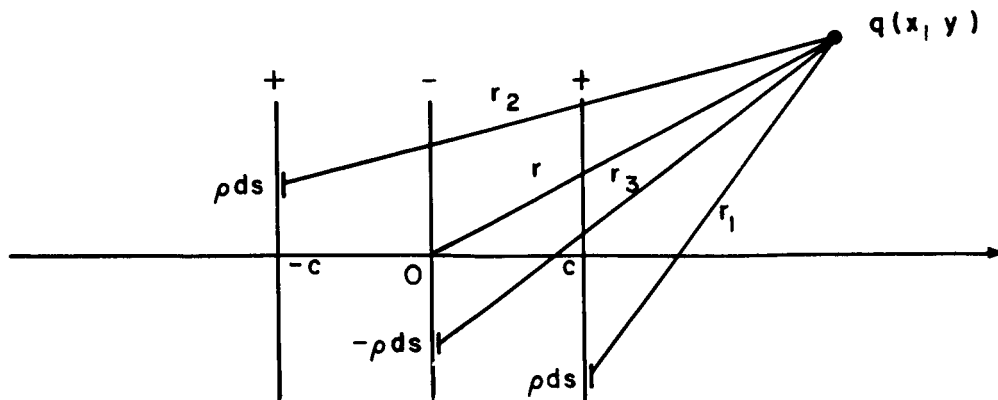
If the positively charged particle q is of mass m and charge $a$ , its equation of motion is (again omitting the $\underline{B}$ term)

$$J\ddot{\underline{r}} = \rho q \int_{-\ell}^{\ell} \left[ \frac{\underline{r}_2}{r_2^3} - \frac{\underline{r}_3}{r_3^3} + \frac{\underline{r}_1}{r_1^3} \right] ds \qquad (D-40)$$

An obvious first integral of (D-40) is

$$J\dot{\underline{r}}^2 = -2\rho q \int_{-\ell}^{\ell} \left[ \frac{1}{r_1} + \frac{1}{r_2} - \frac{1}{r_3} \right] ds + \text{constant} \qquad (D-41)$$

The equi-potential curve therefore has the equation

$$\int_{-\ell}^{\ell} \left[ \frac{1}{r_1} + \frac{1}{r_2} - \frac{1}{r_3} \right] ds = a \qquad (D-42)$$

where

$$a = \frac{J v_\infty^2}{2\rho q} > 0$$

Denoting the coordinates of q on the equi-potential curve by (x, y) and performing the integrations indicated in (D-42) we obtain

$$\left| \frac{\ell - y + \sqrt{(x-c)^2 + (\ell-y)^2}}{\ell + y - \sqrt{(x-c)^2 + (\ell+y)^2}} \cdot \frac{\ell + y - \sqrt{x^2 + (\ell+y)^2}}{\ell - y + \sqrt{x^2 + (\ell-y)^2}} \cdot \frac{\ell - y + \sqrt{(x+c)^2 + (\ell-y)^2}}{\ell + y - \sqrt{(x+c)^2 + (\ell+y)^2}} \right|$$

$$= e^a = \bar{a} > 1 \qquad (D-43)$$

From (D-43) it follows that any possible y-intercepts must satisfy

$$\left| \frac{\ell + y -}{\ell - y +} \left| \frac{\ell + y}{\ell - y} \right| \cdot \left( \frac{\ell - y + \sqrt{c^2 + (\ell-y)^2}}{\ell + y - \sqrt{c^2 + (\ell+y)^2}} \right)^2 \right| = \bar{a} \qquad (D-44)$$

85

Obviously there are no y-intercepts such that $y \geq -\ell$. If $y < -\ell$, then (D-44) is equivalent to

$$\frac{|\ell + y|}{\ell - y} = \overline{a}\left(\frac{|\ell + y| + \sqrt{c^2 + (\ell + y)^2}}{\ell - y + \sqrt{c^2 + (\ell - y)^2}}\right)^2 \qquad \text{(D-45)}$$

To see that (D-45) has no solution for $y < -\ell$, put

$$\left|\ell + y\right| = c \tan \theta, \quad \ell - y = c \tan \phi \qquad \text{(D-46)}$$

where we must have

$$0 < \theta < \phi < \frac{\pi}{2} \qquad \text{(D-47)}$$

Then (D-45) becomes

$$\frac{\tan \theta}{\tan \phi} = \overline{a}\left(\frac{\tan \theta + \sec \theta}{\tan \phi + \sec \phi}\right) \qquad \text{(D-48)}$$

or equivalently

$$\frac{\sin \theta}{\sin \phi} = \overline{a} + (\overline{a} - 1)\sin \theta > 1 \qquad \text{(D-49)}$$

But (D-49) implies that $\theta > \phi$, which contradicts (D-47). Thus we conclude that (D-43) has no y-intercepts.

Any positive x-intercepts of (D-43) must satisfy

$$F(x) = \left(\sqrt{(x-c)^2 + \ell^2} + \ell\right)\left(\sqrt{x^2 + \ell^2} - \ell\right)\left(\sqrt{(x+c)^2 + \ell^2} + \ell\right)$$
$$- a\left(\sqrt{(x-c)^2 + \ell^2} - \ell\right)\left(\sqrt{x^2 + \ell^2} + \ell\right)\left(\sqrt{(x+c)^2 + \ell^2} - \ell\right) = 0 \qquad \text{(D-50)}$$

From (D-50) we note

$$F(o) = -\overline{a}(2\ell)\left(\sqrt{c^2 + \ell^2} - \ell\right)^2 < 0 \qquad \text{(D-51)}$$

$$F(c) = 2\ell\left(\sqrt{c^2 + \ell^2} - \ell\right)\left(\sqrt{4c^2 + \ell^2} + \ell\right) > 0 \qquad \text{(D-52)}$$

$$F(\text{large } x) \sim (1 - \overline{a}) x^3 < 0 \qquad \text{(D-53)}$$

14

Hence, the equi-potential curve (D-43) crosses the positive x-axis between 0 and c, and also beyond x = c.

Since the left member of (D-43) tends to 1 as $y \longrightarrow \pm \infty$, the curve must remain in the finite part of the plane. Also, since

$$F(c/2) = \frac{c^2}{4} \left[ (1 + \overline{a}) \ell - (\overline{a} - 1) \sqrt{\frac{9c^2}{4} + \ell^2} \right] \tag{D-54}$$

one establishes readily that the curve (D-43) crosses the x-axis between 0 and c/2, whenever

$$\ell > \frac{3}{4} c \left[ \frac{\overline{a} - y}{\sqrt{\overline{a}}} \right] \tag{D-55}$$

Calculations in (D-50) can be made readily by putting $x = rc$, $\ell = fc$,

$$x - c = \ell \tan \theta, \quad x + c = \ell \tan \phi, \quad x = \tan \psi \tag{D-56}$$

Then (D-50) can be solved for $\sqrt{\overline{a}}$ in the form

$$\sqrt{\overline{a}} = \pm \frac{\tan \dfrac{\psi}{2}}{\tan \dfrac{\theta}{2} \tan \dfrac{\phi}{2}} \tag{D-57}$$

where the + sign is used for r > 1 and the minus sign for r < 1, and

$$\tan \theta = \frac{r - 1}{f}, \quad \tan \phi = \frac{r + 1}{f}, \quad \tan \psi = \frac{r}{f} \tag{D-58}$$

For $\ell = \dfrac{c}{2}$, and $\overline{a} = 2.21$, we find the intercepts in (D-50) at

$$x = 0.7c, \text{ and } x = 2c \tag{D-59}$$

Equations (D-57) and (D-58) show that as $\ell$ is shortened, $\overline{a} \longrightarrow 1$, implying that $a \longrightarrow 0$, i.e. that the charge density $\rho \longrightarrow \infty$. A sketch of the curve to the right of the y-axis follows for this case.
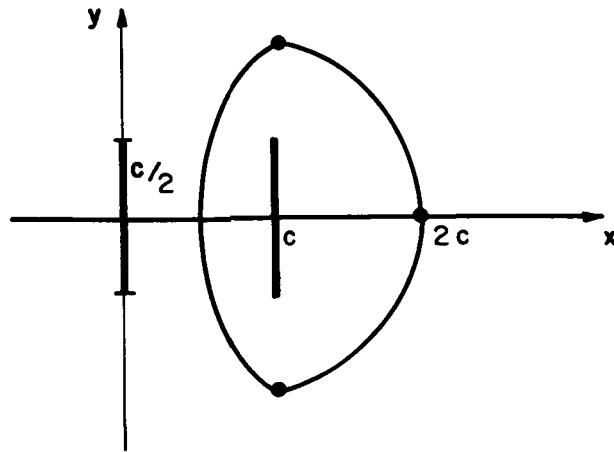
Flux across a surface at a given potential. - Consider the motion of a large

number of electrically charged particles. Assume the number of particles so

large that their distribution can be described in terms of a density function

$$R \equiv R \ (\underline{r}, \ \mu \ ) \tag{D-60}$$

where $\underline{r} \equiv (x, \ y, \ z)$ and $\mu \equiv ( \mu_x, \ \mu_y, \ \mu_z)$ define the location and momentun of

a particle. The particle density is also assumed so small that the interactions

between particles can be neglected.

If dN is the number of particles in $d\underline{r}$ about $\underline{r}$, and $d\underline{\mu}$ about $\underline{\mu}$, then

$$d N = R \, dx \, dy \, dz \, d\mu_x \, d\mu_y \, d\mu_z \tag{D-61}$$

The forces governing the motions of the individual particles are assumed to

be electric in nature, being derivable from a potential function $\phi*$. The

Hamiltonian function appropriate here for any given particle of mass m is

$$H* \ = \ \frac{1}{2m} \ ( \mu_x^2 + \mu_y^2 + \mu_z^2 \ ) \ + m\phi * \tag{D-62}$$

Since H* is different for particles of different masses, we can treat all the

particles on the same footing by considering the Hamiltonian per unit mass $\overline{H}*$:

$$\overline{H}* = \frac{1}{2}(u^2 + v^2 + w^2) + \phi*(x, y, z, \tau) \qquad \text{(D-63)}$$

where u, v, w are the Cartesian components of velocity.

The canonical equations for the motion of any one particle are then

$$\dot{x} = \frac{\partial \overline{H}*}{\partial u}, \quad \dot{y} = \frac{\partial \overline{H}*}{\partial v}, \quad \dot{z} = \frac{\partial \overline{H}*}{\partial w} \qquad \text{(D-64)}$$

$$\dot{u} = -\frac{\partial \overline{H}*}{\partial x}, \quad \dot{v} = -\frac{\partial \overline{H}*}{\partial y}, \quad \dot{w} = -\frac{\partial \overline{H}*}{\partial z} \qquad \text{(D-65)}$$

Liouville's Theorem (see ref. 27), which asserts that the density of any element $d\underline{r}\, d\mu$ of phase space remains constant during its motion according to the canonical equations ( D-64) and (D-65) is now applicable.

Thus, if $\dfrac{D}{D\tau}$ is the Stokes operator

$$\frac{D}{D\tau} \equiv \frac{\partial}{\partial \tau} + \sum_{x, y, z} \left[ \dot{x} \frac{\partial}{\partial x} + \dot{u} \frac{\partial}{\partial u} \right] \qquad \text{(D-66)}$$

we must have

$$\frac{DR}{D\tau} = 0 \qquad \text{(D-67)}$$

Applied to our case, (D-67) becomes

$$\frac{\partial R}{\partial \tau} + \sum_{x, y, z} \left[ \frac{\partial \overline{H}*}{\partial u} \frac{\partial R}{\partial x} - \frac{\partial \overline{H}*}{\partial x} \frac{\partial R}{\partial u} \right] = 0 \qquad \text{(D-68)}$$

If we assume the density to be steady in time, then $\dfrac{\partial R}{\partial \tau} \equiv 0$, and R

satisfies the partial differential equation

$$\sum_{x, y, z} \left[ \frac{\partial \overline{H}*}{\partial u} \frac{\partial R}{\partial x} - \frac{\partial \overline{H}*}{\partial x} \frac{\partial R}{\partial u} \right] = 0 \qquad \text{(D-69}$$

An obvious solution of (D-69) is

$$R = \overline{H}* = \frac{1}{2}(u^2 + v^2 + w^2) + \phi*(x, y, z) = \text{constant} \qquad \text{(D-70)}$$

or

$$R = E + \phi* \tag{D-71}$$

Since the flux of particles across a surface element ds at P is proportional to R at P, we find from (D-71) that the flux across ds at P in the presence of the field $\phi*$ is $1 + \dfrac{\phi*(P)}{E}$ times the flux when $\phi*$ is not present.

In particular, the surface $\phi*(P) = -E$ defines a region of zero flux, i.e. a region into which the charged particles do not enter.

| | | |
|---|---|---|
| a | $\dfrac{Jv_\infty^2}{2qq_1}$ | (see Appendix D) |
| $\bar{a}$ | $e^a$ | |
| A | area | |
| B | magnetic flux density | |
| c | a distance | |
| C | a dimensional constant used in an approximate range-energy equation | |
| C*, C** | constants of integration | |
| D | a maximum, or "dimple" point (see Appendix D) | |
| e | electrostatic charge on particle | |
| E | particle energy | |
| f | a constant (used in Appendix D) | |
| F | force | |
| H | mast height | |
| H* | Hamiltonian function | |
| $\overline{H}$* | Hamiltonian per unit mass | |
| $\bar{i}$ | current density | |
| I | current | |
| J | $4\pi \epsilon_o m$ (see Appendix D) | |
| K | constant of proportionality | |
| K(k) | complete elliptic integral of the first kind | |
| $\ell$ | length | |
| $L_i$ | Loading Index | |
| m | mass of particle | |

| | |
|---|---|
| M | m/Be, proton mass/charge ratio, divided by magnetic density flux |
| h | a constant |
| N | number of particles per $cm^2$ per ster-radian |
| p | pressure |
| q | electrostatic charge |
| r | radius |
| R | a density function, used in Appendix D |
| s | distance |
| t | thickness |
| u, v, w | Cartesian components of velocity |
| v | velocity |
| V | potential |
| $V_{Ref}$ | reference (shielded) volume |
| $w_\infty$ | weight per unit area to stop normally incident protons |
| W | weight |
| x | spacing |
| x, y, z | coordinates |
| $\alpha$ | angle of incident (measured to normal) |
| $\alpha, \beta, \gamma, \varphi, \psi$ | angles |
| $\epsilon_o$ | electrical permittivity of space |
| $\eta$ | a fraction, used in the product $\eta\rho$ to give an effective density, also employed in equation (D-39) |
| $\mu$ | momentum |
| $\rho$ | density |
| $\sigma$ | stress |

$\tau$         time

$\varphi^*$        a potential function

$\chi$         a constant

## Subscripts

| | |
|---|---|
| Ave | average |
| Cir | circle, or circular |
| Cyl | cylinder, or cylindrical |
| eff | effective |
| Elect. | electrode |
| Exit | exit |
| Front | frontal |
| Mast | mast |
| max | maximum |
| o | initial |
| Ref | reference |
| Req'd | required |
| Sph | sphere, or spherical |
| Spectrum | spectrum |
| $\infty$ | at infinity, or of infinite radius |

# REFERENCES

1. Keller, J. W.: Uncertainties in Space Radiation Shielding Calculations. Presented at American Rocket Society "Space Flight Report to the Nation", Preprint No. 2136-61, October 1961.

2. Keller, J. W.: A Study of Shielding Requirements for Manned Space Missions, Convair Report No. FZK-124, Convair Nuclear Research and Development Laboratory, Fort Worth, Texas, October 10, 1960.

3. Tolan, J. H. (editor): Annual Report - 1960, Shielding Problems in Manned Space Vehicles. Lockheed Nuclear Products Co., Report No. NR-140, September 1961.

4. Wallner, Lewis E.; and Kaufman, Harold R.: Radiation Shielding for Manned Space Flight. NASA TN D-681, July 1961.

5. Vosteen, Louis F.: Environmental Problems of Space Flight Structures II. Ionizing Radiation in Space and Its Influence on Spacecraft Design. NASA TN (to be published).

6. Abel, J.: Radiation Considerations for Lunar Missions. Presented at 8th Annual Meeting, American Astronautical Society, Preprint 62-37, Jan. 1962.

7. Rosche', Melvin G.: Private communication. December 14, 1961.

8. Anon.: Neutron Physics Progress Report, Part 8. Oak Ridge National Laboratory, September 1961.

9. Singer, S. F.: Effects of Interplanetary Dust and Radiation Environment on Space Vehicles. Second International Symposium on the Physics and Medicine of the Atmosphere and Space. San Antonio, Texas, November 1958.

10. Dow, Norris F.: Structural Implications of the Ionizing Radiation in Space. General Electric Co. TIS Report No. R60SD376, November 1959.

11. Levy, Richard H.: Radiation Shielding of Space Vehicles by Means of Superconducting Coils. AFBSD TN-61-7, April 1961.

12. Kronzler, J. E.; Buchler, E.; Hsu, F. S. L.; and Wernick, J. H.: Superconductivity in $Nb_3Sn$ at High Current Density in a Magnetic Field of 88 Kgauss. Physical Review Letters, vol. 16, no. 3, Feb. 1, 1961.

13. Barnes, T. G.; Finkelman, E. M.; and Barazotti, A. L.: Radiation Shielding of Lunar Spacecraft. Presented at American Astronautical Society Lunar Flight Symposium, New York City, December 1960.

14. Shanley, F. R.: Weight-Strength Analysis of Aircraft Structures. McGraw-Hill Book Co., 1952.

15. Robey, D. H.: Radiation Shield Requirements for Two Large Solar Flares. Astronautica Acta vol. VI, fasc. 4, June 1960.

16. Dye, D. L.; and Noyes, J. C.: Biological Shielding for Radiation Belt Particles. Journal Astronautical Sciences, vol. VII, no. 3, Fall 1960.

17. Dow, Norris F.: Primary Proton Protection, Part I: Uni-Directional Particles. Space Mechanics Memo #101, General Electric Co. Space Sciences Laboratory, Philadelphia, Pa.; November 1960.

18. Dow, Norris F.: Primary Proton Protection, Part II: Two-Dimensionally Isotropic Particles and Electrostatic Shielding. Space Mechanics Memo #103, General Electric Co. Space Sciences Laboratory, Philadelphia, Pa.; May 1961 (rev.)

19. Dow, Norris F.: Primary Proton Protection, Part III: Geometry, Energy, and Minimum Weight. Space Mechanics Memo #104, General Electric Co. Space Sciences Laboratory, Philadelphia, Pa.; September 1961.

20. Dow, Norris F.: Primary Proton Protection, Part IV: Isotropic Particles and Electromagnetic Shielding. Space Mechanics Memo #105, General Electric Co. Space Sciences Laboratory, Philadelphia, Pa.; December 1961.

21. Atkinson, John H., Jr.; and Willis, Beverly Hill: High Energy Particle Data, vol. II. Univ. of Calif. Report No. UCRL-2426 (rev.), June, 1957.

22. Hughes, Robert F.: On Shielding Satellites and Space Vehicles from High-Energy Particles. General Electric Co. Space Sciences Laboratory, Aerophysics Operation Tech. Memo. No. 148, January 1960.

23. Jacobs, George J. (editor): Proceedings of Conference on Radiation Problems in Manned Space Flight. NASA TN D-588, December 1960.

24. Anon.: Design of Apparatus to Withstand Short-Circuit Forces. General Electric Standards, Section Q103.1, July 1953.

25. Corliss, William R.: Propulsion Systems for Space Flight. The McGraw-Hill Book Co., Inc., New York, 1960.

26. Shen, S. P.: Symposium on Aerospace Radiobiology, II: On the Shielding of Cosmic Rays. Aerospace Medicine 32, 901, 1961.

27. Chandrasekhar, S.: Principles of Stellar Dynamics. Dover Publications, New York, 1960.
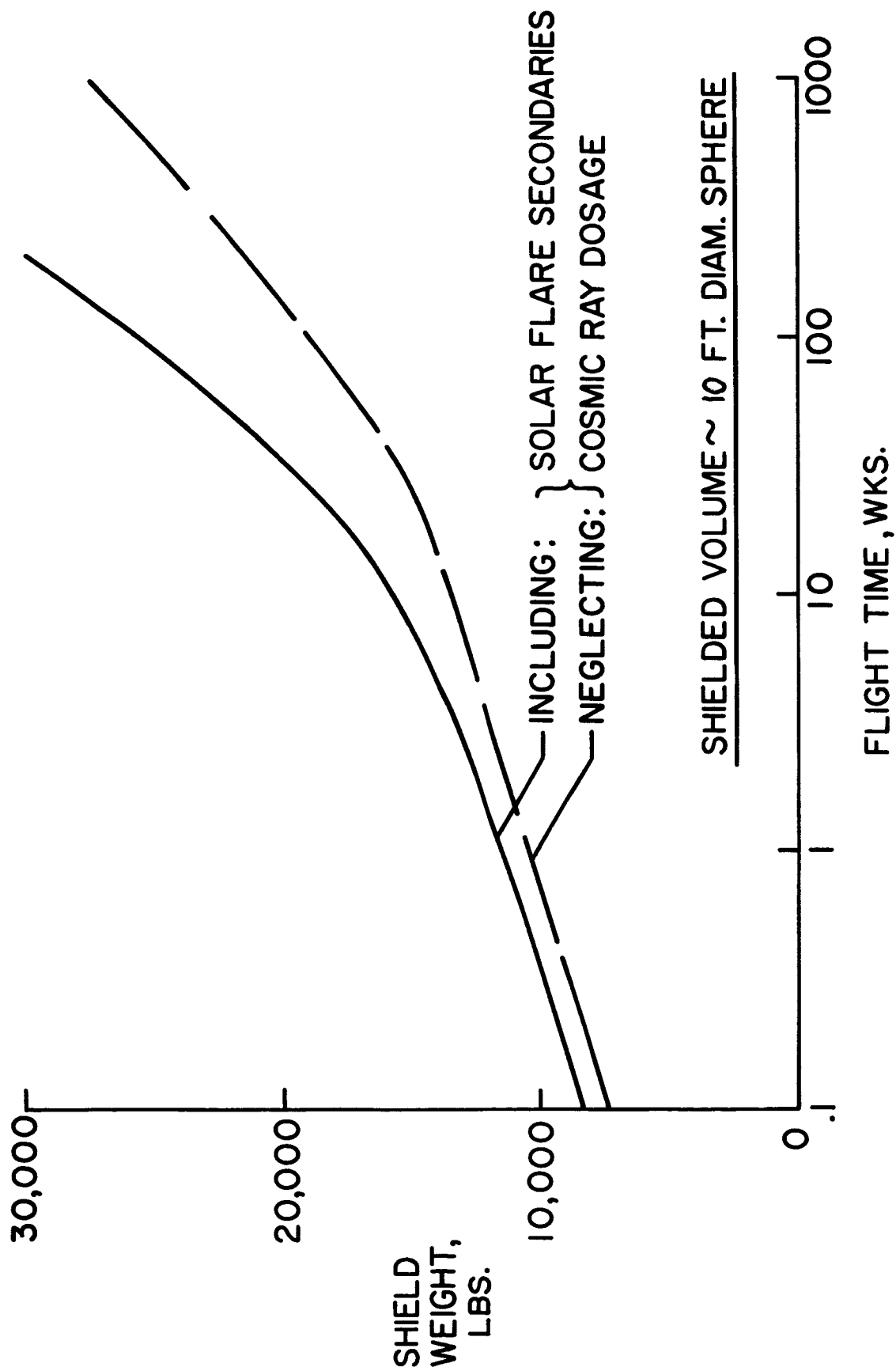
Figure 1. Carbon Shield Weight Required for a 10 Foot Sphere to Give a 99% Probability of Accumulating Less Than 100 Rem Total Dosage (based on refs. 2, 4 and 6).
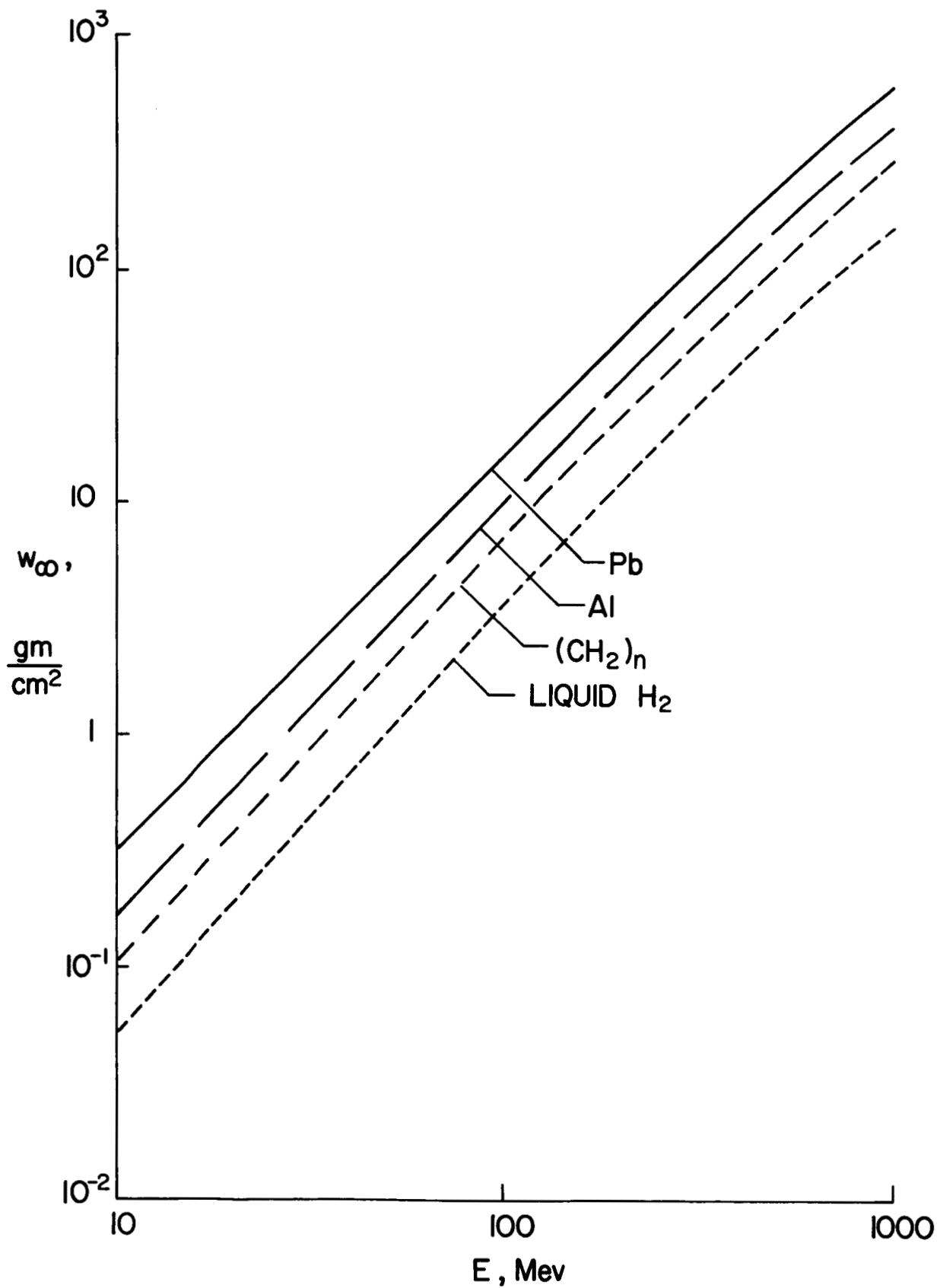
Figure 2. Range-Energy Curves for Attenuation of Protons by Excitation and Ionization of Atoms of Shield Material (based on refs. 17 and 18).
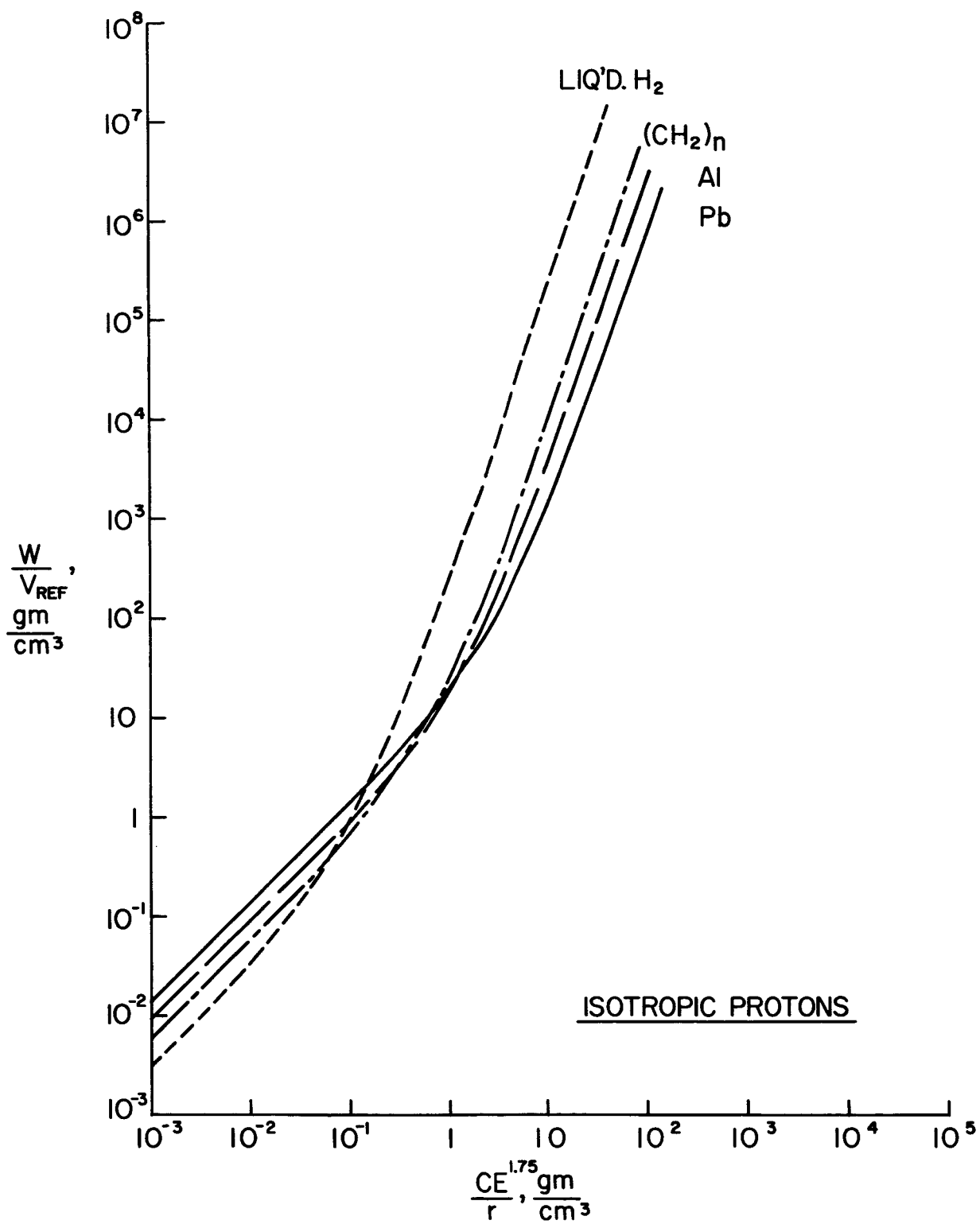
Figure 3. Loading-Index Evaluation of Efficiency of Passive
(Spherical) Shielding for Isotropic Protons.

99
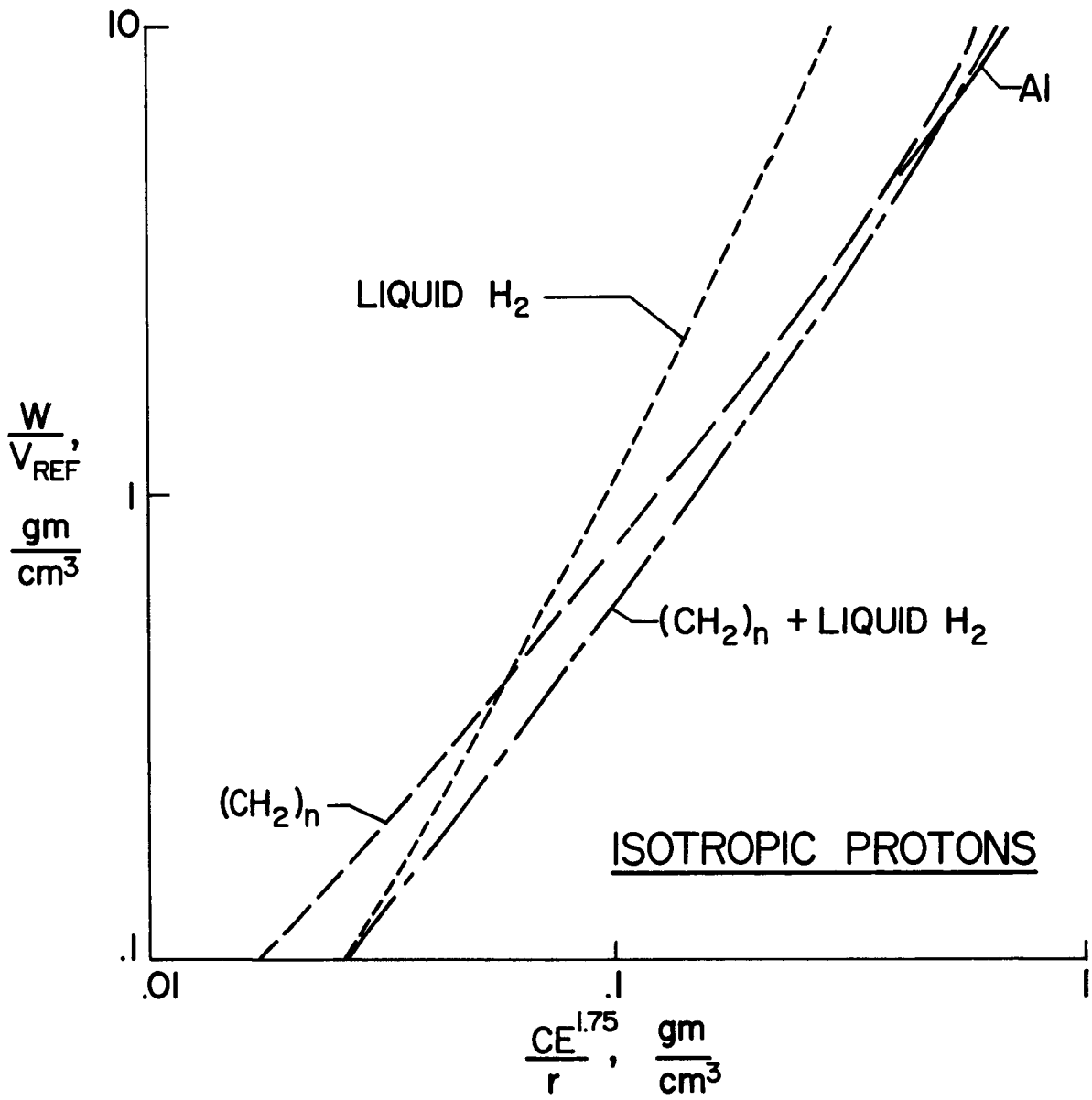
Figure 4. Illustration of Use of Loading-Index Evaluation of Composite-Material (Spherical) Shielding for Isotropic Protons.
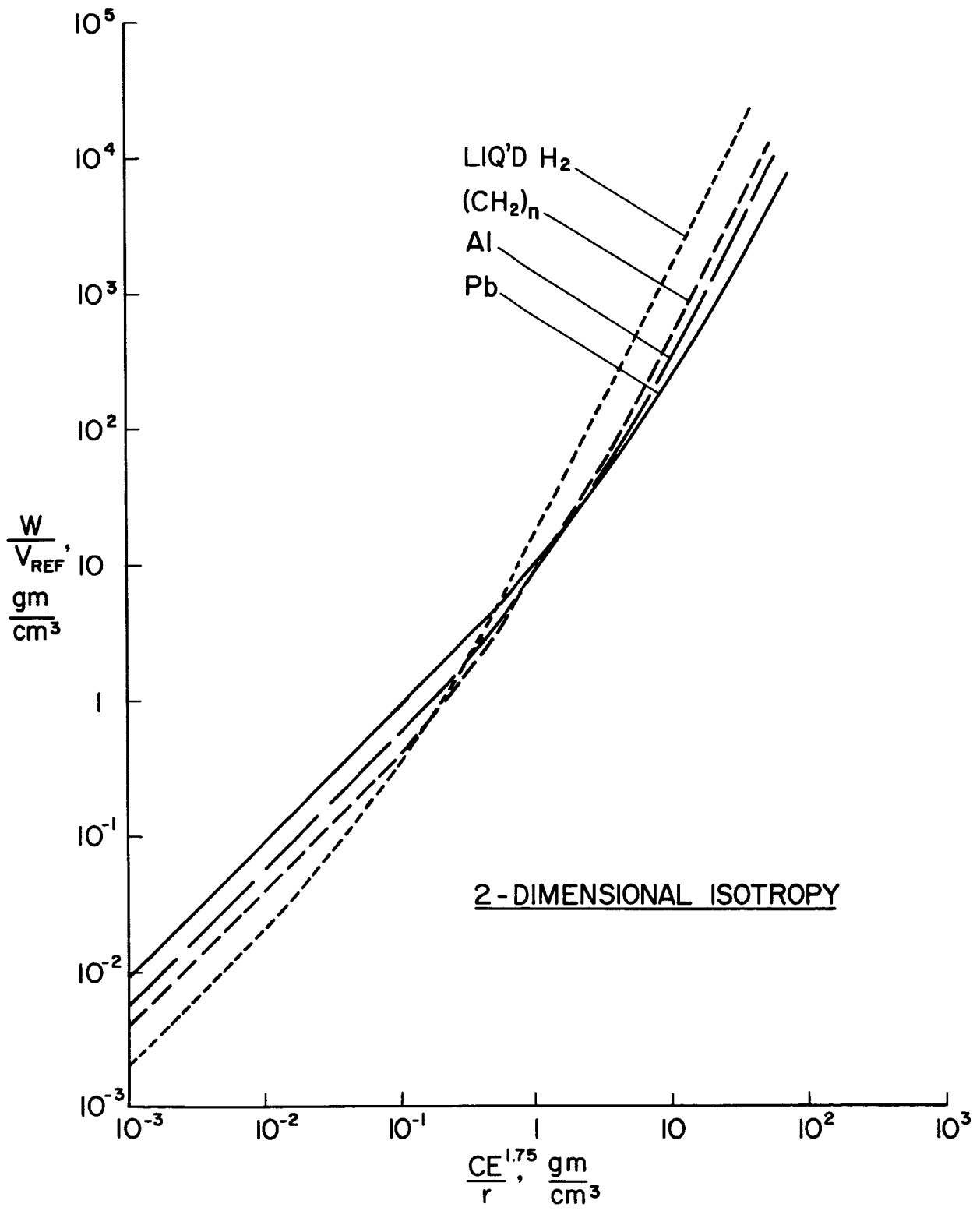
Figure 5. Loading-Index Evaluation of Efficiency of Passive (Cylindrical)
Shielding for 2-Dimensionally Isotropic Protons, with Cylindrical
Volume Shielded Equal to That of Sphere of Same Radius as the
Cylinder.
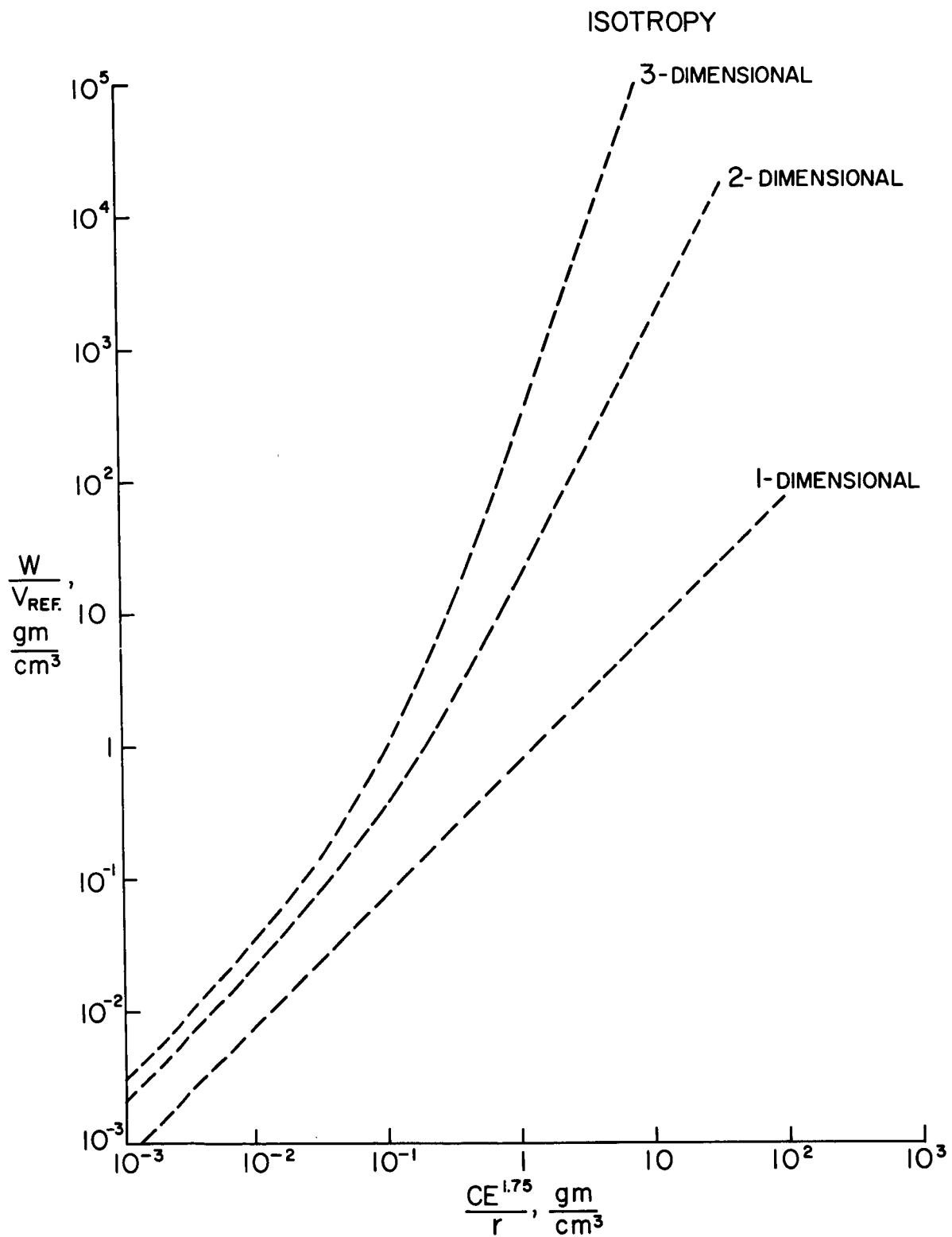
Figure 6. Loading-Index Comparison of Efficiency of Shielding for Various Particle Directionalities, Liquid Hydrogen as the Shield Material, and Spherical (or Equal Radius Cylindrical) Volumes to be Shielded.

102
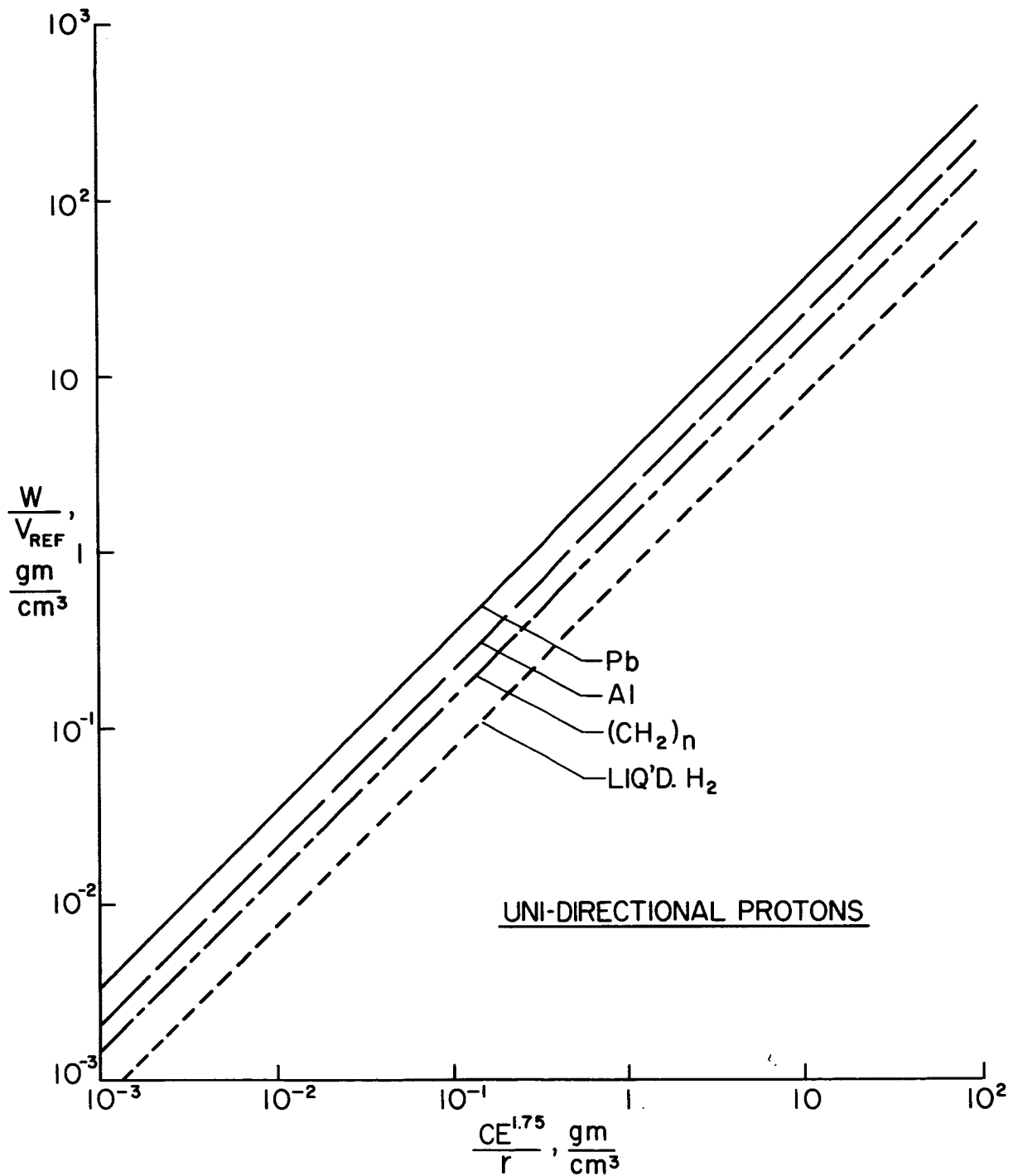
Figure 7. Loading-Index Evaluation of Efficiency of Passive (Disk)
Shielding for Uni-Directional Protons, with Shielded Volume
a Sphere, or an Equal-Radius Cylinder End-on to the Radiation.
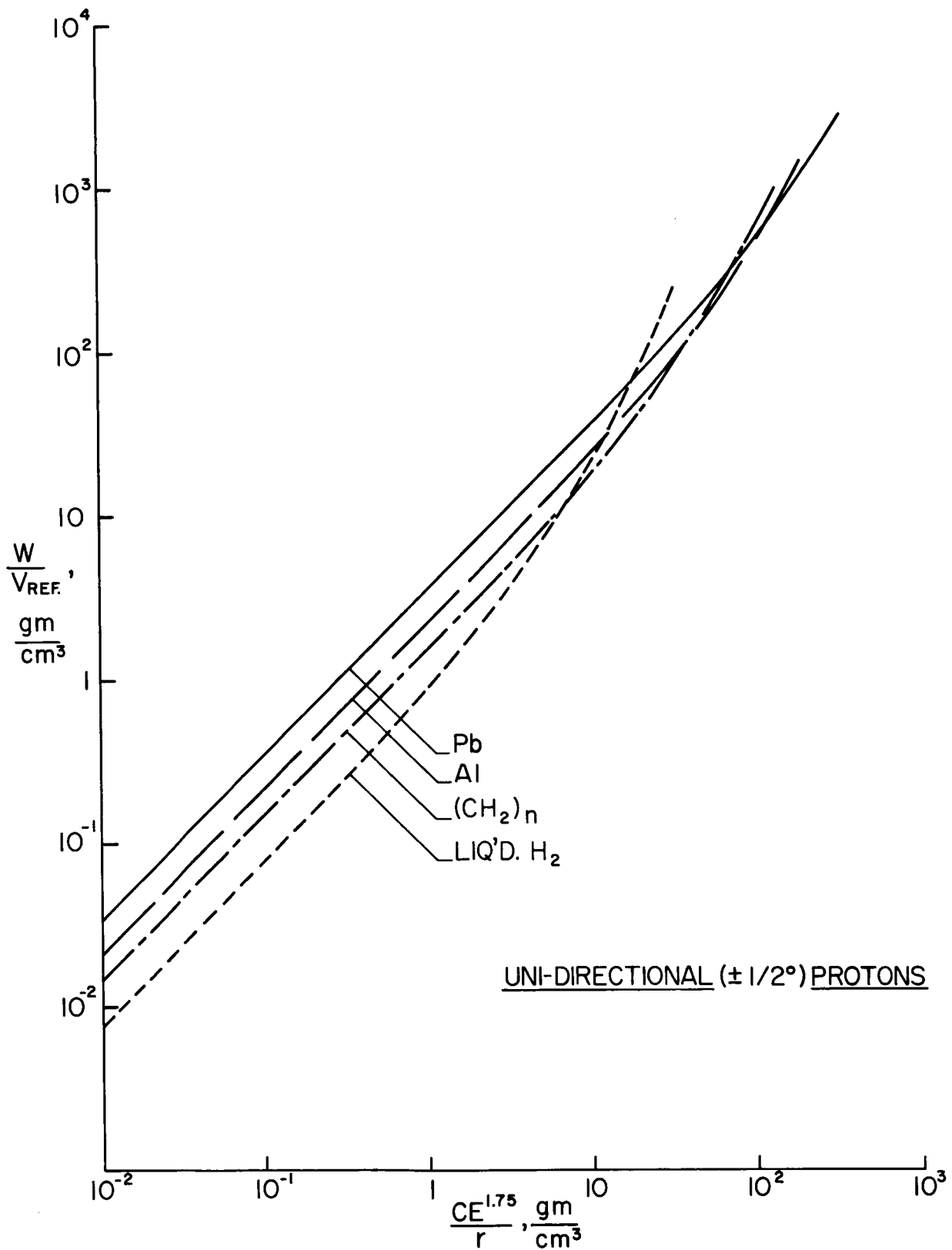
Figure 8. Loading-Index Evaluation of Efficiency of Passive (Umbrella-like) Shielding for Protons Having Slight (1/2°) Angular Deviations from Uni-Directionality. The Shielded Volume is Spherical.
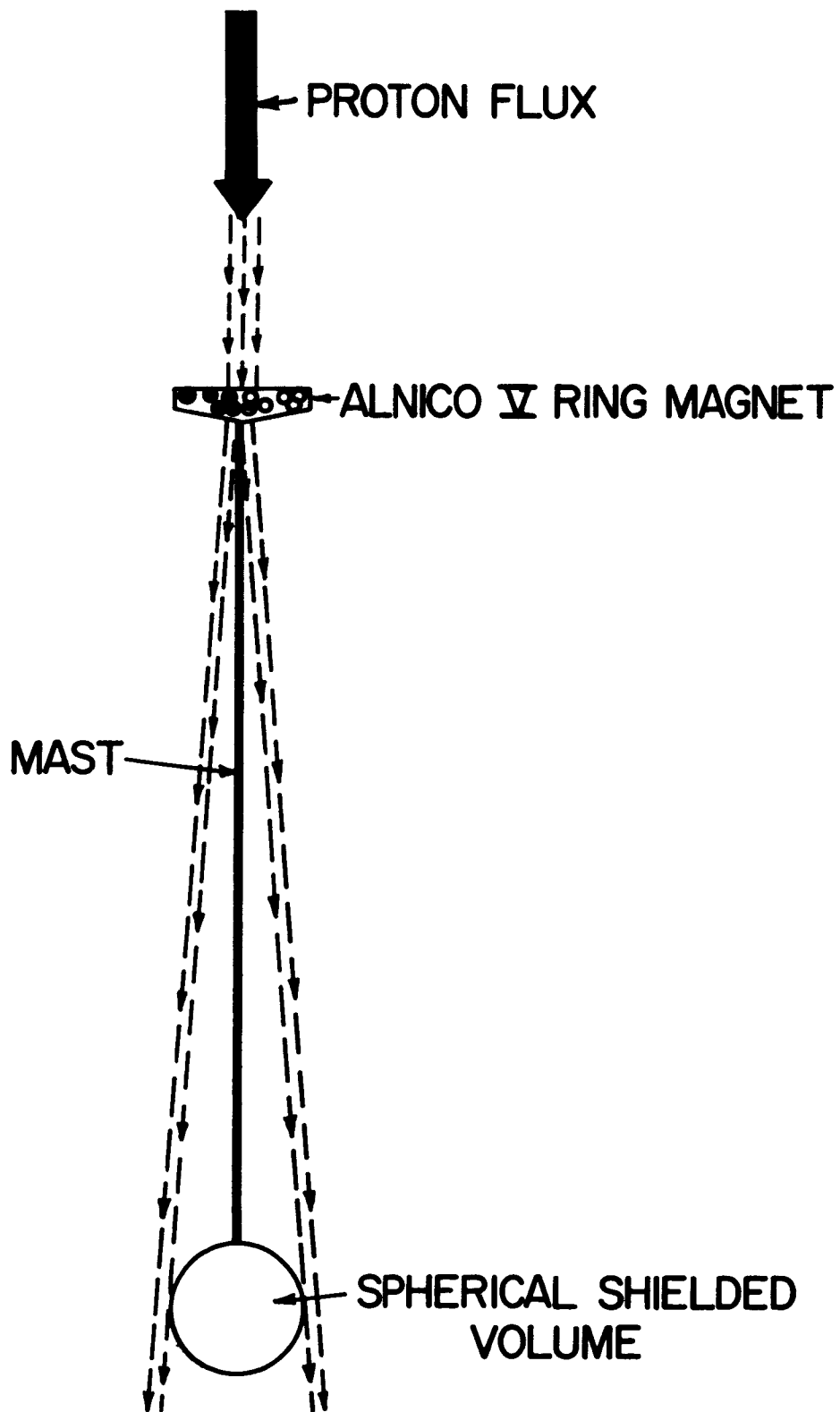
Figure 9. Schematic Representation of Simple, Permanent-Magnet, Active Shielding System Considered for Uni-Directional Protons.
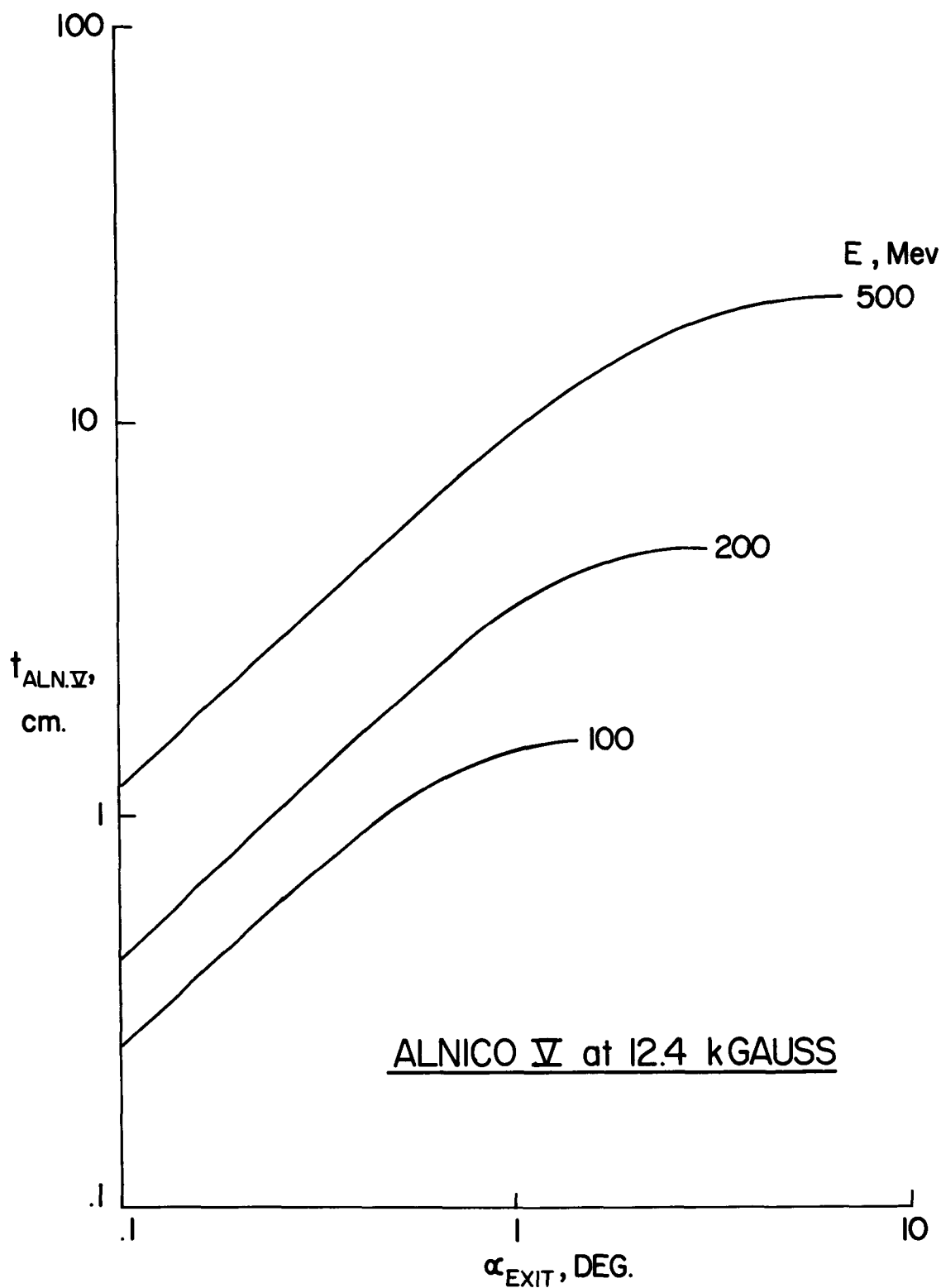
Figure 10. Angles of Diversion $\alpha_{Exit}$ of Protons Normally Incident on Alnico V
Material of Thickness $T_{Aln.\ V}$, and Having a Residual Magnetic Flux
(Normal to the Proton Path) of 12,400 gauss. Curves Calculated by
the Approximate Equations of Appendix A.
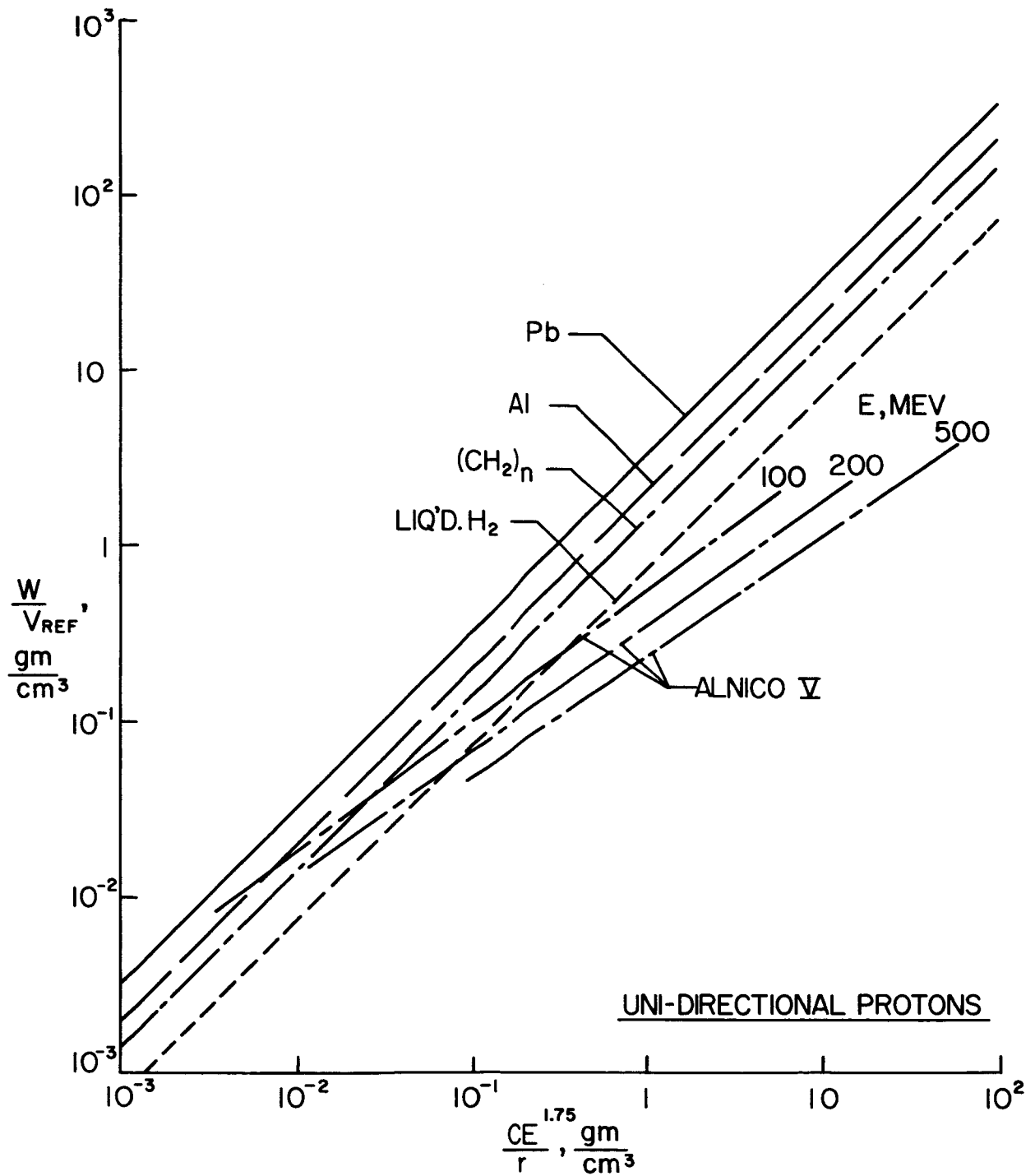
Figure 11. Comparison of Efficiency of Active, Permanent-Magnet, Disk
Shielding with Passive Shielding for the Ideal Case of Uni-
Directional Particles Perfectly Alined with the Axis of the
Shielding System.
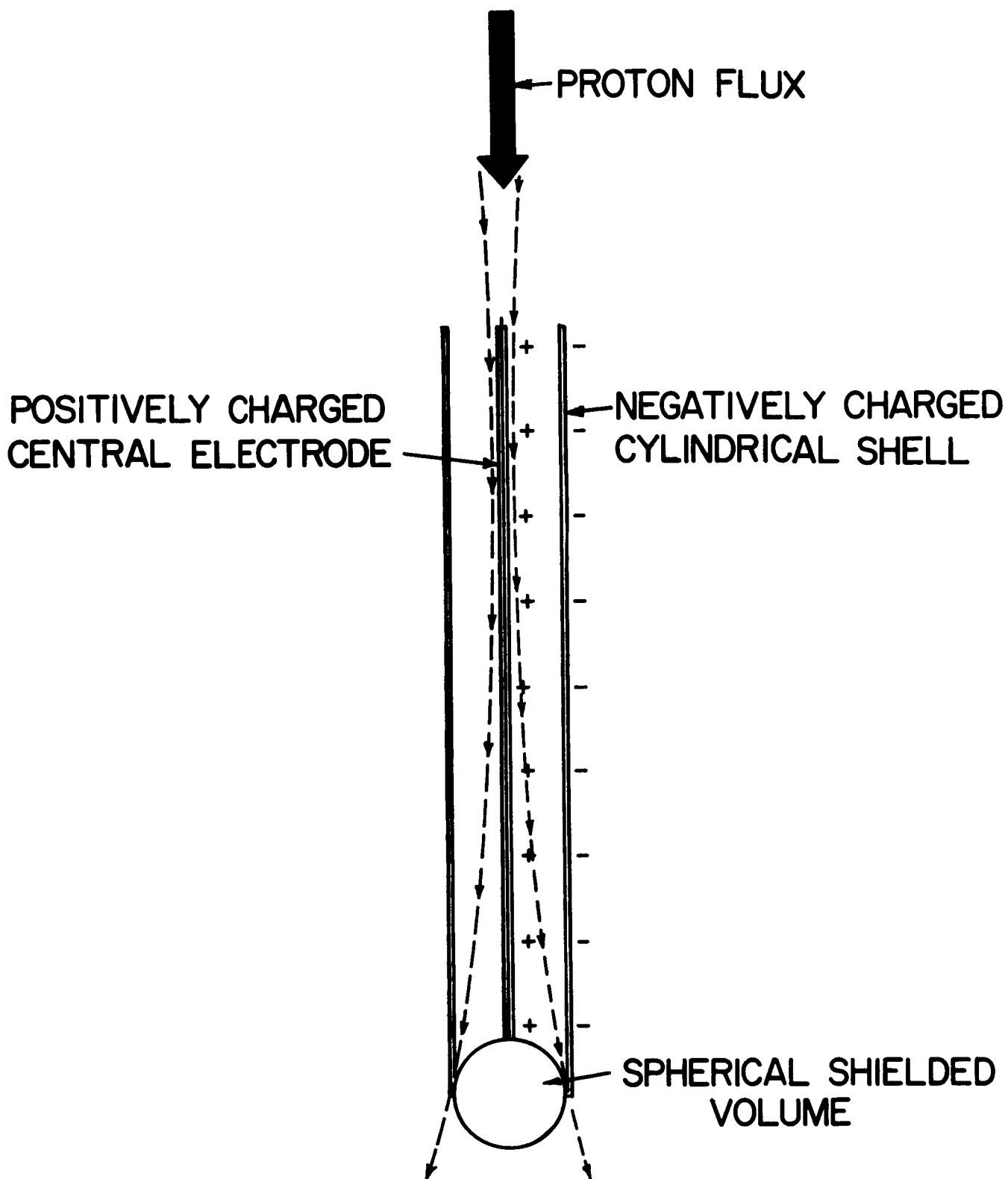
Figure 12. Schematic Representation of Simple Electrostatic Shielding
System Considered for Uni-Directional Protons.
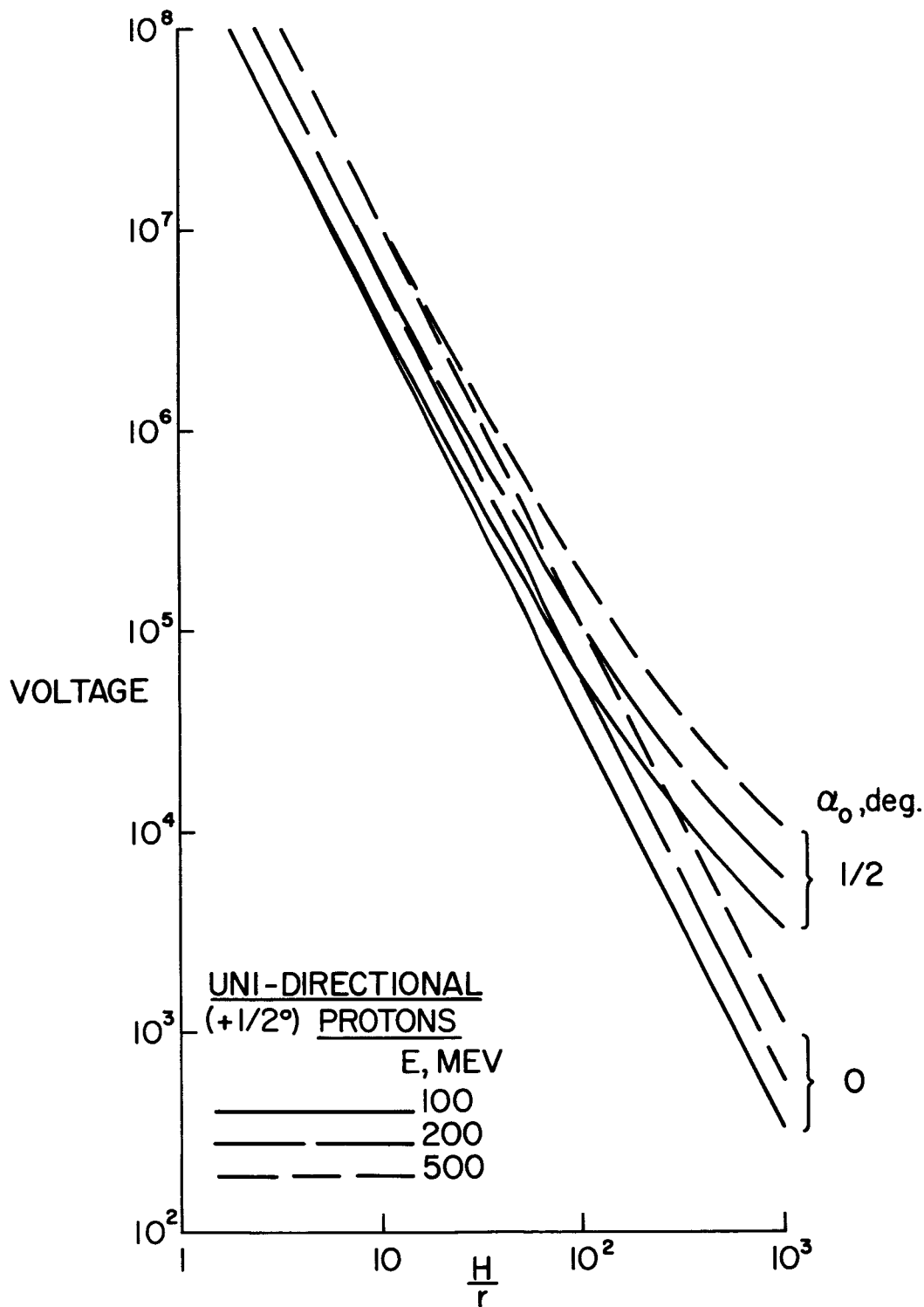
Figure 13. Height/Radius Ratios H/r of Deflecting Electrodes Required
For Diverting Uni-Directional Protons of Given Energies at
Various Applied Electrostatic Voltages.
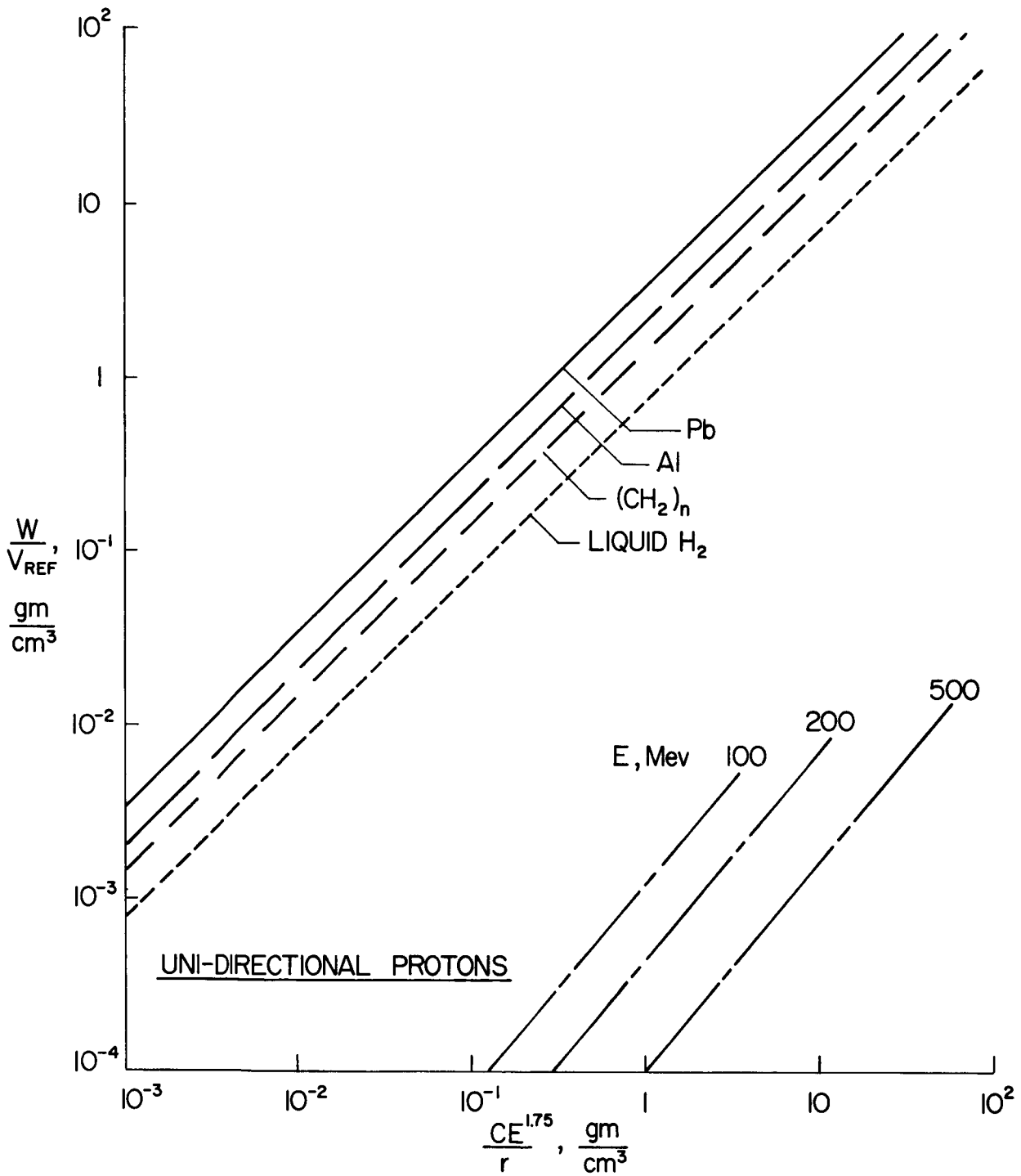
Figure 14. Comparison of Weights of Ideal Active Electrostatic Shielding
Electrodes with Passive Shielding for Perfectly Alined,
Uni-Directional Protons.

110
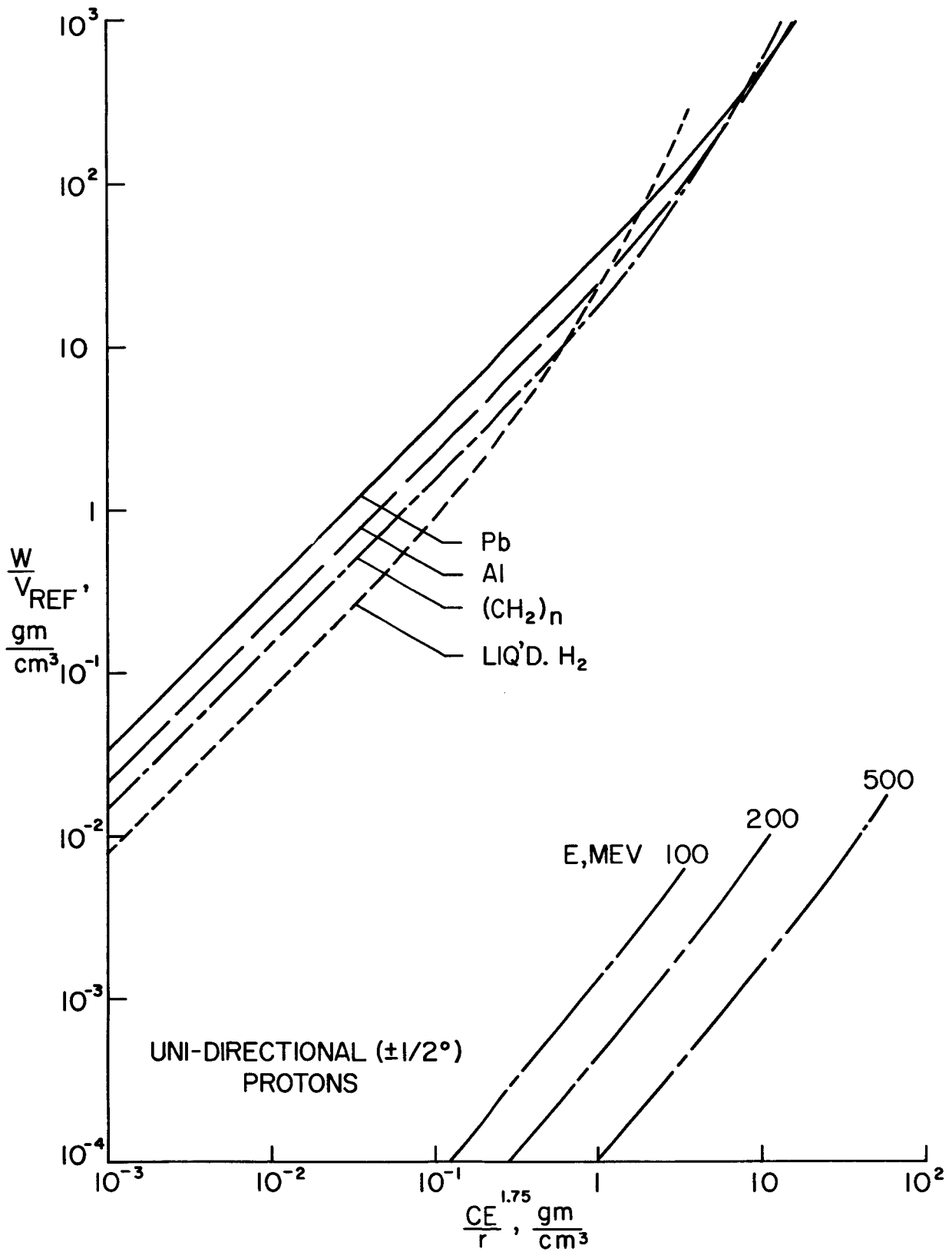
Figure 15. Comparison of Weights of Ideal, Active Electrostatic Shielding
Electrodes with Passive Shielding, for $1/2°$ Angular Misalinement
Between Incident Uni-Directional Protons and Shielding System.

111
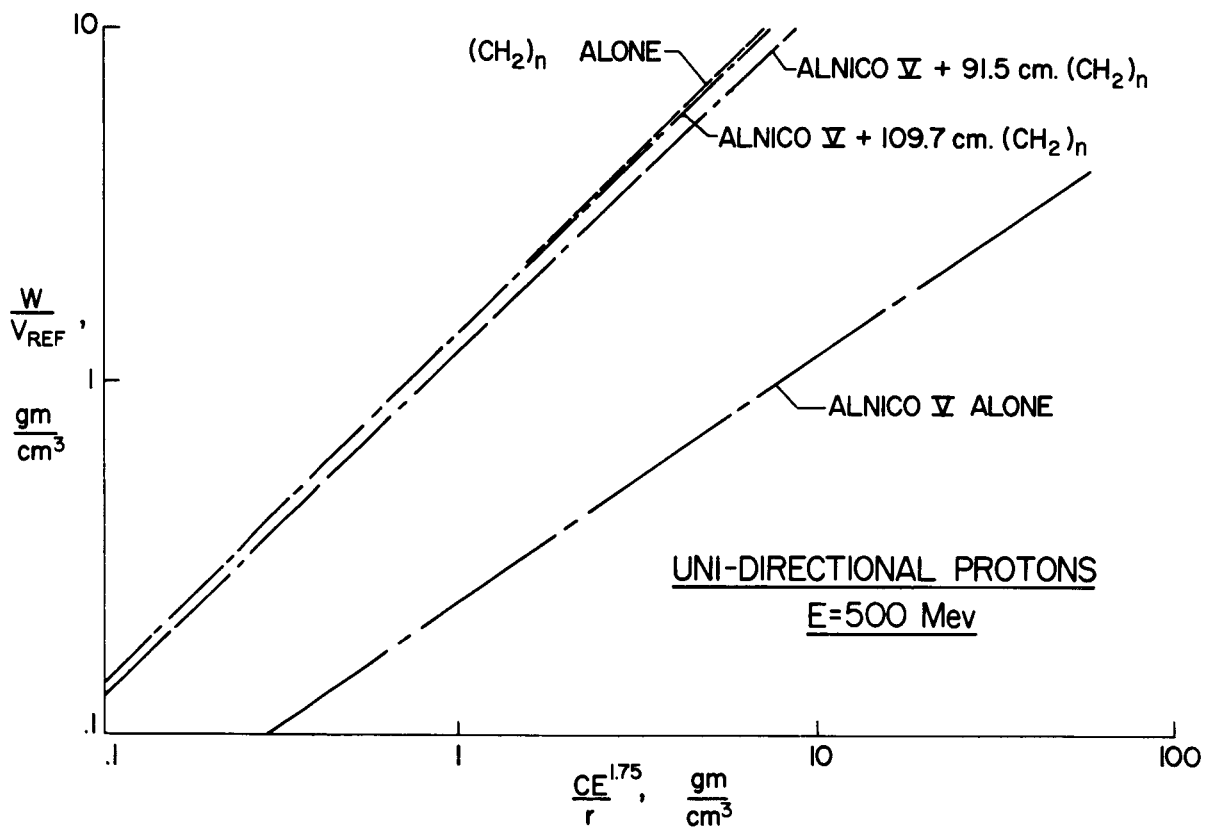
Figure 16. Evaluation of Combination Active, Permanent-Magnet and Passive Polyethylene Shielding System for Uni-Directional Particles.

112
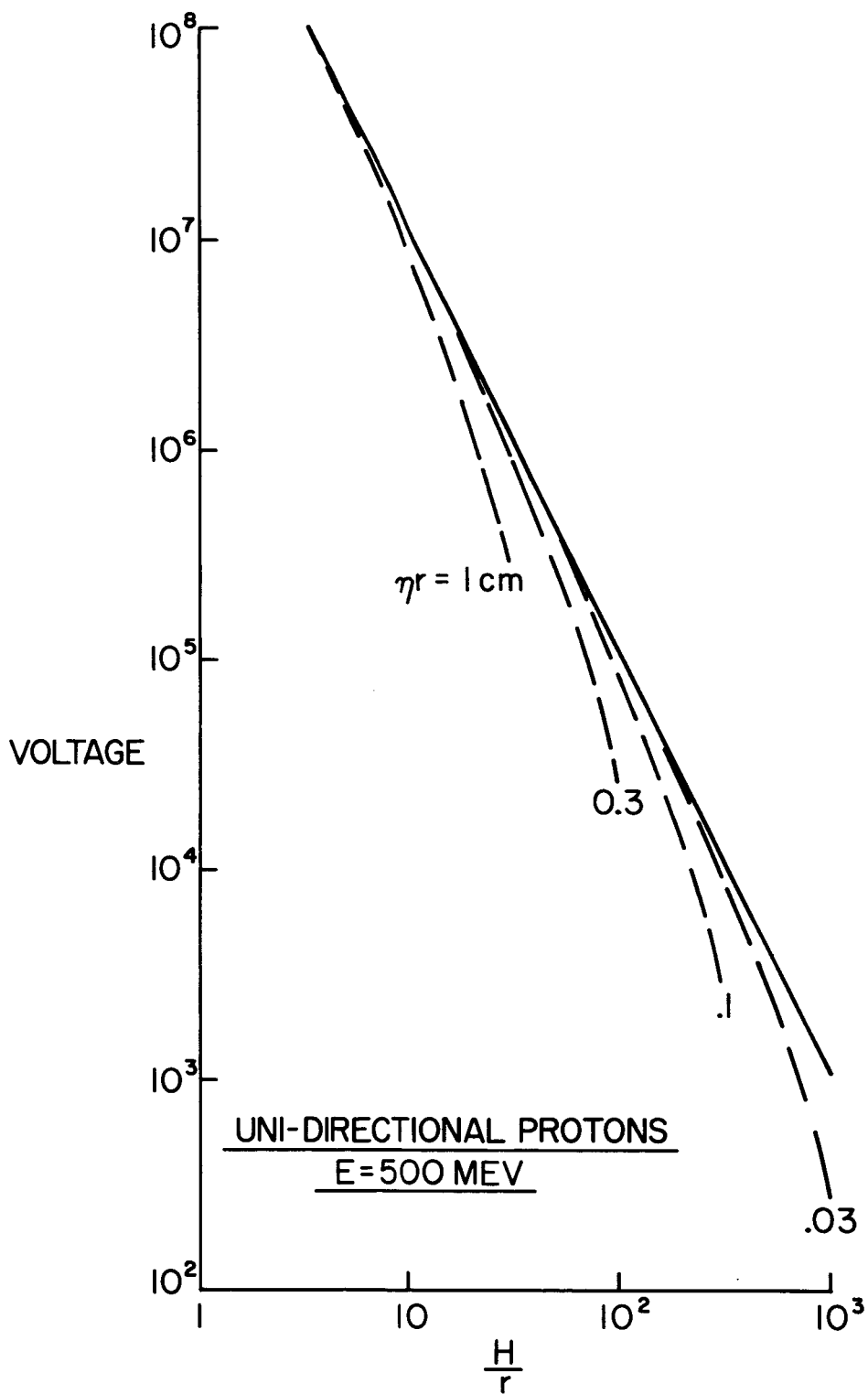
Figure 17. Height/Radius Ratios H/r of Deflecting Electrodes and Voltages Required in Combination with Polyethylene - Distributed so that Its Retarding Thickness is $\eta$ Times the Electrode Length - To Divert Uni-Directional 500 Mev Protons.
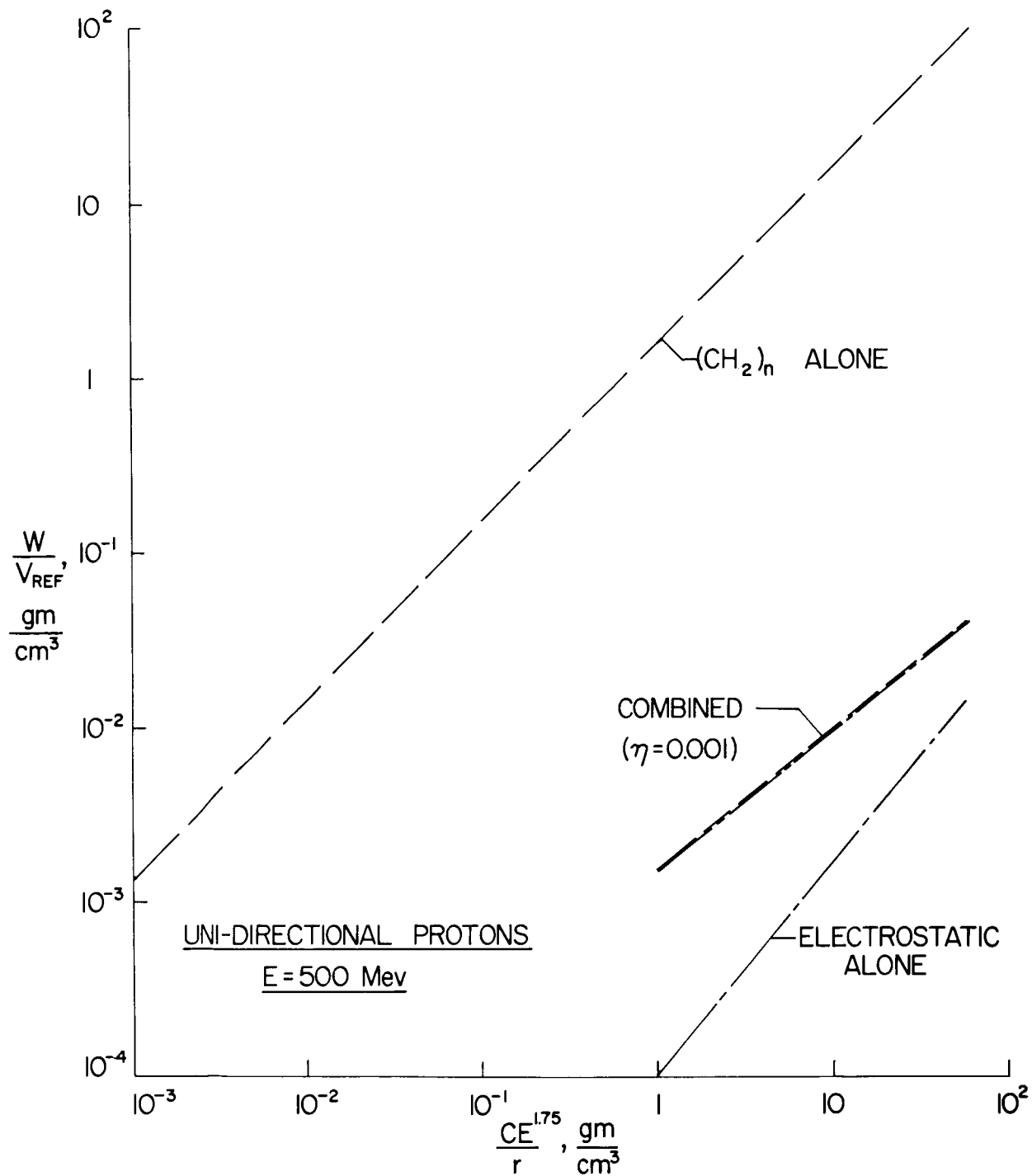
Figure 18. Comparison of: (1) Combination Active, Electrostatic and Passive, Polyethylene Shielding, with (2) Simple Active and Passive Systems For Uni-Directional, 500 Mev Protons, and For a Distributed Density $\eta$ of the Polyethylene of 0.001 in the Combined System.

114
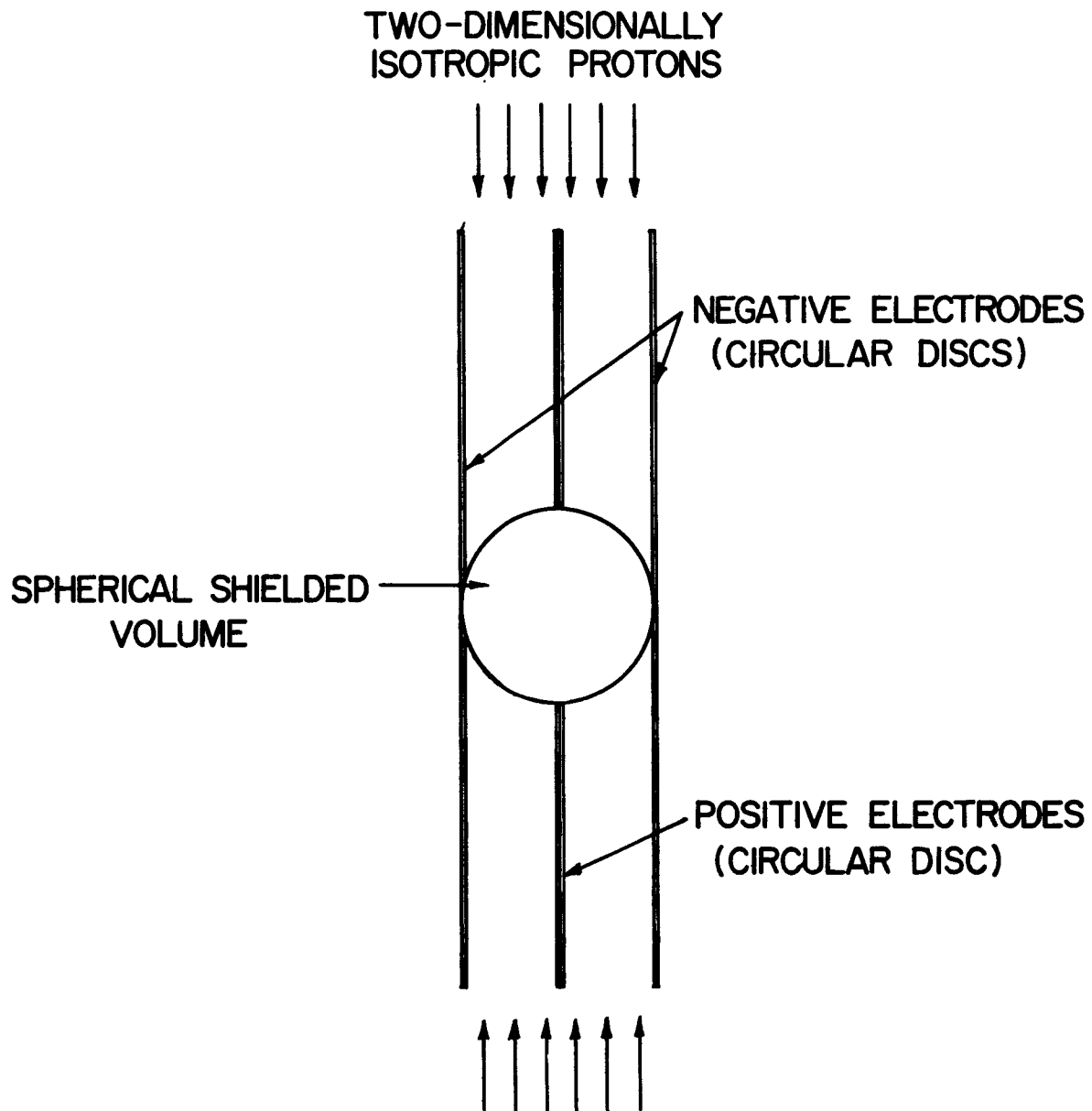
Figure 19.  Schematic Representation of Electrostatic Shielding System
Considered for Two-Dimensionally Isotropic Protons.
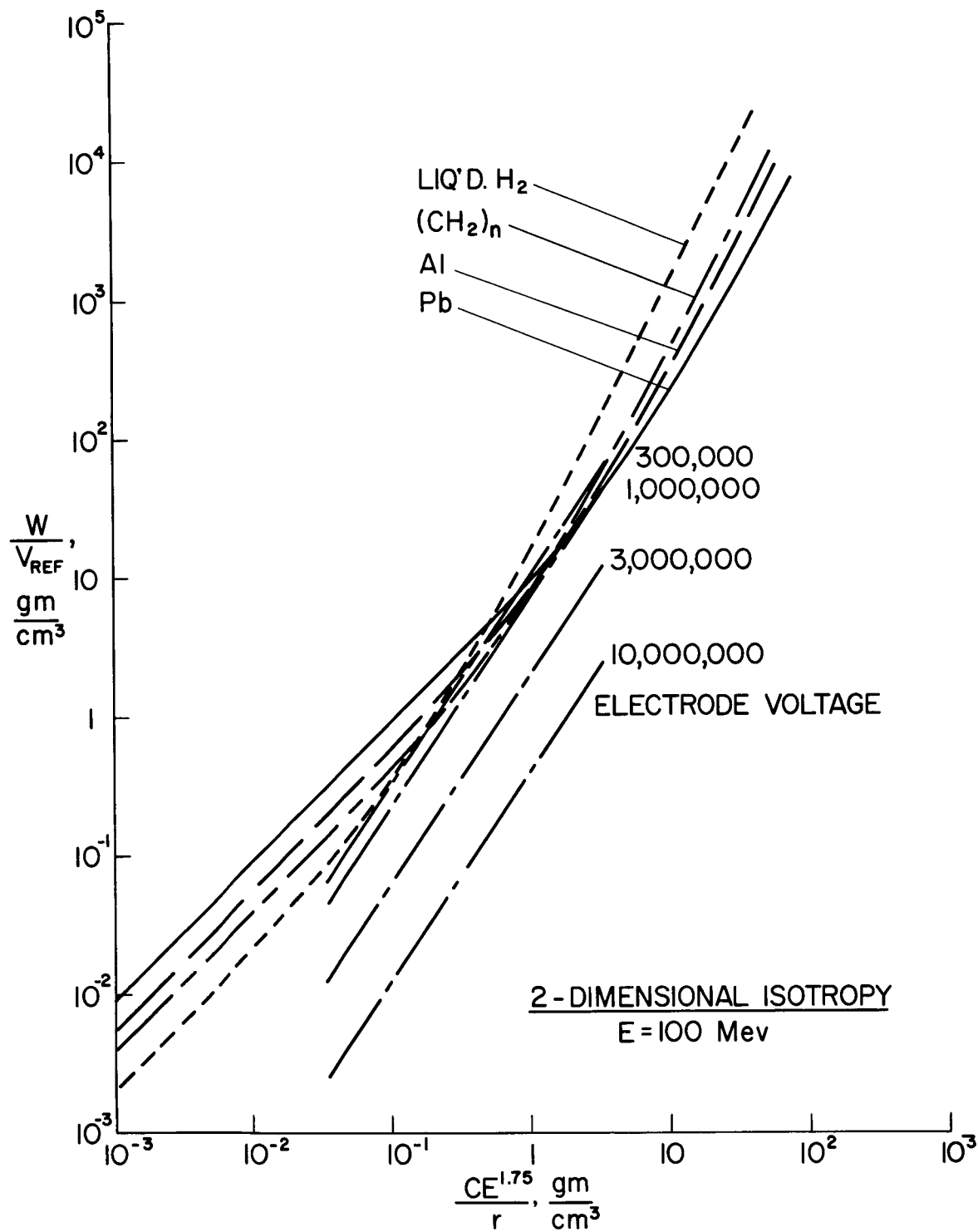
Figure 20. Comparison of Weights of Active, Electrostatic Shielding
Electrodes with Passive Shielding for Two-Dimensionally
Isotropic 100 Mev Protons and for Various Assumed
Deflecting Voltages.

116

W/V_REF, gm/cm³ (y-axis)

$10^5$

$10^4$

$10^3$

$10^2$

$$\frac{W}{V_{REF}}, \frac{gm}{cm^3}$$

$10$

$1$

$10^{-1}$

$10^{-2}$

LIQ'D. $H_2$
$(CH_2)_n$
Al
Pb

E, MEV
500
200
100

2-DIMENSIONAL ISOTROPY
Vr = 1,000,000 VOLTS

$10^{-3}$   $10^{-2}$   $10^{-1}$   $1$   $10$   $10^2$   $10^3$

$$\frac{CE^{1.75}}{r}, \frac{gm}{cm^3}$$
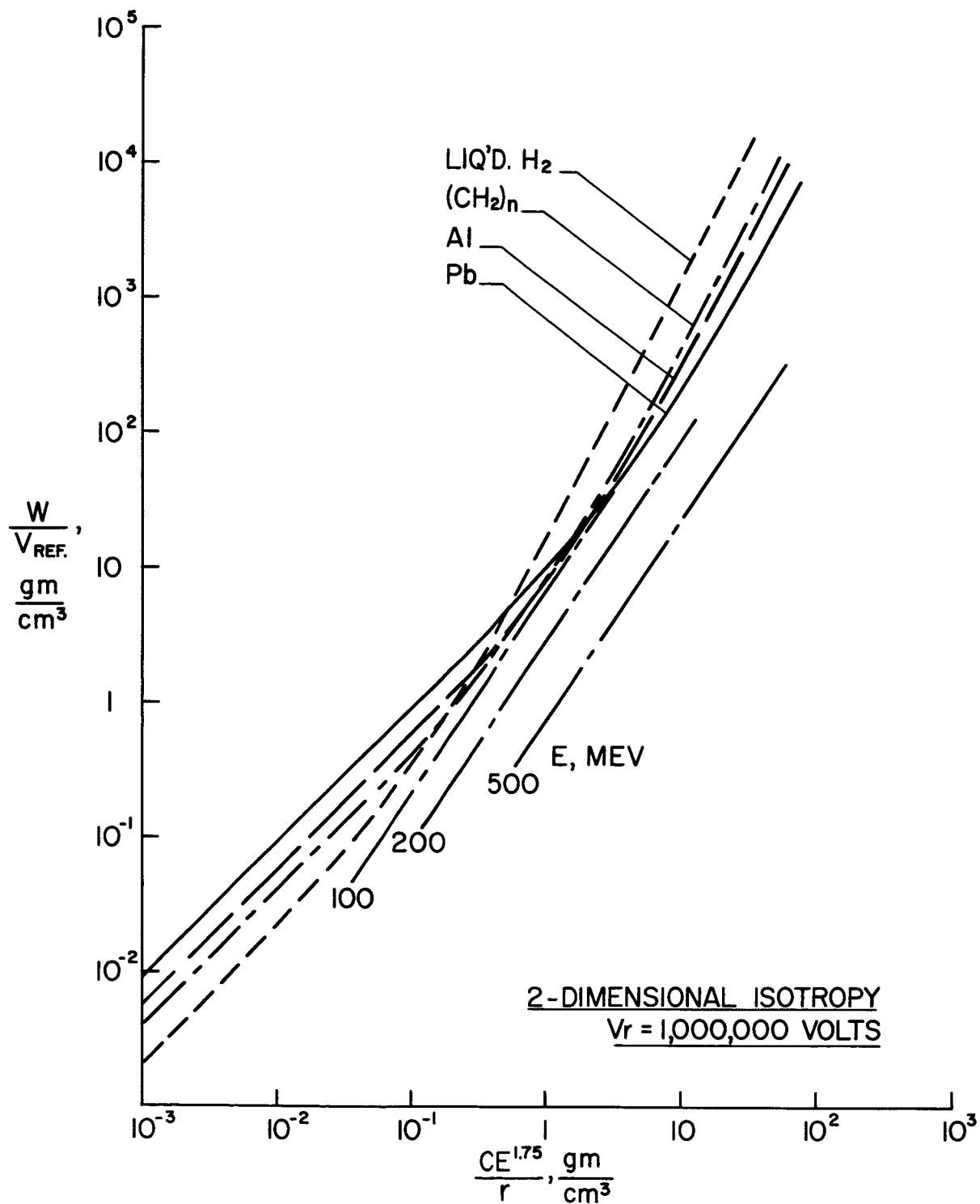
Figure 21. Comparison of Weights of Active, Electrostatic Shielding Electrodes with Passive Shielding for Two-Dimensionally Isotropic Protons of Various Energies at a Constant Deflecting Voltage of 1,000,000 Volts.
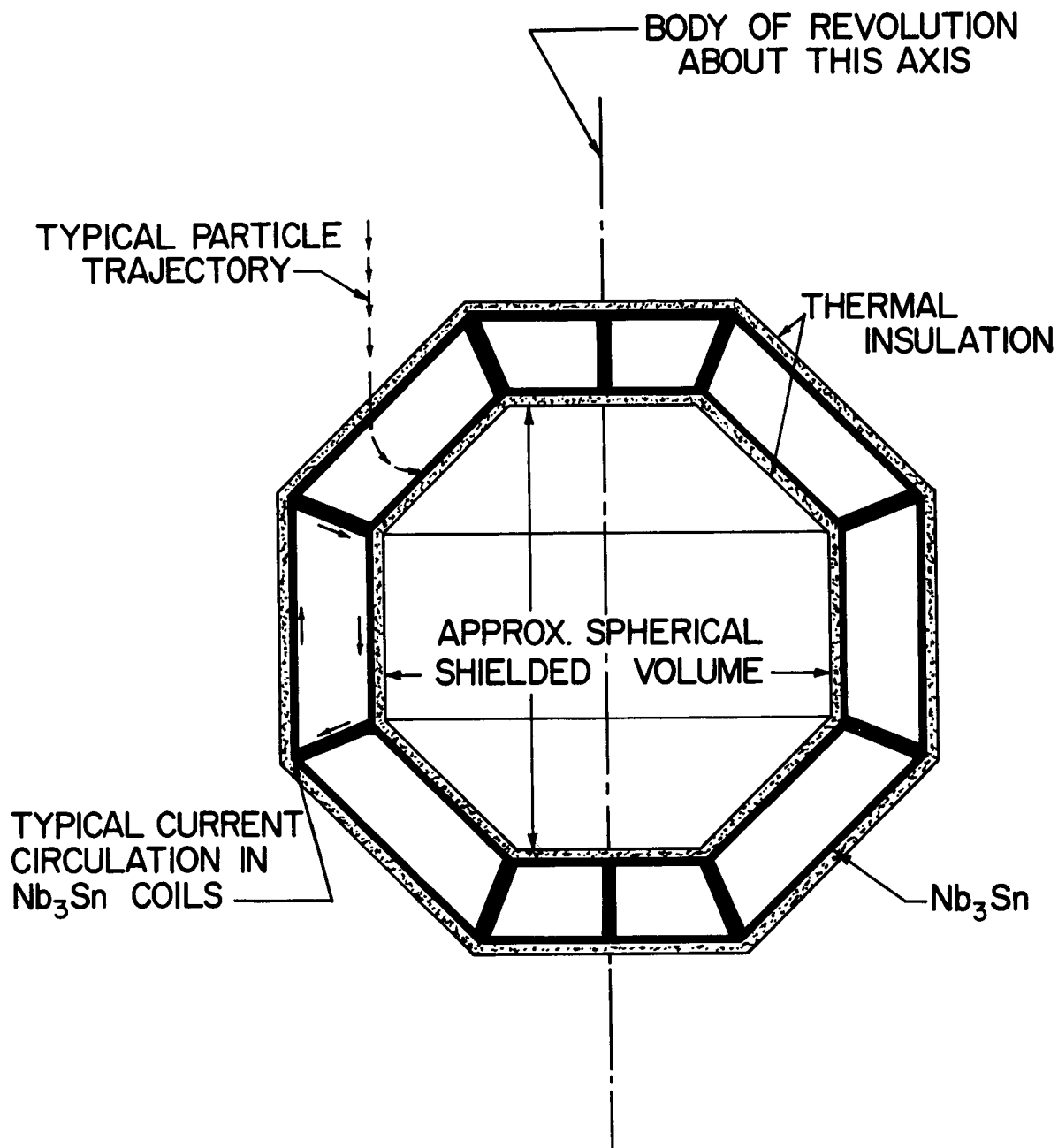
Figure 22.   Schematic Cross-Sectional View of Active Shielding
System Considered for Isotropic Protons.
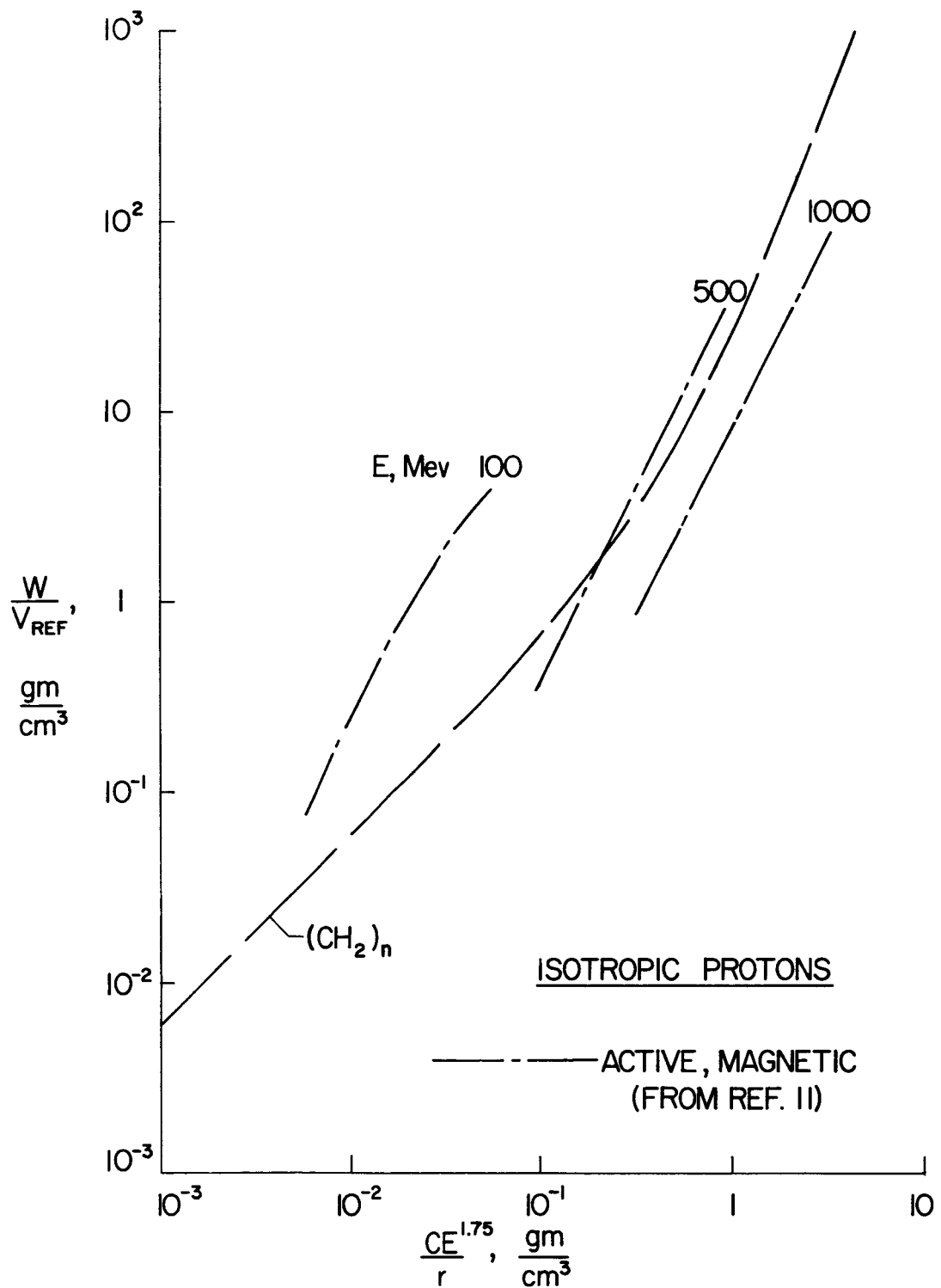
Figure 23. Comparison of Weights of Unconfined-Flux, Superconducting Electromagnetic Shielding for Isotropic Protons (from ref. 11), with Those for Passive, Polyethylene Shielding.
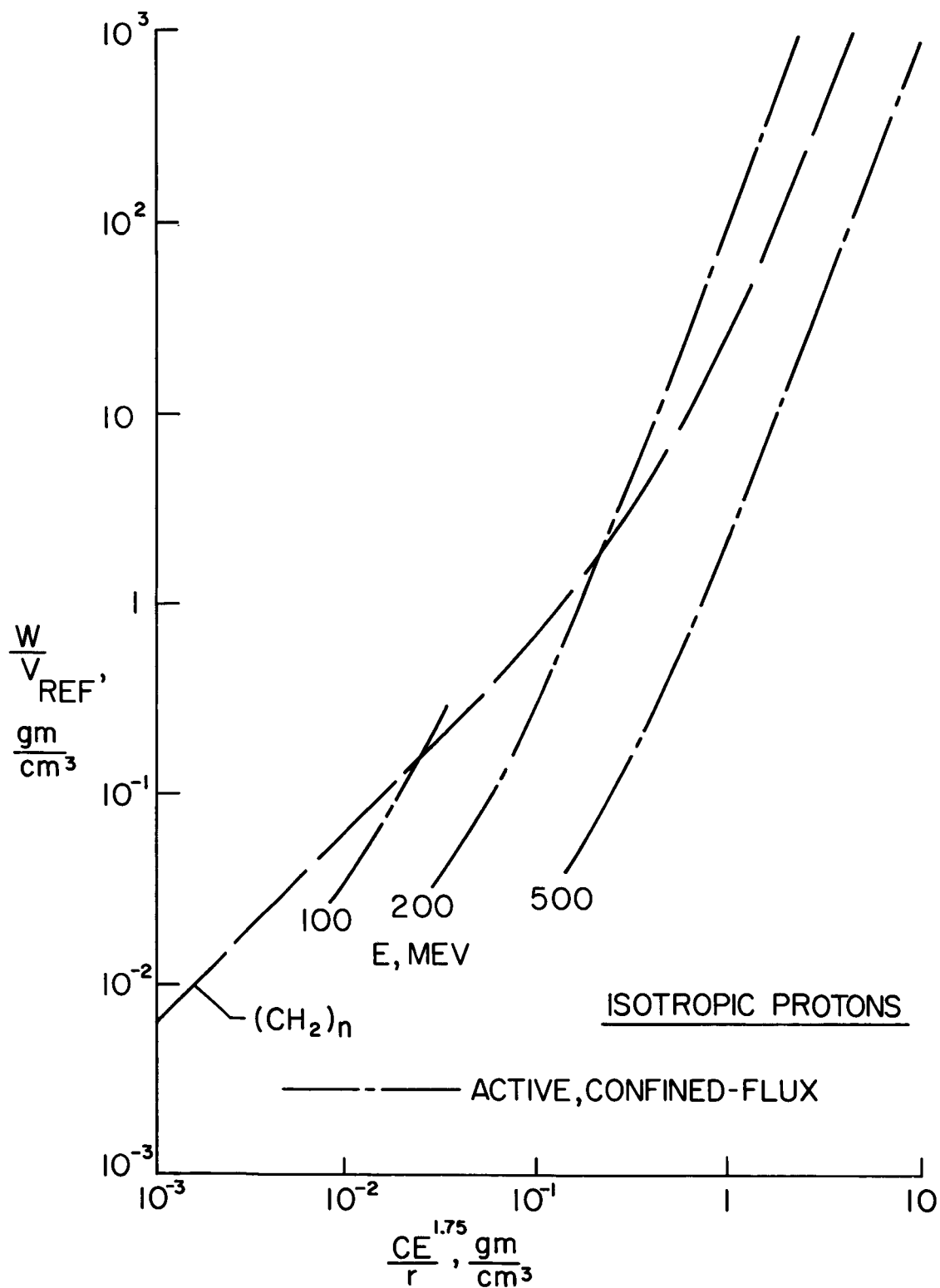
Figure 24. Comparison of Weights of Confined-Flux, Superconducting Electromagnetic Shielding for Isotropic Protons with those for Passive, Polyethylene Shielding.
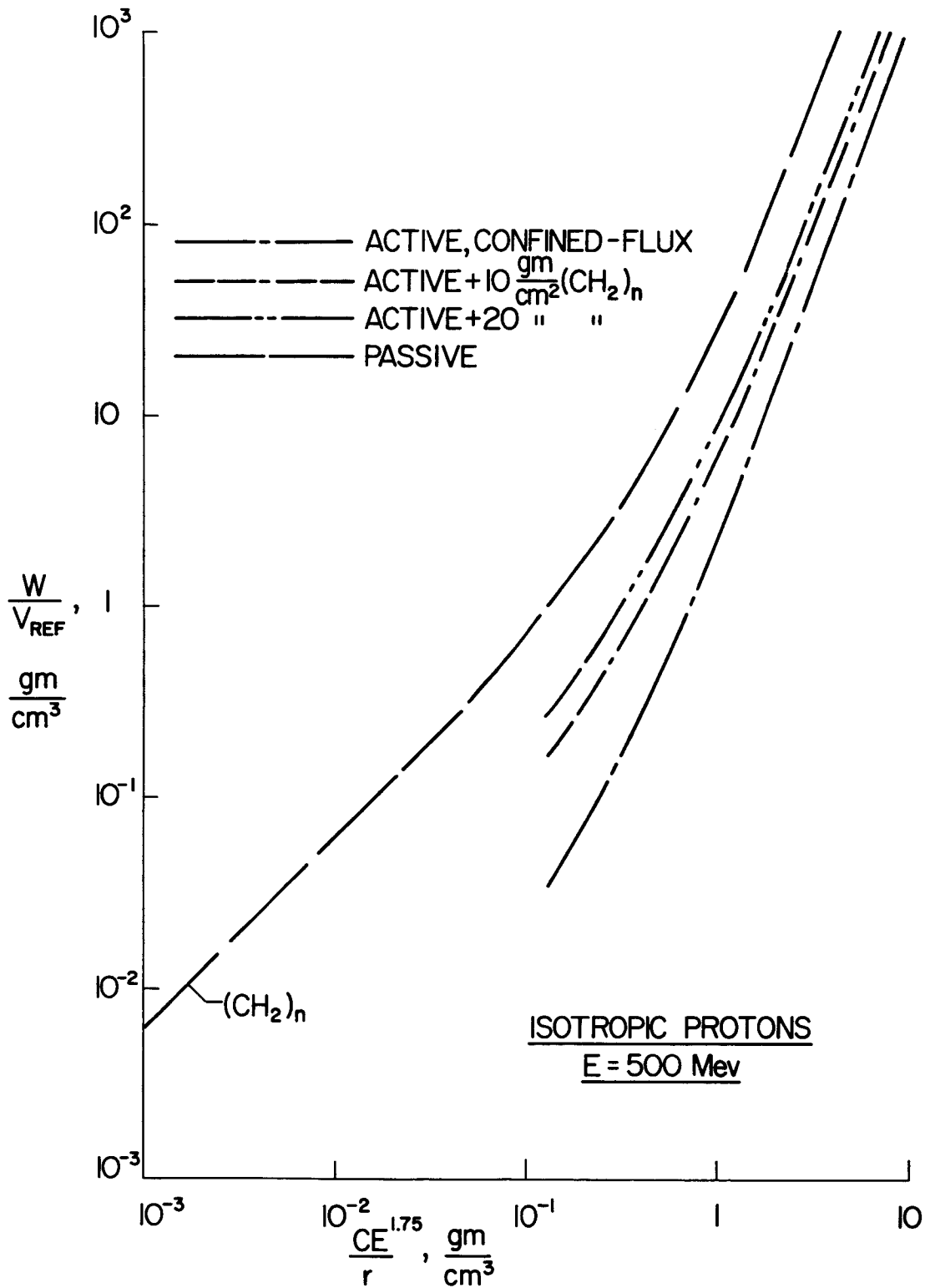
120

Figure 25. Comparison of Weights of Combination Active-Passive
(Superconducting Shielding Covered by Polyethylene)
Systems with those for the Active and Passive Systems
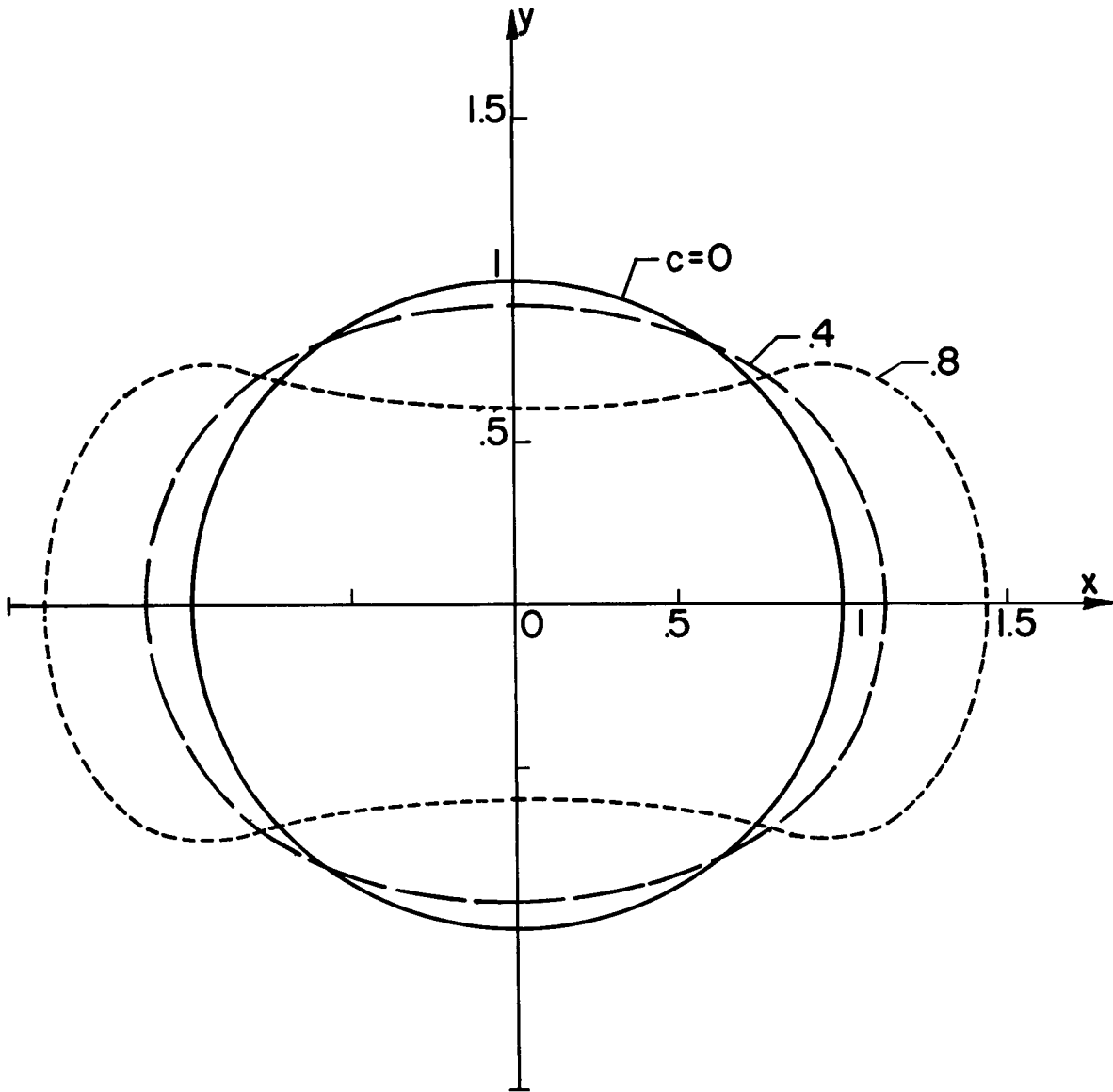Alone for Isotropic, 500 Mev Protons.

121

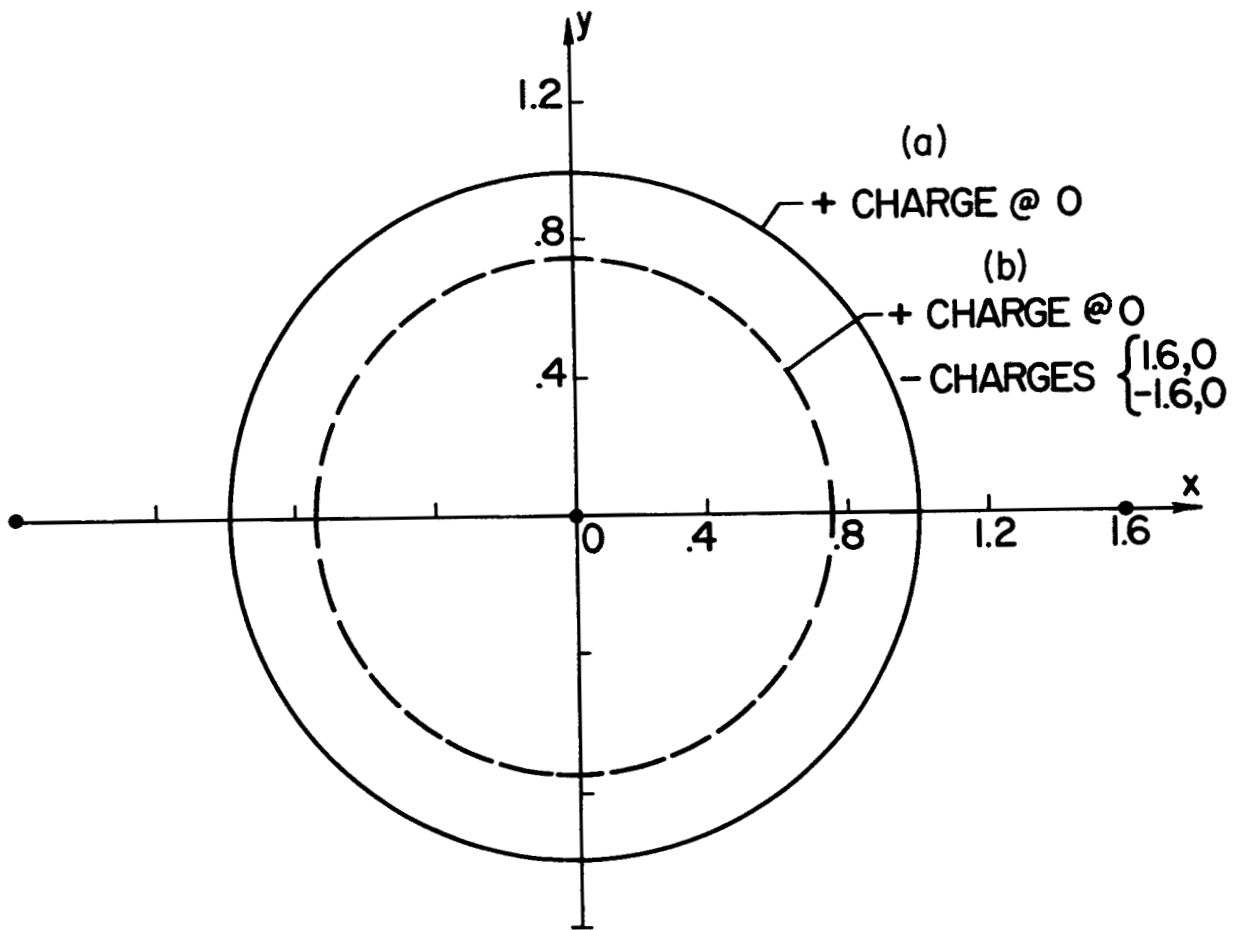Figure 26. Equi-Potential Curves for Two Point Charges Separated by a Distance 2c.

Figure 27. Equi-Potential Curves (a) For One Point Charge, and
(b) One Central Charge Between Two Opposite Charges
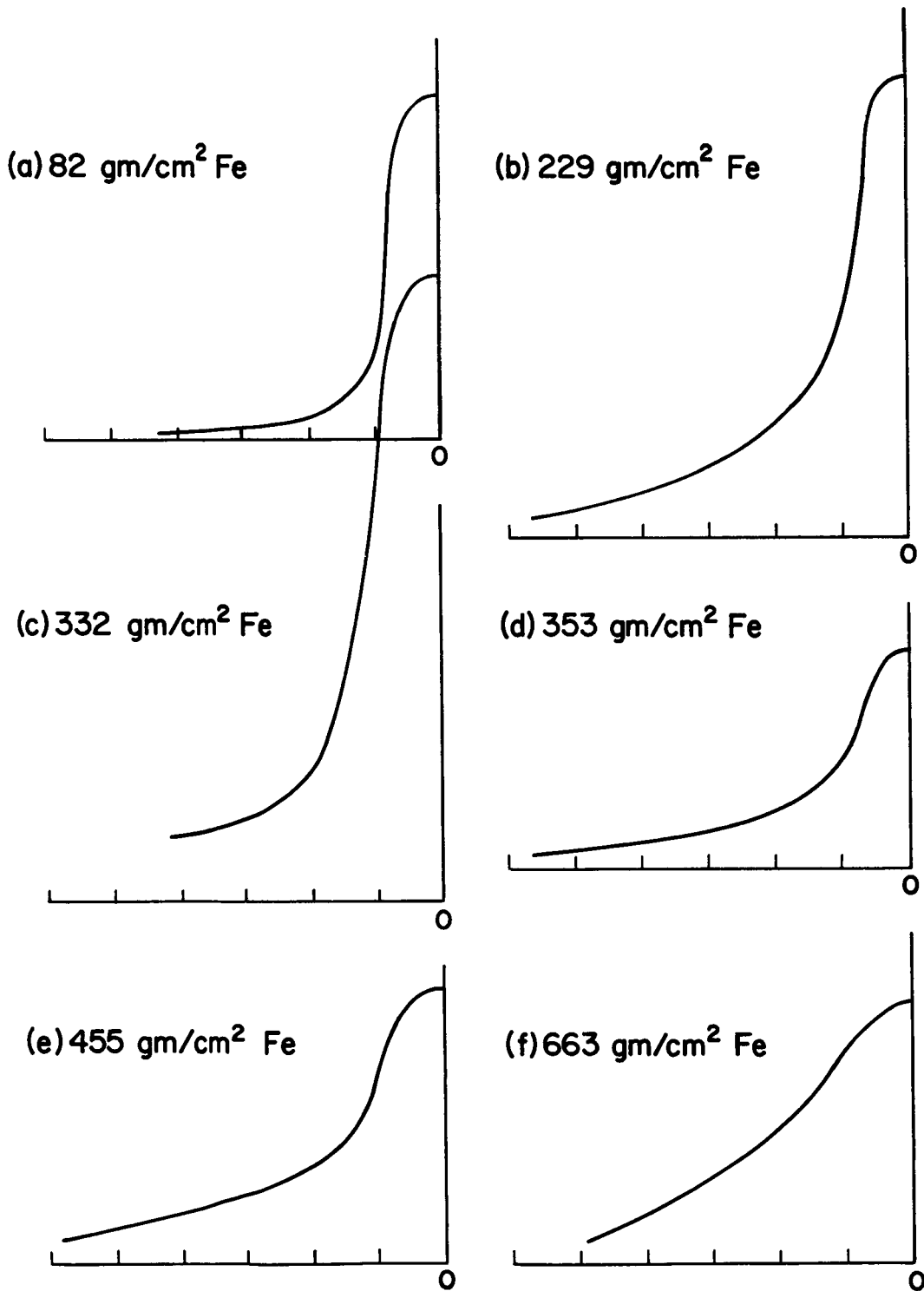Separated by a Distance 2c.

Figure 28.  Lateral Spread of 3-Bev Proton Stream in Iron, Measured by
Na-24 Activity in Aluminum Foils Buried at Indicated Depths
Beneath Surface of Incidence.

# DISTRIBUTION LIST

## TIS R62SD31

### Valley Forge

L. Steg, Rm. 9551
H. Somerson, Rm. 3125
R. Passman, Rm. 3030
E. Fthenakis, Rm. U2408
M. Kornhauser, Rm. U7216
G. Woo, Rm. 7217
V. Szebehely, Rm. 9543 (2)
S. Upham, Rm. 7047B
W. Hoese, Rm. 7047B
J. Farber, Rm. 9539
C. Mannal, Rm. 9533
L. McCreight, Rm. 9533
M. Dank, Rm. 9515
N. Dow, Rm. 7047 (50)
F. Wendt, Rm. 7023H
R. Kirby, Rm. 3223
W. Raithel, Rm. 3222
L. Warzecha, Rm. U7216
L. Lekus, Rm. 3110
R. Lawton, Rm. 3113
E. Merrick, Rm. U7216
R. T. Frost, Rm. 1320
J. Heyda, Rm. 7047
J. P. deVries, Rm. 7023H
G. Arthur, Rm. 3230
R. Haviland, Rm. 3230
J. Abel, Rm. U7216
H. E. Bergeson, Rm. L9531
R. Hughes, Rm. L9169
A. Harrison, Rm. 1308 (2 + tissue)
F. Smith, Rm. 9107L

### Chestnut Street

Documents Library (10 + tissue)
O. Klima, Rm. 5101

G. E. Technical Data Center
One River Road
Schenectady, N. Y. (2 + 6 TIS pages)

Bldg. 28, Rm. 100
G. E., Schenectady, N. Y.
Attn: R. Rochlin

G. E. Tempo Library
735 State Street
Santa Barbara, Calif. (4)

Electronics Park Library
Bldg. 3, Rm. 143
Syracuse, N. Y.
Attn: C. Lukens, Librarian (1 + 3 TIS pages)

Gerald Siesfeld
Young & Rubicam, Inc.
285 Madison Ave.
New York 17, N. Y.

Dr. A. K. Oppenheim
Div. of Aeronautical Sciences
University of California
Berkeley, California

St. Johns University
New York, N. Y.
Attn: L. P. Shen

# GENERAL ⬡ ELECTRIC

SPACE SCIENCES LABORATORY
MISSILE AND SPACE VEHICLE DEPARTMENT

## TECHNICAL INFORMATION SERIES

| AUTHOR | SUBJECT CLASSIFICATION | NO. |
|---|---|---|
| N. F. Dow | Space Flight | R62SD31 |
| S. P. Shen | | **DATE** |
| J. F. Heyda | Nuclear Radiation | April 1962 |

**TITLE**

EVALUATIONS OF SPACE VEHICLE SHIELDING

**ABSTRACT**

A general method of evaluating the efficiency of space vehicle shielding is developed and used to compare various active and passive systems for protection against ionizing radiation. Available permanent magnets are found useless for active shielding, and combined active-passive systems in general are determined to be

| G. E. CLASS | REPRODUCIBLE COPY FILED AT G. E. TECHNICAL INFORMATION CENTER 3198 CHESTNUT STREET PHILADELPHIA, PENNA. | NO. PAGES |
|---|---|---|
| I | | |
| **GOV. CLASS** None | | 124 |

inefficient. On the other hand, evaluations show that active electrostatic shielding may have possibilities for weight savings if electrical conditions (presently unknown) are favorable therefor in space. Further, a positive potential improvement is calculated for an active shielding system which utilizes superconducting $Nb_3Sn$ to provide a confined magnetic flux to deflect incident charged particles; this potential points toward substantial reductions in shield weight for the protection of large vehicles from highly energetic particles. Recommendations are made for further research, particularly for flight experiments to measure directionality of solar flare protons.

**By cutting out this rectangle and folding on the center line, the above information can be fitted into a standard card file.**

AUTHOR

COUNTERSIGNED

DIVISION          Defense Electronics

LOCATION          Valley Forge Space Technology Center, King of Prussia, Pa.